Helicobacter pylori VACA TOXIN:

REGULATION AND STRAIN-SPECIFIC DIFFERENCES IN ACTIVITY

By

Rhonda R. Caston

Dissertation

Submitted to the Faculty of the

Graduate School of Vanderbilt University

in partial fulfillment of the requirements

for the degree of

DOCTOR OF PHILOSOPHY

in

Microbiology and Immunology

May 8, 2020

Nashville, Tennessee

Approved: Date:

D. Borden Lacy, Ph.D.	
Holly Algood, Ph.D.	
Kelli Boyd, D.V.M., Ph.D.	
Matthew Tyska, Ph.D.	
Keith Wilson, M.D.	
Timothy Cover, M.D.	

To my parents and brother, whose endless love got me through

ACKNOWLEDGEMENTS

I would be remiss to not begin this section by acknowledging my mentor, Timothy Cover. I am grateful for the support and guidance I have received throughout the course of my Ph.D. training. Your optimism and ability to find the bright spot in any situation or piece of data was the perfect counter to my moments of discouragement. Thank you for also cultivating a supportive lab environment with an open-door policy that made me feel safe to express my thoughts, opinions, and concerns. Your enthusiasm and backing of lab activities was key in creating an incredible lab culture.

Thank you to all Cover lab members. Past members Arwen Frick-Cheng, Amber Beckett, and Anne Campbell made my transition into lab seamless. Thanks for embracing me, supplying me with coffee, and listening. Aung Soe (Sai) Lin, M. Lorena Harvey, and Jennie Shuman all joined the Cover lab after me. You are all amazing human beings and it has been a privilege to watch you grow as scientists. I also want to thank Nora Foegeding for her willingness to always help and showing me to not be afraid to pursue my passion. Mandy Truelock has worn several hats: summer student, research assistant, team VacA member, graduate student, and kindred spirit. Keep being awesome.

Special thanks to my bonus mentors Mark McClain, John Loh, and Holly Algood. I first worked with Mark during my rotation in the Cover lab and was immediately intimidated. However, I quickly learned that he is sarcastic, understanding, and kind. Thank you for freely sharing your scientific knowledge and life advice. I sat next to John almost every day and I have learned so much about science and life from him. Thank you for our daily banter and always providing your fatherly perspective. Holly, thank you for always being a safe space to vent and cry. You are my role model of a strong woman, mother, and scientist.

I especially want to thank my family and friends. My mother, Barbara Caston, my father, Ronnie Lewis, my brother, Ronnie Lewis Caston, and my sister-in-law, Catrinia Barnes, for

always encouraging me to reach for the highest heights. Growing up I may not have had everything I wanted, but I always had everything I needed and an abundance of love. Your sacrifices did not go unnoticed. Andre, Bianca, Salma, and Turnee are friends that are like family. Thanks for being my biggest cheerleaders and therapists.

Finally, I'd like to thank Michael, for loving me and not being afraid to join me on this journey. I am beyond excited to see what life has in store for us.

TABLE OF CONTENTS

LIST OF TABLES

Table Page

LIST OF FIGURES

Figures Page

Chapter 1

INTRODUCTION

Helicobacter pylori and gastric disease

Helicobacter pylori is a Gram-negative, microaerophilic curved rod-shaped bacteria that colonizes the stomach in about half the world's population (1, 2). *H. pylori* and its link to gastritis and peptic ulcer disease were first identified in the early 1980's by Barry Marshall and J. Robin Warren (3). In 2005, Marshall and Warren won the Nobel Prize in Physiology or Medicine for this seminal finding. Subsequently, this bacterium has been identified as the greatest known risk factor for the development of gastric cancer (4), and the World Health Organization has designated *H. pylori* as a type I carcinogen (5, 6). A majority of those infected with *H. pylori* are asymptomatic, and 1-5% develop peptic ulcer disease or gastric cancer (2, 7). It is not well understood why certain individuals develop severe disease, such as gastric cancer, and others do not.

Gastric cancer is the 5th most commonly diagnosed cancer in the world and the 3rd leading cause of cancer-related deaths. Throughout the world, gastric cancer incidence is about two-fold higher in men than in women (8, 9). Gastric cancer accounts for nearly 800,000 cancer-related deaths worldwide (8). Diagnosis of gastric cancer typically occurs during later stages, when the cancer has already metastasized to other sites of body (10). The incidence of gastric cancer is variable around the world, which can be attributed to geographic differences in dietary factors, *H. pylori* strain type

present in the region, genetic variation among human hosts, and the healthcare infrastructure of the specific countries (8, 9).

Effects of a high salt diet on gastric disease

In many regions of the world, epidemiologic studies have detected an increased risk of gastric cancer associated with a high salt diet (for example, pickled foods and meats that are smoked or salted) (11, 12). Animal studies have recapitulated the trends noted in the epidemiologic studies. Mongolian gerbils fed a high salt diet and infected with *H. pylori* have increased gastric inflammation and a higher incidence of gastric cancer compared to those consuming a normal diet (13). Effects of a high salt diet on gastric pathology in mouse models of *H. pylori* infection also have been reported (14). There are multiple possible mechanisms by which a high salt diet might enhance gastric cancer risk, including effects of high salt concentrations of *H. pylori* or effects on host tissue.

Growth of *H. pylori* in high salt conditions *in vitro* increases expression of *H. pylori* CagA (13, 15-18), a bacterial oncoprotein that is translocated from adherent bacteria into host cells via the *cag* PAI-encoded type IV secretion system (19-23). Sequence analysis of the *cagA* promoter revealed that strains in which CagA is upregulated by high salt contain one or two copies of a (TAATGA) motif (16), which is absent in strains in which CagA is not regulated by salt. Upon entry into host cells, CagA can contribute to carcinogenesis in a variety of ways, including binding and activating Src homology 2 (SH2) domain-containing protein tyrosine phosphatase 2 (SHP2), a phosphatase that relays positive signals for cell growth (24).

Several studies detected additional alterations in *H. pylori* gene expression or proteomic composition in response to high salt conditions (18, 25). Specifically, production of the *H. pylori* adhesin and outer membrane protein HopQ is increased in response to high salt, which might enhance *H. pylori* interactions with CEACAM proteins (Hop Q receptors) on host cells (9, 18, 25). Modification of host diet could prove to be an effective method to reduce an individual's risk of developing gastric cancer.

H. pylori vacuolating toxin (VacA)

Shortly after *H. pylori* was discovered, it was noted that addition of *H. pylori* culture supernatants to cultured eukaryotic cells resulted in cell vacuolation. Subsequently, the vacuolating protein component in the supernatant was purified and became known as vacuolating cytotoxin A (VacA) (26-31). *H. pylori* VacA is categorized as a pore-forming toxin, but the amino acid sequence and structure of VacA are unrelated to sequences and structures of other known bacterial pore-forming toxins.

The transcriptional start site of *vacA* is located 120 nucleotides upstream from the start codon (ATG) (30, 32). *vacA* transcript levels are highest during late log phase growth phase and are potentially altered when *H. pylori* is facing environmental stress (32-34). One study reported that *vacA* mRNA levels are reduced when *H. pylori* is incubated in acidic media for 30 minutes and significantly increased when the bacteria are grown in the presence of high salt for an hour (compared to normal pH and normal salt conditions) (34). Another study did not detect any change in *vacA* transcription when the bacteria are grown in a high salt medium, a difference that may be due to *H. pylori* strain variation (17). Although some studies suggest that *vacA* transcription is

regulated in response to salt concentration, iron concentration, low pH, or contact with host cells, there has not been an in-depth analysis of the mechanisms by which *vacA* expression is regulated in response to environmental changes.

The *vacA* gene encodes a 140 kDa protein, which undergoes Sec-dependent cleavage of an amino terminal signal sequence (Figure 1A) (27, 30, 31). After export from the cytoplasm to the periplasmic space, the toxin is secreted by an autotransporter or type V secretion system (26, 27, 30, 31, 35, 36). The VacA C-terminal β-barrel domain is inserted into the outer membrane and undergoes proteolytic cleavage by an unidentified protease. This cleavage event yields a 12 kDa peptide of unknown function and an 88 kDa protein with vacuolating toxin activity. The 88 kDa protein is secreted and released into the extracellular space and also can be retained on the surface of the bacteria (26, 33, 35, 36).

VacA structure

The secreted 88 kDa VacA protein is comprised of an N-terminal p33 domain and a C-terminal p55 domain, both of which contain regions of allelic diversity(Figure 1) (31, 37). The p33 and p55 domains are important for VacA binding and internalization into host cells (38). When expressed intracellularly, VacA amino acid residues 1-422, which includes the entire p33 domain and 111 amino acids from the p55 domain, are sufficient to induce cell vacuolation (39).

The p33 domain contains a hydrophobic region at its N-terminus comprised of 32 uncharged amino acids (40-42). This region includes three tandem GXXXG motifs that

are predicted to insert into membranes in host cells (40, 41). Mutating residues within this region eliminates VacA channel formation and vacuolating activity (41, 43, 44).

Once secreted, soluble VacA a monomers can oligomerize into soluble flower or snowflake-like structures (Figure 1B) (45-49). Both single layer (hexamers and heptamers) and double-layered (dodecamers and tetradecamers) have been observed. When water soluble VacA oligomers are exposed to acidic pH or alkaline pH, they disassemble into monomers (50, 51). VacA preparations exposed to low pH or high pH have greater cytotoxic activity compared to oligomeric VacA preparations maintained at neural pH (52, 53). When acid-activated VacA is added to liposomes comprised of various lipid compositions, primarily hexamers are observed on the surface of liposomes (54). Thus, it is thought that VacA interacts with the plasma membrane of host cells as a monomer and subsequently oligomerizes and inserts to form channels.

Prior studies of the p55 domain resulted in a 2.4-Å crystal structure, which revealed a right-handed β-helix structure characteristic of autotransporter passenger domains (55). Additionally, a 19-Å cryoelectron microscopy (cryo-EM) structure of a dodecamer localized the p33 domain to the central region and the p55 domain to the peripheral arms of the oligomer (56). Recently, near-atomic resolution structures of water soluble VacA oligomers have been resolved using cryo-EM (48, 49). The resolved structure consists of amino acids 27–299 (p33 domain) and 335–811 (p55 domain) (49). The p33 domain is a right-handed β-helix that extends into the p55 domain. While the p33 β-helix is formed by multiple ~30 amino acid repeats, the p55 domain is composed of ~25 amino acid repeats (49). Protomer- protomer interaction domains have been mapped to amino acids 47–75 of the p33 domain and amino acids 338-350 of the p55

domain (48, 49). These data are consistent with previous findings indicating that VacA mutants with residues 49-57 or 346-347 deleted fail to oligomerize (56-58). Thus far, all structural studies have utilized the s1i1m1 VacA type. No structural studies have been reported for other forms.

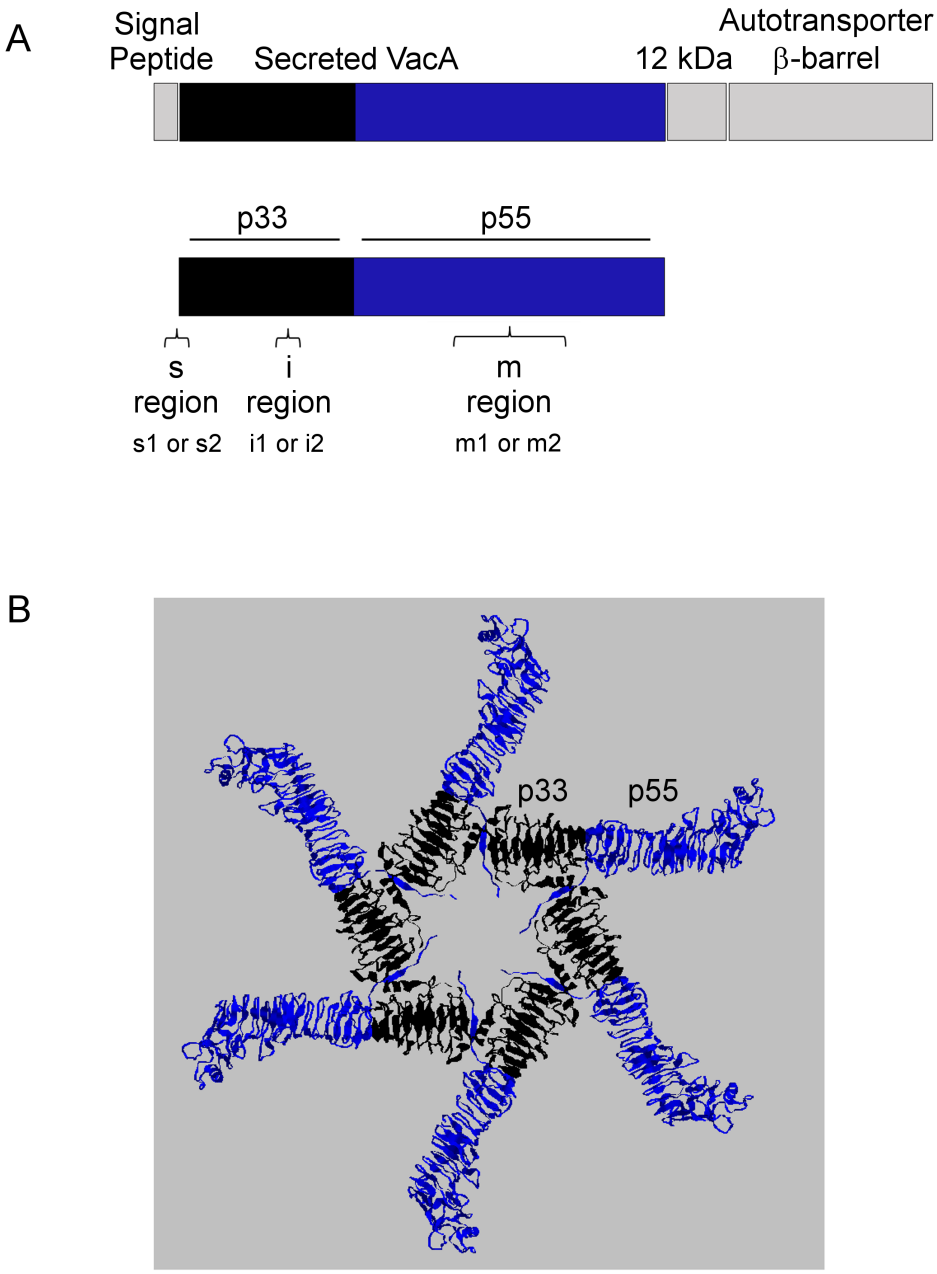

Figure 1. Schematic depiction of VacA protein. (A) In the schematic, the amino-terminal signal peptide, the 12 kDa peptide of unknown function, and a carboxy-terminal autotransporter domain with a predicted β-barrel structure are depicted in gray. The secreted 88 kDa VacA toxin depicts the p33 domain of VacA in black, the p55 domain in blue. Three regions of sequence diversity (s-, i-, and m-regions) are shown. (B) The cryo-EM structure of a hexamer formed by VacA from wild-type 60190 (type s1i1m1 VacA) is shown (PDB 6NYF) (49).

Effects of VacA on host cells

Multiple putative VacA receptors have been reported, including receptor protein tyrosine phosphatases (RPTP) α and β, low-density lipoprotein receptor-related protein-1 (LRP1), epidermal growth factor receptor (EGFR), and sphingomyelin on epithelial cells, and β2 integrin subunit (CD18) on T cells (51, 59-65). VacA binds lipid raft domains, but the specific receptors mediating this interaction have not been defined (66-69). It is unclear if VacA oligomerization occurs prior to membrane insertion, concomitant with insertion, or subsequent to insertion. VacA is subsequently internalized by a clathrin-independent, Cdc43 and Rac1-dependent route (70-73). VacA is internalized into endosomal compartments and has also been reported to associate with mitochondria, the Golgi apparatus, and the endoplasmic reticulum (70, 71, 74-76).

Changes in cell signaling after VacA intoxication are thought to be due to VacA receptor interactions. VacA activates p38, a mitogen-activated protein (MAP) kinase, in AZ-521 cells and T cells (77-79). Activation of this pathway leads to expression of cyclooxygenase 2 (COX-2), which results in increased prostaglandin E2 production, or activation of activating transcription factor 2 (ATF-2), but the receptors involved are unknown (78, 79). Additionally, VacA can activate G protein-coupled receptor kinase interactor (Git1), which is known to be activated by ligand interaction with RPTP β, resulting in upregulation of vascular endothelial growth factor (VEGF) and the β-catenin signaling pathway (59, 80, 81).

It is proposed that once VacA is internalized, vacuolation of cells, the function for which vacuolating toxin A is named, can occur when VacA anion channels form in endosomal membranes coupled with the activity of the vacuolar ATPase induce

swelling of the endosomal compartments (82-84). In addition to inducing vacuolation, VacA has been shown to induce autophagy, disrupt epithelial barriers, and induce cell death (74, 85-92). AZ-521 cells, a duodenal cell line, for unknown reasons are particularly susceptible to VacA-induced cell death. Treatment of cells with VacA has been reported to lead to decreased mitochondrial membrane potential, activation of proapoptotic factors Bax and Bak and cytochrome c release (93). The toxin's effects are not limited to epithelial cells. For example, VacA inhibits activation and proliferation of human T cells and B cells (77, 94-96). In macrophages, VacA can promote the formation of megasomes and stunts the maturation and function of vesicular compartments, which can inhibit the ability of macrophages to engulf *H. pylori* (97, 98).

VacA diversity

Early studies noted that there is considerable variation in vacuolating toxin activity among *H. pylori* strains (28). Additionally, there are differences among strains in levels of VacA secretion (32). At present, it is not known whether differences among strains in secretion are primarily due to differences in *vacA* transcription, differences in transcript stability, or differences in the efficiency with which various forms of VacA are secreted.

All *H. pylori* strains contain a *vacA* gene, and in most strains the *vacA* open reading frame is intact. Frameshift mutations, resulting in an absence of VacA protein production in *vacA,* are present in a small proportion of isolates (99). Phylogenetic analysis of *vacA* sequences from a large number of *H. pylori* strains has revealed the existence of several distinct groups of *vacA* alleles, several of which have distinct

geographical distributions (100). For example, *vacA* alleles found in many *H. pylori* strains isolated in East Asia are considerably different from the *vacA* alleles typically found in strains isolated in Europe or Africa (100, 101). Divergence among groups of *vacA* alleles is principally due to positively selected sequence changes in the region of *vacA* encoding the p55 domain and corresponds to surface-exposed sites in the p55 crystal structure (100).

Three main regions of diversity in VacA sequences have been recognized: the signal sequence region (s-region), the intermediate region (i-region), and middle region (m-region) (Figure 1). Within each of these regions, sequences can be classified into two main types (s1 or s2, i1 or i2, and m1 or m2) (102, 103). The s-region of VacA corresponds to the amino-terminal signal sequence and the amino-terminus of the secreted toxin (102, 104-106). The i-region is found within the p33 domain of VacA (103). The m-region corresponds to part of the p55 domain (102). Homologous recombination occurs commonly in *H. pylori*, and consequently, *vacA* alleles can contain multiple possible combinations of s-, i- and m-region types (s1-i1-m1; s2-i2-m2; s1-i1-m2, etc.) (102). An analysis of 735 *H. pylori* strains from 24 countries found 42% of strains contained s1m1 alleles, 26% s1m2, about 15% s2m2, and about 17% contained chimeric s1s2 and/or m1m2 sequences (107). However, s2m1 *vacA* alleles were not detected. In all countries that were a part of the study, s1 alleles were more common than s2 alleles, and m1 and m2 alleles were similar in prevalence, except on the Iberian Peninsula and in Central and South America, where strains containing the m1 allele were more abundant (107).

A region of sequence variation at the junction between VacA p33 and p55 domains has been termed the “d-region”. (108). A ~20 amino acid insertion is present in this region in some strains but not others. The *vacA* genes containing this deletion are termed d1 and those that do not contain the deletion are termed d2 (108). One study reported that type d2 forms of VacA form membrane channels that are less anion-selective and have a lower conductance than channels formed by d1 forms of VacA (109). Conversely, the presence or absence of the d-region insertion does not influence vacuolating activity of the protein (110).

Unlike the s1 forms of VacA, type s2 forms of VacA do not cause vacuolation of mammalian cells (102, 104-106). Differences in activity are attributed to different sites of signal sequence cleavage in s1 and s2 VacA proteins. Specifically, a hydrophilic 12 amino acid N-terminal extension is present in type s2 forms of the secreted 88 kDa protein but absent from type s1 proteins (106). One study reported that the i-region (within the p33 domain) is a determinant of vacuolating toxin activity in strains that produce type s1-m2 forms of VacA (103). Type i1 forms of VacA are more active than type i2 forms of VacA in experiments conducted with Jurkat T cells (111). Several studies have reported that type m1 and m2 forms of VacA exhibit distinct cell-type specificities. For example, the m1 VacA type is more active than the m2 type when added to HeLa cells (human cervix origin). However, both m1 and m2 forms are highly active in RK-13 cells (rabbit kidney origin) (112, 113). The difference in activity of m1 and m2 VacA proteins has been attributed to cell-type dependent variations in VacA binding to host cells and may also be attributable to differences in channel-forming properties (109, 113). Cell type specificity has been mapped to a 148-residue segment

within the m-region of VacA (112). m1 and m2 forms of VacA remain intact in most strains despite a high level of recombination (i.e. m1 and m2 forms of *vacA* are common, whereas chimeric forms are relatively rare) (100).

VacA and disease

Epidemiologic studies have demonstrated a correlation between the type of *vacA* allele present in *H. pylori* strains and the risk of gastric disease. Specifically, the risk of gastric cancer or peptic ulcer disease is higher in persons infected with strains containing type s1i1m1 forms of vacA, compared to persons infected with strains containing type s2i2m2 forms of vacA (9, 102, 103, 114-116). Additionally, strains containing types s1 and m1 *vacA* alleles have also been associated with an increased severity of gastric inflammation, epithelial damage, or ulceration, compared to strains containing type s2 or m2 *vacA* alleles (107, 117, 118). The increased risk of disease observed with strains containing s1, i1, or m1 forms of vacA is probably attributable not only to the effects of VacA, but also to the effects of additional virulence determinants. Specifically, strains containing a type s1 *vacA* allele typically harbor the *cag* pathogenicity island (which encodes CagA and a type IV secretion system) and the outer membrane protein adhesin BabA, whereas strains containing a type s2 *vacA* allele typically lack the *cag* pathogenicity island and often lack *babA* (9).

Mice and gnotobiotic piglets have been used to evaluate the role of VacA in gastric disease; however, neither develop gastric cancer. To study the effects of VacA *in vivo*, purified VacA or *H. pylori* extracts containing VacA have been directly administered into the stomachs of mice, resulting in damage to the gastric mucosa and

the recruitment of inflammatory cells (59, 119, 120). No differences in gastric inflammation were observed in several studies where gnotobiotic piglets or mice were inoculated with wild-type or VacA null *H. pylori* strains (121, 122). Conversely, one study of mice infected with wild-type or VacA null *H. pylori* reported stronger Th1 and Th17 responses and more severe pathology in mice colonized with a *vacA* null mutant strain, compared to the wild-type strain (123). Several studies have found that VacA-producing strains colonize better than a VacA null mutant strain (122-124). One study compared the different forms of the i-region in a mouse model. Mice infected with an s1/i1 form of VacA had a greater degree of spasmolytic polypeptide-expressing metaplasia (SPEM) than mice infected with a strain producing the s2/i2 form of VacA (124).

The role of VacA in *H. pylori*-mediated disease has been understudied in the gerbil model. *H. pylori* strain 7.13 is commonly used in studies of gastric cancer in the gerbil model (125, 126). Strain 7.13 does not produce detectable VacA, indicating that VacA is not required for gastric carcinogenesis in the gerbil model (127). A study using *H. pylori* strain TN2 did not detect differences in gastric inflammation in gerbils colonized with a wild-type strain or a *vacA* mutant strain, but animals infected with the wild-type strain did experience a higher incidence of gastric ulceration (128).

Goals of study

Previous studies have shown that expression and production of specific outer membrane proteins are increased when *H. pylori* is grown in high salt environments, and expression and secretion of key *H. pylori* virulence factors, such as CagA, are altered in response to environmental salt (11, 13, 16-18, 25). There are conflicting

reports of whether VacA is regulated in response to high salt. Previous studies have used proteomic approaches to define effects of high salt conditions on the *H. pylori* membrane proteome, but there had not been any systematic efforts to analyze effects of salt on secreted *H. pylori* proteins. Therefore, I utilized proteomic methods and transcriptomics to gain a more thorough understanding of how environmental sodium chloride concentration influences the composition of the *H. pylori* exoproteome and specifically to determine if expression and secretion of VacA are altered under high salt conditions.

Structural studies have only analyzed the m1 VacA form and functional studies of the secreted toxin have primarily utilized the m1 toxin type (48, 49, 55, 56). Previous studies that analyzed functional properties of the m2 form of toxin have had limitations. These include testing m1 and m2 VacA proteins produced by wild-type *H. pylori* strains, which contain differences outside of the m-region of VacA, using polyclonal antibodies that may differ in affinities, and challenges standardizing *H. pylori* broth culture supernatants or water extracts so that they contain equal concentrations of m1 and m2 VacA (112, 113, 129). Non-gastric cell lines, such as HeLa and RK-13, have been used in many previous studies to compare activities of m1 and m2 VacA proteins. To further investigate the role of the m-region in VacA activity, I generated *H. pylori* strains producing chimeric proteins in which segments of the VacA p55 domain of a parental strain (type m1 VacA) were replaced by corresponding m2 sequences. I then tested the activities of these proteins in an assortment of biologically relevant model systems. I hypothesized that the m2 form of VacA would have a reduced ability to bind host cells, resulting in decreased internalization and a reduction in VacA-mediated activities.

A version of the following section (Chapter 2, Effect of environmental salt concentration on the

Helicobacter pylori exoproteome) was previously published in Journal of Proteomics

Caston RR, Loh JT, Voss BJ, McDonald WH, Scholz MB, McClain MS, Cover TL. Effect of environmental salt concentration on the *Helicobacter pylori* exoproteome**.** J. Proteomics 2019; 202:103374.

Chapter 2

EFFECT OF ENVIRONMENTAL SALT CONCENTRATION ON THE *Helicobacter pylori* EXOPROTEOME

Introduction

H. pylori strains from unrelated individuals exhibit a high level of genetic diversity, and this variation among strains is an important factor that influences the risk of gastric cancer (9, 130, 131). For example, *H. pylori* strains vary in the production of a pore-forming toxin known as VacA. The VacA proteins secreted by some strains cause vacuolation (and many other alterations) in gastric epithelial cells, whereas VacA proteins secreted by other strains lack vacuolating activity (9, 31, 132, 133). *H. pylori* strains producing highly active forms of VacA (designated type s1/i1/m1) are associated with a higher risk of gastric cancer, compared to strains producing less active forms of the protein (designated s2/i2/m2) (9, 134). *H. pylori* strains also vary in the presence or absence of a chromosomal region known as the *cag* pathogenicity island (19-23, 135) and in the production of outer membrane proteins (BabA, SabA and HopQ) mediating adherence to host cells (9, 136-138) *H. pylori* strains containing the *cag* PAI, producing active forms of VacA, and producing BabA, SabA and type I HopQ are associated with a higher risk of gastric cancer and peptic ulcer disease, compared to strains lacking *the cag* PAI, producing inactive forms of VacA, and lacking these adhesins (9, 139).

The risk of gastric cancer is influenced not only by strain-specific bacterial constituents, but also by genetic variation among human hosts, environmental factors,

and dietary factors (140). Epidemiologic studies in many regions of the world have detected an increased risk of gastric cancer associated with a high salt diet (12, 140). One study reported that a high salt diet increased the risk of *H. pylori*-induced gastric cancer in a Mongolian gerbil model (141), and effects of a high salt diet on gastric pathology in mouse models of *H. pylori* infection also have been reported (142). There are multiple possible mechanisms by which a high salt diet might enhance gastric cancer risk. For example, high salt conditions in the stomach may have direct effects on *H. pylori* that influence the interactions between the bacteria and the gastric mucosa. In support of this hypothesis, several studies detected alterations in *H. pylori* gene expression or proteomic composition in response to high salt conditions (15-18, 143). *H. pylori* growth in media containing high salt concentrations augments CagA production and alters the expression of genes encoding outer membrane proteins (16, 18, 25, 144).

Within the stomach, *H. pylori* localizes in the gastric mucus layer and attaches to gastric epithelial cells, but rarely invades human cells. *H. pylori*-induced alterations in the gastric mucosa have been attributed, at least in part, to the actions of secreted *H. pylori* proteins. CagA is translocated from adherent bacteria into human cells through a type IV secretion system (19-23). VacA is secreted through a type V secretion system and released into the extracellular space as a soluble protein (132, 145, 146). Many other *H. pylori* proteins are also released into the extracellular space (33, 35, 147, 148), either by specific secretion pathways or non-specifically as a consequence of bacterial autolysis.

Previous studies identified *H. pylori* proteins released into the extracellular space using proteomic methods, typically involving either 2D gel electrophoresis and or other protein separation methods, followed by mass spectrometric analysis (33, 35, 147, 148). Most of the previous studies endeavored to distinguish between *H. pylori* proteins selectively released into the extracellular space and proteins non-specifically released as a consequence of autolysis. In the current study, we tested the hypothesis that environmental sodium chloride concentration influences the composition of the *H. pylori* exoproteome. Specifically, we cultured *H. pylori* in media containing varying concentrations of sodium chloride, and then analyzed the composition of the exoproteome under each of the culture conditions tested. In parallel, we used RNA-seq methodology to analyze effects of environmental sodium chloride concentration on *H. pylori* gene transcription and identified salt-responsive genes encoding proteins that are released into the extracellular space. We report that high salt conditions alter the abundance of numerous *H. pylori* proteins released into the extracellular space. Increased levels of VacA in the extracellular space in response to high salt conditions is relevant to the increased risk of gastric cancer observed in persons who consume a high salt diet.

Materials and Methods

Bacterial strains and culture conditions

H. pylori strain 26695 was passaged on Trypticase soy agar plates containing 5% sheep blood at 37° C in room air supplemented with 5% CO_2. Liquid cultures were

grown in a modified form of sulfite-free Brucella broth (149) containing only low molecular mass (< 3 kDa) components (Brucella broth filtrate), supplemented with 1X cholesterol (Gibco), as described previously (33). The use of this medium facilitates subsequent mass spectrometric analysis with minimal interference from high molecular mass proteins present in unfractionated Brucella broth. The Brucella broth used for routine *H. pylori* culture contains 0.5% added sodium chloride. In the current study, we also used modified forms of Brucella broth filtrate containing higher levels of added sodium chloride (1.0% or 1.25% NaCl).

Bacteria were harvested from plates and inoculated into liquid medium (10 ml volume, initial OD_{600} = 0.02) with the compositions described above (0.5% added sodium chloride). The seed cultures were grown with shaking for about 18 h, and then were inoculated into fresh Brucella broth filtrate [containing varying amounts of NaCl (0.5%, 1.0%, or 1.25%)] at an initial OD_{600} of 0.02. A previous study showed that the composition of the exoproteome is growth phase-dependent (33), so we collected aliquots at two different time points (24 h and 36 h post-inoculation, corresponding to late log and stationary phase). The culture aliquots were centrifuged at 4500 x g at 4° C, yielding broth culture supernatants and bacterial pellets that were processed as described below.

Processing of broth culture supernatants

Culture supernatants were processed as described previously (33). Specifically, the supernatants were passed through a 0.22 μm filter to remove any residual bacteria. Filtered supernatants were concentrated using a 10 kDa cut-off centrifugal filter

ultrafiltration unit. The concentration of any residual low molecular mass Brucella broth components was reduced by buffer exchange with Tris-buffered saline. The resulting preparations were centrifuged at 100,000 x g for 2 h at 4° C to remove outer membrane vesicles and other insoluble components, and the samples was further concentrated using centrifugal filter ultrafiltration units (10 kDa cut-off). Protein concentrations were determined by bicinchoninic acid (BCA) assay (Pierce).

Bacterial fractionation

Bacteria were fractionated into preparations enriched in membrane components or soluble components (cytoplasmic and periplasmic proteins), as described previously (18, 33). Specifically, the bacterial pellets were washed twice in TNKCM buffer [50 mM Tris (pH 7.4), 100 mM NaCl, 27 mM KCl, 1 mM $CaCl_2$, 0.5 mM $MgCl_2$] and re-suspended in suspension lysis buffer [50 mM Tris (pH 7.4) containing 1 mM $MgCl_2$ and EDTA-free protease inhibitor cocktail (Roche)]. The re-suspended pellets were sonicated (5 pulses, 20 seconds on/40 seconds off, 20% amplitude), and lysates were centrifuged at 4500 x g at 4° C. The resulting supernatant was collected and subjected to ultracentrifugation at 100,000 x g at 4° C for 2 h. The resulting insoluble fraction (pellet) is enriched in membrane proteins, and the soluble fraction (supernatant) is enriched in cytoplasmic and periplasmic proteins (33, 150). Both the supernatants and solubilized protein fractions were concentrated by ultrafiltration with a 10 kDa cutoff membrane, and protein concentrations were quantified by BCA assay (Pierce).

Analysis of samples by mass spectrometry

Samples prepared as described above were run 2 cm into a 10% BisTris NuPAGE gel. Gels were stained with Coomassie blue and an in-gel trypsin digest was performed. Single dimensional LC-MS/MS was performed using ThermoFisher LTQ equipped with a nano-electrospray source and attached to a Nanoacuity (Waters) HPLC unit with an autosampler (33). Peptides were resolved via reversed phase separation (90 min total cycle time). Peptide MS/MS spectra were acquired data-dependently with one full scan MS followed by 5 MS/MS scans. The peptide MS/MS spectral data were queried using SEQUEST (full tryptic specificity) and searched against the *H. pylori* 26695 protein database, to which both common contaminants and reversed versions of *H. pylori* protein sequences had been added. Peptide identifications were filtered and collated to proteins using Scaffold 4 (Proteome Systems). Protein identifications required a minimum of 2 unique peptides per protein, and were filtered to a 5% false discovery rate (both peptide and protein).

Analysis of mass spectrometry data

H. pylori was cultured under each of the experimental conditions on three separate days, and the resulting samples were analyzed by mass spectrometry. Spectral counts (peptides assigned to a given protein) detected in LC-MS/MS analyses of the three independent samples from each condition were summed and normalized. To identify proteins that were selectively released into the extracellular space, proteomic data for the broth culture supernatant fraction were compared to proteomic data for the cytoplasmic/periplasmic fraction, using previously described methods (33). Specifically, for each protein, we compared the relative abundance of assigned spectra in the

supernatant to the relative abundance of assigned spectra in the cytoplasm/periplasm fraction by calculating an enrichment value (E_{sup} = % $abundance_{sup}$/% $abundance_{CP/PP}$)(33). To facilitate further analysis, the levels of enrichment were expressed as log_2 values (log_2 E_{sup}). Proteins enriched in the supernatant compared to the cytoplasm/periplasm fraction are assigned positive log_2 E_{sup} values, while those enriched in the cytoplasm compared to the supernatant are assigned negative log_2 E_{sup} values.

As an additional analytic approach for identifying selectively released proteins, the significance of differences in numbers of assigned spectra in supernatants compared to cytoplasm/periplasm fractions was calculated using a Fisher's exact test (FET) with Benjamini-Hochberg (BH) multiple test correction. Selectively released proteins were defined as proteins with log_2 E_{sup} value ≥ 1 (a 2-fold or greater abundance in the supernatant vs the cytoplasm/periplasm) and exhibiting statistically significant differences based on Fisher's Exact test with Benjamini-Hochberg correction (false discovery rate = 0.1). This approach successfully discriminated between proteins previously reported to be selectively released into the extracellular space (33) and ribosomal proteins (data not shown).

To assess the effect of salt concentration on the relative abundance of selectively released proteins detected in culture supernatant, assigned spectral counts for individual proteins detected in LC-MS/MS analyses of supernatants from all cultures containing 0.5% salt (both 24 h and 36 h time points) were summed, and a similar approach was used for spectral counts from all cultures containing 1.0% salt or 1.25% salt. The numbers of spectral counts in samples from different conditions were then

compared. Proteins exhibiting a ≥2-fold difference in the number of normalized spectral counts when comparing cultures containing high salt concentrations (1.0% or 1.25%) with cultures containing routine salt concentrations (0.5% NaCl) were considered to be salt-responsive. This analysis was restricted to selectively released proteins (Table 1) for which a minimum of 10 spectral counts were detected in either high salt or low salt conditions.

Western blotting

H. pylori was inoculated into Brucella broth filtrate supplemented with cholesterol and containing 0.25%, 0.5%, 1.0% or 1.25% NaCl, at a starting OD_{600} of ~0.02, as described above. After 24 h and 36 h, aliquots of the cultures were removed and centrifuged at 4500 x g for 15 minutes. The supernatant fraction was concentrated using a 10 kDa cut-off centrifugal filter ultrafiltration unit, and protein concentrations were determined using a BCA protein assay (Pierce). In addition to analyses of cultures grown in Brucella broth filtrate, *H. pylori* were also inoculated into unfractionated Brucella broth supplemented with cholesterol and containing either 0.5% or 1.25% NaCl at OD_{600} ~0.30 and incubated for 1 h with shaking. This latter condition mimicked the *H. pylori* growth conditions used for RNA analyses (see below). Supernatant samples were processed as described above.

Western blot analyses were performed using samples standardized by protein concentration (40 ug of total protein per sample). Proteins were separated on a gradient (4-20%) acrylamide gel and transferred to a nitrocellulose membrane. Membranes were immunoblotted using rabbit polyclonal antisera to VacA (151) followed

by an anti-rabbit secondary antibody conjugated to horseradish peroxidase (Promega). Enhanced chemiluminescent reaction-generated signals were detected using x-ray film.

RNA isolation

H. pylori was grown in unfractionated Brucella broth supplemented with 1X cholesterol (Gibco) to an OD_{600} of ~0.5, and was subcultured into Brucella broth containing either 0.5% NaCl or 1.25% NaCl at a starting OD_{600} of ~0.3. Following growth for 1 h, the cultures were centrifuged, bacterial pellets were resuspended in RNA*later* (Ambion) for 40 min, and the pellets were stored at -80^{o} C. RNA was prepared using TRIzol reagent (Ambion), using the manufacturer's instructions. All RNA samples were digested with RQ1 RNase-free DNase (Promega) to remove contaminating DNA, before being subjected to a clean-up step using Qiagen RNeasy columns.

Preparation of RNA-seq library and analysis

The preparation of RNA-seq libraries and subsequent analysis was performed as described previously (143). Briefly, RNA quality was determined using 2100 Bioanalyzer (Agilent), and 200 ng of DNase-treated total RNA (RNA integrity number greater than 9) was used to generate rRNA-depleted/mRNA-enriched libraries using TruSeq Ribo-Zero bacterial RNA kits (Illumina). Library quality was assessed using the 2100 Bioanalyzer (Agilent), and libraries were analyzed using KAPA library quantification Kits (KAPA Biosystems). Pooled libraries were subjected to 75-bp paired-end sequencing according to the manufacturer's protocol (Illumina HiSeq 3000).

Bcl2fastq2 conversion software (Illumina) was used to generate demultiplexed Fastq files. Six independent RNA-seq libraries prepared from *H. pylori* cultures grown in media containing either 0.5% or 1.25% NaCl (three cultures of each) were sequenced. The numbers of sequence reads for each sample ranged from 2.28×10^7 to 5.12×10^7.

RNA-seq data were trimmed to remove all bases below a quality of Q3, and adapter sequences were removed using FastQ quality control software (FaQCs) (152). Kallisto pseudocounting (153) was applied to all annotated genes in the *H. pylori* 26695 reference genome (154) (GenBank accession number GCA_000008525.1). The expected counts fields from Kallisto outputs were used for all analysis steps. Transcripts associated with a total of 1,562 *H. pylori* genes were identified by RNA-seq. The EdgeR (155) package for R was used to analyze count files. Data from individual samples were normalized within EdgeR and analyzed using the generalized linear model (GLM).

The RNA-seq data were analyzed by calculating for each gene a transcript abundance ratio (number of sequence reads from bacteria grown in high salt conditions divided by the number of sequence reads from bacteria grown in routine conditions). The mean ± SD of all the calculated transcript abundance ratios for the 1562 identified genes was 1.01 ± 0.3. Specific genes were classified as upregulated or downregulated in response to high salt conditions (1.25% NaCl) if the calculated transcript ratios were $\geq$2 standard deviations above or below the mean transcript abundance ratios (i.e. $\geq$1.61 or $\leq$0.62), with a false discovery rate (FDR) of <0.05.

Analysis of vacA by real time RT-qPCR

H. pylori total RNA was isolated using Trizol reagent (Gibco). RNA samples were digested with RQ1 RNAse-free DNAse (Promega) and subjected to a clean-up step using RNAeasy columns (Qiagen), as described above. Purified RNA (100 ng) was then used for cDNA synthesis with random hexamer primers using the iScript cDNA synthesis kit (Biorad). Real-time reverse transcription quantitative PCR (RT-qPCR) was completed using 1:20 dilutions of cDNA. Control reactions were performed in the absence of reverse transcriptase. Real time analysis was performed using an ABI real-time PCR machine and SYBR green fluorophore (iTaq universal SYBR mix; Bio-Rad), with transcript abundance determined using the ΔΔCT method. In addition to analyzing expression of *vacA* and other genes of interest, we analyzed expression of the housekeeping genes *gyrB* (DNA gyrase subunit B) and *atpA* (encoding ATP synthase F1 α subunit) and 16S rRNA as controls. Prior to analysis, the transcript levels of target genes in each sample were normalized to the abundance of the 16S rRNA internal control. The normalized transcript signals from high-salt conditions and routine conditions were then compared. The primers used for real-time RT-qPCR analysis were as follows: 5'-ACAACAAACACACCGCAAAA- 3' and 5' CCTGAGACCGTTCCTACAGC -3' for *vacA*; 5'- GGAGTACGGTCGCAAGATTAAA -3' and 5'-CTAGCGGATTCTCTCAATGTCAA -3' for 16S rRNA; 5'-CGTGGATAACGCTGTAGATGAGAGC -3' and 5' -GGGATTTTTTCCGTGGGGTG -3' for *gyrB;* and 5'-CTTCACGCAATTCGCTTCTG-3' and 5'-AAGCCCTTAGCCCCAGCATA-3' for *atpA.*

Results

Analysis of selectively released proteins

To determine the effect of environmental salt concentration on composition of the *H. pylori* exoproteome, we cultured *H. pylori* in media containing three different concentrations of sodium chloride (0.5%, 1.0%, or 1.25%), as described in Methods. Culture medium containing 0.5% NaCl is used for routine culture of *H. pylori*, whereas 1.0% or 1.25% NaCl concentrations correspond to elevated salt concentrations. Aliquots were removed at 24 h and 36 h post-inoculation (corresponding to late-log phase and stationary phase), and the samples were centrifuged to yield bacterial pellets and culture supernatants. The broth culture supernatant fractions were processed to remove outer membrane vesicles and other insoluble components, and the bacterial pellets were processed to yield a soluble cellular fraction enriched in cytoplasmic and periplasmic proteins, as described in Methods. The broth culture supernatant and soluble cellular fractions were then analyzed by LC-MS/MS. *H. pylori* can potentially release proteins into the extracellular space through specific secretion pathways or non-specifically as a result of autolysis (33, 35, 147, 148, 156). To identify proteins that were selectively released into the extracellular space, we used a previously described approach (33) in which the relative abundance of individual proteins in the supernatant fraction is compared to the relative abundance of the corresponding proteins in the cytoplasmic/periplasmic fraction, as described in Methods.

Twenty-five proteins met the criteria for selective release into the extracellular space (as defined in Methods) in all 6 of the culture conditions tested [i.e. medium

containing 0.5%, 1.0%, or 1.25% NaCl, and time points of 24 h or 36 h] (Table 1), and 35 proteins met criteria for selective release in at least 5 of the 6 conditions tested (Table 2). These included several proteases [HP0657, HP1012, and HP1019 (serine protease, HtrA)], several cysteine-rich proteins belonging to the Sel-1-like protein family (HP0211, HP0235, and HP1098, designated HcpA, HcpE and HcpC, respectively)(157, 158), HP0104 (2',3'-cyclic-nucleotide 2'-phosphodiesterase, CpdB), and HP0410 (neuraminyllactose-binding hemagglutinin homolog). Many of the proteins listed in Table 2 [including HP0175 (159-161), HP0211 (HcpA) (162, 163), HP1019 (serine protease, HtrA) (164, 165), HP1118 (γ-glutamyltranspeptidase, GGT) (123, 166, 167), HP1173 (168), HP1286 (169, 170), and HP1454] (171) are capable of causing alterations in host cells. The majority of the proteins listed in Table 2 are predicted to contain Sec-dependent signal sequences. Many of the proteins listed in Table 2 were also identified as selectively released proteins in a previous study that analyzed *H. pylori* protein release when cultured in medium containing 0.5% sodium chloride (33) (Table 2, asterisks). Proteins identified as selectively released under all conditions in the current study but not the previous study (33) included HP0175 (cell binding factor 2, also known as peptidyl prolyl cis,trans-isomerase) and HP0389 (superoxide dismutase). These data confirm that specific proteins are selectively released into the extracellular space under routine culture conditions, and indicate that most of these proteins are also selectively released under high salt conditions.

Culturing *H. pylori* in medium containing increased salt concentrations could potentially lead to multiple bacterial alterations that affect the composition of the exoproteome. For example, high salt conditions might alter the release of proteins from

the bacterial surface into the culture supernatant, might alter expression of genes encoding released proteins, or might promote bacterial autolysis. As an initial approach for distinguishing among these possibilities, we assessed whether high salt conditions changed the selectivity of release of the proteins listed in Table 2 (i.e., resulting in higher or lower $\log_2 E_{sup}$ values than observed under routine culture conditions). As shown in Table 2, culturing *H. pylori* in high salt conditions was associated with an increased selectivity of release of the listed proteins (mean $\log_2 E_{sup}$ values of 2.59 for cultures containing 0.5% salt, 3.17 for cultures containing 1.0% salt, and 3.52 for cultures containing 1.25% salt). In contrast, culturing *H. pylori* in high salt conditions did not result in any change in the selectivity of release of ribosomal proteins (data not shown). These results indicate that *H. pylori* growth in medium containing elevated salt concentrations does not promote autolysis.

89 proteins met the criteria for selective release in fewer than 5 of the conditions tested (Table 1). Examples included numerous outer membrane proteins (OMPs) and VacA (vacuolating toxin) (Table 1). Selective release of OMPs was mainly detected at the 24 h time point (Table 1). Collectively, these data indicate that numerous proteins are selectively released into the extracellular space under both routine conditions and high salt conditions (Table 2).

Table 1. Proteins selectively released into the extracellular space under 1 or more culture conditions

Gene/Protein[a]	Description	E_{sup} values for the indicated culture conditions[b]					
		24 h 0.5%	24 h 1.0%	24 h 1.25%	36 h 0.5%	36 h 1.0%	36 h 1.25%
HP0003	3-deoxy-d-manno-octulosonic acid 8-phosphate synthetase (KdsA)				1.16		
HP0006*	pantoate-beta-alanine ligase (PanC)	2.31					
HP0025*	outer membrane protein (Omp2)		1.74	2.06			1.68
HP0089	pfs protein (Pfs)	2.81	1.81		3.08		
HP0097	hypothetical protein			4.93			
HP0104*	2',3'-cyclic-nucleotide 2'-phosphodiesterase (CpdB)	7.64	4.79	7.21	4.12	7.37	5.34
HP0105	conserved hypothetical protein						2.47
HP0107	cysteine synthetase (CysK)			3.17			
HP0127	outer membrane protein (Omp4)			4.74			
HP0129*	hypothetical protein	3.04	2.48	5.61		2.94	5.48
HP0130	hypothetical protein		2.31	2.34			
HP0162	conserved hypothetical protein	1.82	1.86		2.14		
HP0166	response regulator (OmpR)	1.39					
HP0175	cell binding factor 2	1.10	1.56	1.93	1.34	2.15	2.43
HP0176	fructose-bisphosphate aldolase (Tsr)	1.27	1.66	1.38	1.42	1.40	1.09
HP0194*	triosephosphate isomerase (Tpi)				1.83		2.47
HP0204*	hypothetical protein	2.16		3.60		3.91	
HP0211*	conserved hypothetical secreted protein		4.26	4.50	3.07	5.73	2.79
HP0218*	hypothetical protein	1.49		1.57			
HP0224	peptide methionine sulfoxide reductase (MsrA) [1.8.4.6]	1.03	1.36	1.76		1.24	1.15
HP0227	outer membrane protein (Omp5)		4.90				
HP0229*	outer membrane protein (Omp6)		5.52	3.61			
HP0231*	hypothetical protein	2.02	2.04	2.53	2.06	2.98	3.09
HP0233*	conserved hypothetical protein	2.51		2.15			
HP0235*	conserved hypothetical secreted protein	2.03	3.07	3.75	5.10	6.15	3.91
HP0237	porphobilinogen deaminase (HemC)	4.69					
HP0240*	octaprenyl-diphosphate synthase (IspB)	2.34					
HP0252	outer membrane protein (Omp7)			3.75			
HP0275*	ATP-dependent nuclease (AddB)		3.21			3.03	4.30
HP0298*	dipeptide ABC transporter, periplasmic dipeptide-binding protein (DppA)	2.80	3.51	3.98	2.68	5.25	3.75
HP0304*	hypothetical protein	5.19		5.38	5.01	5.12	4.87
HP0305	hypothetical protein	1.58	1.16	1.68			
HP0317*	outer membrane protein (Omp9)		1.78	2.40			
HP0318	conserved hypothetical protein			1.11			
HP0319*	arginyl-tRNA synthetase (ArgS)	2.23			2.75		
HP0323*	membrane bound endonuclease (Nuc)	3.74	3.01	4.73	2.18	2.90	2.57
HP0377*	thiol:disulfide interchange protein (DsbC), putative	2.83	3.57	4.73	3.02	5.73	5.33
HP0389	superoxide dismutase (SodB)	2.01	1.31	2.06	1.19	1.15	
HP0390	adhesin-thiol peroxidase (TagD)		1.25		1.14	1.30	1.21
HP0408*	hypothetical protein	2.25	2.85			4.13	4.24
HP0410*	putative neuraminyllactose-binding hemagglutinin homolog (HpaA)	5.04	4.74	5.50	3.94	3.20	3.21
HP0472*	outer membrane protein (Omp11)	4.48	5.19	5.09			
HP0473	molybdenum ABC transporter, periplasmic molybdate-binding protein (ModA)					4.69	4.76
HP0480	GTP-binding protein, fusA-homolog (YihK)				1.03		
HP0485*	catalase-like protein	3.34	2.71	4.31	2.59	3.90	4.19
HP0545*	cag pathogenicity island protein (Cag24)					3.09	
HP0604	uroporphyrinogen decarboxylase (HemE)	2.06		1.75			
HP0618	adenylate kinase (Adk)	2.07	1.76	2.04			1.74
HP0620	inorganic pyrophosphatase (Ppa)	1.72		1.53			
HP0630	modulator of drug activity (Mda66)	1.48	1.66	2.21	1.54	1.78	
HP0642*	NAD(P)H-flavin oxidoreductase	2.08	3.07	2.46	1.58		
HP0657*	processing protease (YmxG)	2.66	2.11	2.87	2.01	3.25	2.40
HP0671	outer membrane protein (Omp14)			3.75			
HP0686	iron(III) dicitrate transport protein (FecA)			3.03			

HP0709	conserved hypothetical protein					4.69	4.64
HP0710*	conserved hypothetical protein		6.29	7.35			5.16
HP0720	hypothetical protein	2.42	2.85				
HP0721*	hypothetical protein			2.77			2.63
HP0723*	L-asparaginase II (AnsB)		2.49	2.95		3.86	3.10
HP0735*	xanthine guanine phosphoribosyl transferase (Gpt)		2.27				
HP0736	phosphoserine aminotransferase (SerC)				2.66		
HP0783*	hypothetical protein			3.75	2.67	4.81	
HP0785*	conserved hypothetical secreted protein		5.42			3.99	
HP0797*	flagellar sheath adhesin (HpaA)		3.21	1.86			
HP0824	thioredoxin (TrxA)	1.13	1.21	1.16			1.25
HP0825	thioredoxin reductase (TrxB)	1.25	1.31		1.23		1.16
HP0827	ss-DNA binding protein 12RNP2 precursor				2.99		
HP0863	lipoprotein, putative			4.74			
HP0865	deoxyuridine 5'-triphosphate nucleotidohydrolase (Dut)			2.46			
HP0866	transcription elongation factor GreA (GreA)		1.71				
HP0871*	CDP-diglyceride hydrolase (Cdh)	3.38	3.36	4.41		4.92	5.68
HP0875*	catalase	1.22		1.59		1.56	
HP0884	hypothetical protein					4.81	2.47
HP0887*	vacuolating cytotoxin (VacA)		1.67	1.39		3.13	2.67
HP0896*	outer membrane protein (Omp19)			3.38			
HP0912	outer membrane protein (Omp20)		3.17	2.59			
HP0913	outer membrane protein (Omp21)			2.50			
HP0940*	amino acid ABC transporter, periplasmic binding protein (YckK)	5.76	3.36	4.74			
HP0953*	hypothetical protein	2.27	2.05	3.38		3.82	3.06
HP0966	conserved hypothetical protein	2.56					
HP0973*	hypothetical protein	2.23	3.29	2.77	2.47	5.21	4.65
HP0974*	phosphoglycerate mutase (Pgm)	2.23					
HP1012*	protease (PqqE)	2.26	1.87	2.69	2.66	2.44	2.38
HP1019*	serine protease (HtrA)	5.56	6.23	6.36	4.21	4.97	5.31
HP1037	conserved hypothetical protein		1.14	1.02	1.03		
HP1067	chemotaxis protein (CheY)			1.82		1.98	
HP1083	hypothetical protein			3.60			
HP1098*	conserved hypothetical secreted protein	2.97	2.45	3.58	3.18	4.81	4.28
HP1099	2-keto-3-deoxy-6-phosphogluconate aldolase (Eda)			1.85			
HP1117*	conserved hypothetical secreted protein						4.51
HP1118*	gamma-glutamyltranspeptidase (GGT)	2.72	3.13	3.61	2.90	3.91	4.05
HP1126*	colicin tolerance-like protein (TolB)			5.24		4.92	4.98
HP1161	flavodoxin (FldA)	1.00	1.14	1.10			
HP1164	thioredoxin reductase (TrxB)	1.88	1.70	2.06	1.72	1.28	1.52
HP1173*	hypothetical protein	5.04	4.86	7.35	2.50	6.71	6.56
HP1177	outer membrane protein (Omp27)		1.54	2.52			
HP1179	phosphopentomutase (DeoB)		2.21				2.47
HP1186*	carbonic anhydrase	2.56	2.47	4.23		5.84	3.52
HP1218	glycinamide ribonucleotide synthetase (PurD)	1.46	1.65				
HP1227*	cytochrome c553	1.82	2.79	2.58		3.19	3.69
HP1243*	outer membrane protein (Omp28)			2.77			
HP1285*	conserved hypothetical protein	2.84	2.30	4.13	2.97	4.67	4.17
HP1286*	conserved hypothetical secreted protein	1.85	1.66	2.75	2.00	2.70	3.05
HP1299*	methionine amino peptidase (Map)		3.36				
HP1376*	(3R)-hydroxymyristoyl-(acyl carrier protein) dehydratase (FabZ)					3.09	4.12
HP1395*	outer membrane protein (Omp30)		4.74	5.81			
HP1399	arginase (RocF)		1.49				
HP1441	peptidyl-prolyl cis-trans isomerase B, cyclosporin-type rotamase (Ppi)		1.82		1.79	2.04	
HP1454*	hypothetical protein	1.98	2.31	5.46	2.80	4.77	4.61
HP1455*	hypothetical protein	5.04					
HP1456*	membrane-associated lipoprotein (Lpp20)		2.56	2.31			
HP1458	thioredoxin	1.84	1.30	1.88	1.54	1.50	1.70
HP1461	cytochrome c551 peroxidase		2.36				
HP1469	outer membrane protein (Omp31)		3.07	3.51			
HP1477	hypothetical protein	4.48					
HP1494	UDP-MurNac-tripeptide synthetase (MurE)	3.57			2.18		3.10

HP1495	transaldolase (Tal)	2.23	1.90				
HP1501	outer membrane protein (Omp32)			4.01			
HP1512	iron-regulated outer membrane protein (FrpB)		1.90	3.30			
HP1526	exodeoxyribonuclease (LexA)	2.23	1.95				
HP1547	leucyl-tRNA synthetase (LeuS)				1.33		
HP1561*	iron(III) ABC transporter, periplasmic iron-binding protein (CeuE)	2.57	2.54	2.84	2.48	3.24	3.33
HP1562*	iron(III) ABC transporter, periplasmic iron-binding protein (CeuE)	2.72	2.73	3.42	2.51	3.23	3.08
HP1564*	outer membrane protein	2.14	2.00	2.50	2.28	2.90	3.09

[a]asterisks (*) represent proteins also shown to be selectively released in Snider et al. (33).

[b] *H. pylori* were grown under varying conditions (medium containing 0.5%, 1.0% or 1.25% NaCl for 24 or 48 h). The E_{sup} values shown (log_2) in the table are all >1 (consistent with selective release). Blank cells indicate conditions for which log_2 Esup values were <1 and/or results were not statistically significant.

Table 2. Proteins selectively released into the extracellular space under ≥5 culture conditions

Gene/Protein	Description	Enrichment of proteins in culture supernatant compared to the soluble bacterial fraction under the indicated culture conditions[a,b]				
		0.5 % NaCl	1.0% NaCl	1.25% NaCl	Average E_{sup}[c]	Predicted cleavage site[d]
HP0104*[e]	2',3'-cyclic-nucleotide 2'-phosphodiesterase (CpdB)	5.88	6.08	6.28	6.08	18-19
HP0129*	hypothetical protein	2.64	2.71	5.54	3.63	21-22
HP0175	cell binding factor 2; peptidyl prolyl cis,trans-isomerase	1.22	1.85	2.18	1.75	26-27
HP0176	fructose-bisphosphate aldolase (Tsr)	1.34	1.53	1.23	1.37	-
HP0211*	hypothetical secreted protein (HcpA)	2.74	4.99	3.64	3.79	25-26
HP0224	peptide methionine sulfoxide reductase (MsrA)	0.94	1.30	1.45	1.23	22-23
HP0231*	hypothetical protein; DsbK (thioloxidoreductase)	2.04	2.51	2.81	2.45	26-27
HP0235*	hypothetical secreted protein (HcpE)	3.57	4.61	3.83	4.00	24-25
HP0298*	dipeptide ABC transporter, periplasmic dipeptide-binding protein (DppA)	2.74	4.38	3.87	3.66	22-23
HP0304*	alginate lyase	5.10	3.86	5.12	4.69	19-20
HP0323*	membrane bound endonuclease (Nuc); NucT	2.96	2.95	3.65	3.19	16-17
HP0377*	thiol:disulfide interchange protein (DsbC), putative	2.92	4.65	5.03	4.20	24-25
HP0389	superoxide dismutase (SodB)	1.60	1.23	1.54	1.46	-
HP0410*	putative neuraminyllactose-binding hemagglutinin homolog (HpaA paralog)	4.49	3.97	4.36	4.27	24-25
HP0485*	catalase-like protein	2.97	3.31	4.25	3.51	24-25
HP0630	modulator of drug activity (Mda66)	1.51	1.72	1.67	1.63	-
HP0657*	processing protease (YmxG)	2.34	2.68	2.63	2.55	20-21
HP0871*	CDP-diglyceride hydrolase (Cdh)	3.81	4.14	5.05	4.33	21-22

HP0953*	hypothetical protein	1.98	2.93	3.22	2.71	20-21
HP0973*	hypothetical protein	2.35	4.25	3.71	3.44	28-29
HP1012*	protease (PqqE)	2.46	2.15	2.54	2.38	26-27
HP1019*	serine protease (HtrA)	4.89	5.60	5.84	5.44	-
HP1098*	hypothetical secreted protein (HcpC)	3.08	3.63	3.93	3.55	25-26
HP1118*	gamma-glutamyltranspeptidase (Ggt)	2.81	3.52	3.83	3.39	27-28
HP1164	thioredoxin reductase (TrxB); flavodoxin: quinone reductase (FqrB)	1.80	1.49	1.79	1.69	-
HP1173*	hypothetical protein	3.77	5.79	6.96	5.51	26-27
HP1186*	carbonic anhydrase	1.97	4.16	3.87	3.33	18-19
HP1227*	cytochrome c553	1.81	2.99	3.13	2.64	19-20
HP1285*	5'-nucleotidase, lipoprotein e(P4) family	2.90	3.48	4.15	3.51	-
HP1286*	polyisoprenoid-binding protein (YceI)	1.92	2.18	2.90	2.34	17-18
HP1454*	Lpp20 domain containing protein	2.39	3.54	5.03	3.65	19-20
HP1458	thioredoxin-2 (Trx 2)	1.69	1.40	1.79	1.63	-
HP1561*	iron(III) ABC transporter, periplasmic iron-binding protein (CeuE1)	2.52	2.89	3.09	2.83	31-32
HP1562*	iron(III) ABC transporter, periplasmic iron-binding protein (CeuE2)	2.62	2.98	3.25	2.95	29-30
HP1564*	putative outer membrane protein	2.21	2.45	2.79	2.48	-
Average[f]		**2.59**	**3.17**	**3.52**	**3.09**	

[a] E_{sup} values (log_2) were calculated and analyzed as described in Methods. The reported data represent the average of E_{sup} values (log_2) from broth cultures grown under the indicated conditions for 24 and 36 h. All proteins listed in the table were selectively released in at least 5 of the 6 conditions tested (see Table 1).

[b]Raw data with complete list of selectively released proteins (1 or more condition) are shown in Table 1.

[c]Average E_{sup} values (log_2) for each protein, based on analysis of 6 culture conditions.

[d]Predicted signal sequence cleavage site, based on use of SignalP 5.0 (172). Numbers represent positions of amino acids at the site of predicted cleavage. Dash (-) indicates that no signal sequence is predicted.

[e] Asterisks (*) represent proteins also selectively released in Snider et al. (33)

[f]Average E_{sup} value for allof the listed proteins.

Selectively released proteins exhibiting altered relative abundance in culture supernatant in response to high salt conditions

We next sought to identify the subset of selectively released proteins that differed in relative abundance when comparing supernatant fractions from cultures grown in medium containing 0.5% sodium chloride with supernatant fractions from cultures grown in medium containing higher levels of sodium chloride. As described in Methods, we calculated ratios of spectral counts (high salt vs normal salt) for the selectively released proteins listed in Table 1. Numerous OMPs and VacA (as well as multiple other proteins) were selectively released into the supernatant and were more abundant in one or both of the high salt conditions (1.0% and/or 1.25% NaCl) compared to routine salt conditions (Table 3). A smaller number of proteins were more abundant in supernatants from cultures grown in the normal salt condition (0.5% salt) compared to supernatants from cultures grown in the higher salt conditions (i.e. decreased abundance in high salt conditions) (Table 3). These experiments demonstrate that the proportional abundance of specific proteins in the extracellular space is altered during *H. pylori* growth under high salt conditions compared to growth under routine conditions.

Table 3. Selectively released proteins that exhibit altered abundance in supernatant in response to high salt conditions

Protein	Description	Fold change[a]		
		1.0% vs. 0.5%	1.25% vs. 0.5%	Predicted cleavage site[b]
Downregulated				
HP0089	Pfs; Mtn; MqnB	(0.75)	0.44	-
HP0966	P-loop NTPase and CrfC domain containing protein	(0.73)	0.24	-
HP1526	exodeoxyribonuclease (LexA)	(0.86)	0.41	-
Upregulated				
HP0097	hypothetical protein	2.05	2.55	15-16
HP0127	outer membrane protein (Omp4, HorB)	5.62	19.46	20-21
HP0130	hypothetical protein	(1.92)	2.35	17-18
HP0227	outer membrane protein (Omp5, HopM)	21.78	23.57	18-19
HP0229	outer membrane protein (Omp6, HopA)	9.40	14.53	16-17
HP0252	outer membrane protein (Omp7, HopF)	10.24	27.37	23-24
HP0317	outer membrane protein (Omp9, HopU)	3.10	6.29	20-21
HP0472	outer membrane protein (Omp11, HorE)	(1.62)	2.19	18-19
HP0671	outer membrane protein (Omp14, HorF)	7.93	27.37	23-24
HP0686	iron(III) dicitrate transport protein (FecA1)	12.55	27.37	17-18
HP0709	S-adenosylmethionine hydrolase	3.48	3.09	21-22
HP0710	putative outer membrane protein	6.53	16.45	16-17
HP0797	flagellar sheath adhesin (HpaA)	6.14	13.20	27-28
HP0863	lipoprotein, putative; plasminogen-binding protein (PgbB)	5.62	19.46	17-18
HP0884	hypothetical protein	2.15	2.95	-
HP0887	vacuolating cytotoxin (VacA)	8.77	10.58	33-34
HP0896	outer membrane protein (Omp19, BabB)	(1.25)	5.52	19-20
HP0912	outer membrane protein (Omp20, HopC, AlpA)	5.85	11.74	21-22
HP0913	outer membrane protein (Omp21, HopB, AlpB)	2.52	6.52	41-42
HP1083	putative outer membrane protein	4.19	7.42	26-27
HP1117	hypothetical secreted protein (HcpX)	(1.43)	3.17	23-24
HP1126	colicin tolerance-like protein (TolB)	2.10	2.70	16-17
HP1177	outer membrane protein (Omp27, HopQ)	2.96	7.24	21-22
HP1243	outer membrane protein (Omp28, BabA)	17.16	74.74	20-21
HP1376	(3R)-hydroxymyristoyl-(acyl carrier protein) dehydratase (FabZ)	(1.14)	2.26	-
HP1395	outer membrane protein (Omp30, HorL)	(1.74)	4.61	21-22
HP1456	membrane-associated lipoprotein (Lpp20)	2.16	3.63	21-22
HP1461	cytochrome c551 peroxidase	7.38	2.92	18-19
HP1469	outer membrane protein (Omp31, HorJ)	2.43	3.90	17-18

HP1501	outer membrane protein (Omp32, HorK)	4.19	19.13	-
HP1512	iron-regulated outer membrane protein (FrpB)	3.51	10.25	21-22

[a] To identify selectively released proteins that differed in proportional abundance in the culture supernatant in response to salt concentration, we analyzed proteomic data for the proteins listed in Table 1. The fold change in response to high salt conditions was calculated as a ratio (total spectral counts from 24 h and 36 h time points in 1.0% or 1.25% high salt conditions compared to total spectral counts in the 0.5% condition). The analysis was restricted to proteins with ≥10 total assigned spectral counts in either the 0.5% NaCl condition or high salt conditions. Proteins with fold change values >2 or <2 were considered salt-responsive. The proteins listed met these criteria in at least one of the two high salt conditions. Values in parentheses did not have fold values > 2 for that condition or did not meet the criteria for ≥10 total assigned spectral counts.
[b]Predicted signal sequence cleavage site, based on use of SignalP 5.0 (172). Numbers represent positions of amino acids at the site of predicted cleavage. Dash (-) indicates that no signal sequence is predicted.

Release of VacA toxin in response to high salt conditions

As described above, the relative abundance of VacA in culture supernatant was higher in cultures containing elevated sodium chloride concentrations than in supernatant from cultures containing 0.5% salt. Western blot analysis of samples from 3 independent cultures using a polyclonal antibody to the 88 kDa secreted VacA protein confirmed that VacA levels in the culture supernatant were increased in cultures containing high salt concentrations, compared to cultures containing 0.5% salt (Figure 2A).

We also analyzed whether VacA levels in the culture supernatant were increased after exposure of the bacteria to high salt conditions for a relatively short time period (1 h). *H. pylori* was grown overnight and subcultured at OD_{600} ~0.3 into either the standard medium (0.5% NaCl) or medium containing 1.25% NaCl. As shown in Figure 2B, higher levels of VacA were detected in *H. pylori* supernatants from cultures containing 1.25% NaCl than in supernatants from cultures containing 0.5% NaCl. Therefore, the Western blotting data corroborate the results obtained by analysis of mass spectrometry data, and provide further evidence indicating that the levels of VacA in the extracellular space are increased in response to high salt conditions.

Under routine culture conditions, the 88 kDa VacA toxin and a small VacA peptide are released into the extracellular space, and the carboxy-terminal VacA β-barrel domain remains associated with the bacteria (31, 36). To determine whether *H. pylori* exposure to high salt conditions altered this pattern of release, we analyzed proteomic data for samples containing elevated salt concentrations and mapped the location of detected VacA peptides relative to the full-length VacA amino acid sequence

(Figure 3A). Nearly all of the VacA peptides detected in the supernatant mapped to the secreted 88 kDa toxin. VacA peptides corresponding to the predicted C-terminal β-barrel domain of VacA were not detected in the culture supernatant, similar to what has been observed previously when analyzing VacA secretion in medium containing 0.5% salt (33). For comparison, we analyzed the distribution of peptides assigned to two salt-responsive OMPs [(HP0710 (HomA), HP1177 (HopQ), Table 3)]. We detected peptides in the supernatant that were mapped throughout the entire length of the HopQ and HomA outer membrane proteins, including the predicted C-terminal β-barrel domains (Figure 3B and C) (173).

Effect of high-salt conditions on *vacA* transcription

To further investigate the mechanisms by which high salt conditions led to increased levels of VacA in the extracellular space, we performed real-time reverse transcription (RT)-PCR analysis. We compared *vacA* transcription in *H. pylori* cultured for one hour in medium containing 0.5% NaCl compared to medium containing 1.25% NaCl, as described in Methods. RT-qPCR analysis confirmed that *vacA* transcript levels were significantly upregulated in a high salt environment, compared to transcription of control genes (*gyrB* and *atpA*) ($p<0.05$, 1-way ANOVA) (Figure 2C).

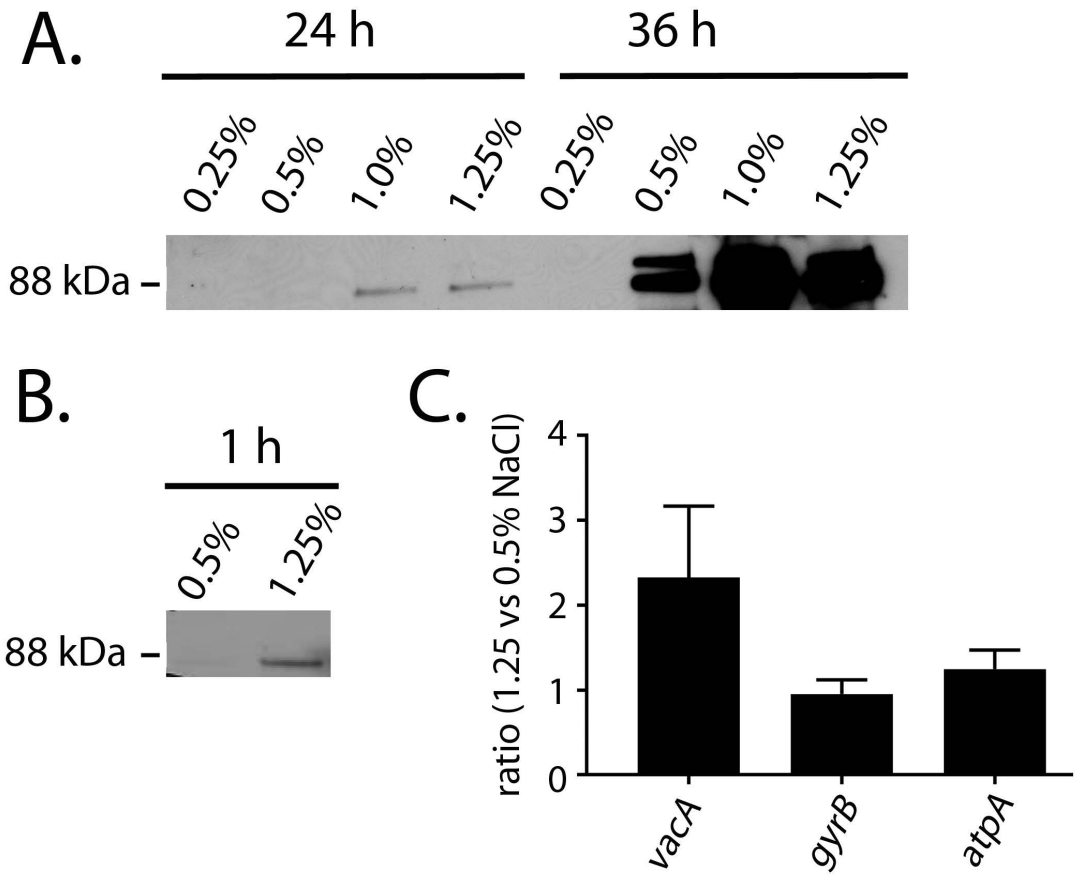

Figure 2. VacA protein and transcript levels are increased in response to high salt concentration. *H. pylori* was cultured in Brucella broth filtrate supplemented with cholesterol and containing the indicated concentrations of NaCl (0.25%, 0.5%, 1.0% and 1.25%). (A) Western blot analysis of VacA in culture supernatant samples from 24 and 36 h time points (standardized at 40 µg protein per sample). (B) Cultures were inoculated at an OD_{600} of about 0.3, and samples from a 1 h time point (100 µg protein per sample) were analyzed by Western blotting. The results are representative of analyses of three independent sets of cultures. (C) *H. pylori* was cultured for 1 h in Brucella broth-cholesterol containing 0.5% NaCl or 1.25% NaCl. Transcript abundance was analyzed by RT-qPCR. Normalized transcripts signals from bacteria grown in 1.25% NaCl were compared to those from bacteria grown in 0.5% NaCl. RNA was isolated from four independent experiments. The mean and standard error of the mean are shown. A significant difference ($P < 0.05$, 1-way ANOVA) was observed when comparing the effect of high salt on *vacA* transcript levels, compared to effects on control genes (*gyrB* and *atpA*).

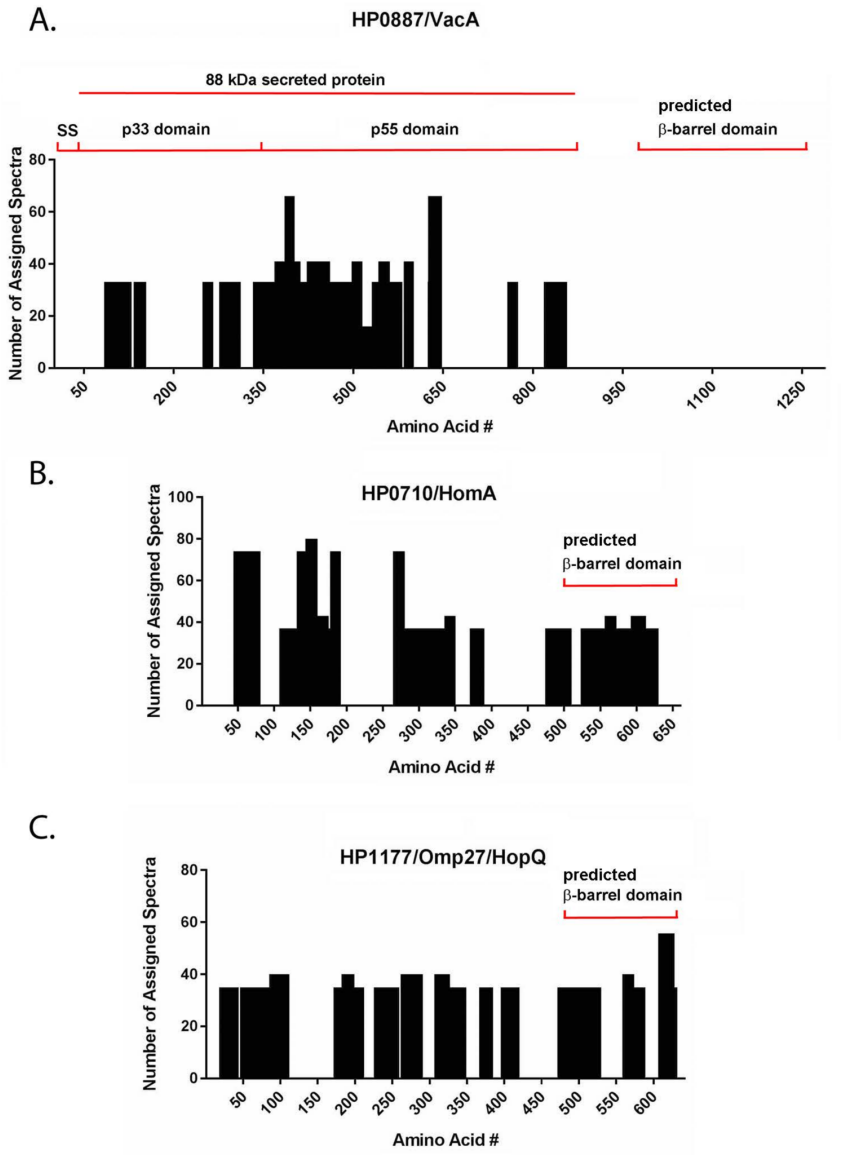

Figure 3. Analysis of VacA and Omp peptide distribution. *H. pylori* was grown in high salt conditions (1.25% NaCl for 24 h), and broth culture supernatants were processed as described in Methods. Spectral counts for peptides assigned exclusively to VacA, HomA, or HopQ were analyzed. The x -axis corresponds to the amino acid position for each protein and the y-axis indicates the number of assigned spectra. Regions of VacA corresponding to a signal sequence (SS), p33 domain, p55 domain, and C-terminal β-barrel domain are shown. The C-terminal portions of HomA and HopQ are predicted to have a β-barrel architecture, based on use of the program BOCTOPUS, a transmembrane β-barrel topology prediction tool (http://boctopus.bioinfo.se/)(173).

Differential expression of H. pylori genes in response to high salt

To investigate the effects of high salt concentrations on *H. pylori* gene transcription, we used RNA-seq analysis to compare the transcriptomes of bacteria cultured for 1 h in medium containing 0.5% or 1.25% NaCl. Based on the criteria described in the Methods, 173 genes were differentially expressed in response to varying salt concentration (127 downregulated and 46 upregulated in response to high salt conditions) (Table 4). In many cases, we detected differential expression of multiple genes that are predicted to be transcribed within the same operons. Based on the predicted *H. pylori* operon structure reported by Sharma et al. (174), we identified 27 operons that were downregulated and 5 operons that were upregulated in response to high salt conditions (Figure 4). Sixteen of the 124 selectively released proteins shown in Table 1 were salt-responsive, based on RNA-seq analyses (Table 5).

We hypothesized that many of the genes encoding salt-responsive proteins identified in the proteomic analysis might be differentially transcribed in response to variations in salt concentration. To test this hypothesis, we compared the list of salt-responsive proteins identified in the proteomic analysis (Table 3) with the list of salt-responsive genes identified in the RNA-seq analysis. Overall, there was relatively little concordance in the set of salt-responsive proteins or genes identified by these two approaches. Transcription of HP0089 was downregulated in response to high salt concentrations, and the corresponding protein exhibited decreased abundance in culture supernatants in response to high salt conditions. Upregulated transcription of *vacA* (HP0887) in response to high salt concentrations was consistent with elevated levels of these proteins detected in culture supernatant under high salt conditions.

Upregulated transcription of *vacA* (HP0887) in response to high salt concentrations was also consistent with the results of RT-qPCR experiments (Figure 2).

Table 4. Genes that are differentially expressed in response to high salt conditions

Genes downregulated in high salt	Description	fold (1.25% vs 0.5%)[a]
HP0002	riboflavin synthase beta chain (*ribE*)	0.45
HP0003	3-deoxy-d-manno-octulosonic acid 8-phosphate synthetase (*kdsA*)	0.61
HP0034	aspartate 1-decarboxylase (*panD*)	0.53
HP0035	hypothetical	0.54
HP0089	pfs protein (*pfs*)	0.50
HP0102	hypothetical protein	0.60
HP0103	methyl-accepting chemotaxis protein (*tlpB*)	0.58
HP0109	chaperone and heat shock protein 70 (*dnaK*)	0.53
HP0110	co-chaperone and heat shock protein (*grpE*)	0.54
HP0144	cytochrome c oxidase (*fixN*)	0.45
HP0145	cytochrome c oxidase (*fixO*)	0.60
HP0153	recombinase (*recA*)	0.41
HP0154	enolase (*eno*)	0.47
HP0160	hypothetical secreted protein	0.33
HP0193	fumarate reductase, cytochrome b subunit (*frdC*)	0.47
HP0195	enoyl-(acyl-carrier-protein) reductase (NADH) (*fabI*)	0.53
HP0196	UDP-3-0-(3-hydroxymyristoyl) glucosamine N-acyltransferase (*lpxD*)	0.48
HP0197	S-adenosylmethionine synthetase 2 (*metX*)	0.55
HP0198	nucleoside diphosphate kinase (*ndk*)	0.52
HP0201	fatty acid/phospholipid synthesis protein (*plsX*)	0.55
HP0202	beta-ketoacyl-acyl carrier protein synthase III (*fabH*)	0.52
HP0204	hypothetical protein	0.54
HP0215	CDP-diglyceride synthetase (*cdsA*)	0.48
HP0220	synthesis of [Fe-S] cluster (*nifS*)	0.60
HP0221	nifU-like protein	0.47
HP0259	exonuclease VII, large subunit (*xseA*)	0.56
HP0285	hypothetical protein	0.58
HP0294	aliphatic amidase (*amiE*)	0.58
HP0335	hypothetical protein	0.53
HP0336	hypothetical protein	0.59
HP0341	hypothetical protein	0.28
HP0423	hypothetical protein	0.58
HP0509	glycolate oxidase subunit (*glcD*)	0.58
HP0514	ribosomal protein L9 (*rpl9*)	0.60
HP0515	heat shock protein (*hslV*)	0.38
HP0559	acyl carrier protein (*acpP*)	0.51
HP0560	hypothetical protein	0.40
HP0561	3-ketoacyl-acyl carrier protein reductase (*fabG*)	0.57
HP0594	hypothetical protein	0.49
HP0603	hypothetical protein	0.53
HP0617	aspartyl-tRNA synthetase (*aspS*)	0.53
HP0618	adenylate kinase (*adk*)	0.46
HP0626	tetrahydrodipicolinate N-succinyltransferase (*dapD*)	0.61
HP0627	hypothetical protein	0.44
HP0628	hypothetical protein	0.44
HP0630	modulator of drug activity (*mda66*)	0.57
HP0663	chorismate synthase (*aroC*)	0.33
HP0677	conserved hypothetical integral membrane protein	0.57
HP0681	hypothetical protein	0.27
HP0682	hypothetical protein	0.24
HP0683	UDP-N-acetylglucosamine pyrophosphorylase (*glmU*)	0.61

HP0691	3-oxoadipate coA-transferase subunit A (*yxjD*)	0.60
HP0692	3-oxoadipate coA-transferase subunit B (*yxjE*)	0.48
HP0716	conserved hypothetical protein	0.61
HP0755	molybdopterin biosynthesis protein (*moeB*)	0.54
HP0756	hypothetical protein	0.47
HP0757	beta-alanine synthetase homolog	0.52
HP0773	hypothetical protein	0.55
HP0777	uridine 5'-monophosphate (UMP) kinase (*pyrH*)	0.47
HP0794	ATP-dependent clp protease proteolytic component (*clpP*)	0.62
HP0801	molybdopterin converting factor, subunit 1 (*moaD*)	0.56
HP0802	GTP cyclohydrolase II (*ribA*)	0.60
HP0812	hypothetical protein	0.51
HP0829	inosine-5'-monophosphate dehydrogenase (*guaB*)	0.52
HP0845	thiamin phosphate pyrophosphorylase kinase (*thiM*)	0.57
HP0865	deoxyuridine 5'-triphosphate nucleotidohydrolase (*dut*)	0.60
HP0883	Holliday junction DNA helicase (*ruvA*)	0.52
HP0889	iron(III) dicitrate ABC transporter (*fecD*)	0.58
HP0916	iron-regulated outer membrane protein (*frpB*)	0.52
HP0924	4-oxalocrotonate tautomerase (*dmpI*)	0.61
HP0970	nickel-cobalt-cadmium resistance protein (*nccB*)	0.54
HP1031	flagellar motor switch protein (*fliM*)	0.54
HP1034	ATP-binding protein (*ylxH*)	0.50
HP1055	hypothetical protein	0.55
HP1097	hypothetical protein	0.30
HP1098	hypothetical secreted protein	0.35
HP1099	2-keto-3-deoxy-6-phosphogluconate aldolase (*eda*)	0.58
HP1108	pyruvate ferredoxin oxidoreductase, gamma subunit	0.52
HP1117	conserved hypothetical secreted protein	0.54
HP1118	gamma-glutamyltranspeptidase (*ggt*)	0.49
HP1140	biotin acetyl coenzyme A carboxylase synthetase (*birA*)	0.53
HP1143	hypothetical protein	0.56
HP1150	hypothetical protein	0.56
HP1151	ribosomal protein S16 (*rpS16*)	0.59
HP1163	hypothetical protein	0.58
HP1204	ribosomal protein L33 (*rpL33*)	0.59
HP1212	ATP synthase F0, subunit c (*atpE*)	0.47
HP1241	alanyl-tRNA synthetase (*alaS*)	0.59
HP1288	hypothetical protein	0.40
HP1298	translation initiation factor EF-1 (*infA*)	0.57
HP1299	methionine amino peptidase (*map*)	0.54
HP1300	preprotein translocase subunit (*secY*)	0.52
HP1301	ribosomal protein L15 (*rpl15*)	0.55
HP1302	ribosomal protein S5 (*rps5*)	0.44
HP1303	ribosomal protein L18 (*rpl18*)	0.37
HP1304	ribosomal protein L6 (*rpl6*)	0.51
HP1305	ribosomal protein S8 (*rps8*)	0.54
HP1306	ribosomal protein S14 (*rpS14*)	0.37
HP1307	ribosomal protein L5 (*rpl5*)	0.61
HP1308	ribosomal protein L24 (*rpl24*)	0.54
HP1309	ribosomal protein L14 (*rpl14*)	0.58
HP1310	ribosomal protein S17 (*rps17*)	0.55
HP1311	ribosomal protein L29 (*rpL29*)	0.44
HP1312	ribosomal protein L16 (*rpl16*)	0.50
HP1313	ribosomal protein S3 (*rps3*)	0.58
HP1314	ribosomal protein L22 (*rpl22*)	0.48
HP1315	ribosomal protein S19 (*rps19*)	0.51

HP1316	ribosomal protein L2 (*rpl2*)	0.60
HP1317	ribosomal protein L23 (rpl23)	0.59
HP1318	ribosomal protein L4 (*rpl4*)	0.43
HP1319	ribosomal protein L3 (*rpl3*)	0.58
HP1358	hypothetical protein	0.62
HP1373	rod shape-determining protein (*mreB*)	0.56
HP1400	iron(III) dicitrate transport protein (*fecA*)	0.31
HP1406	biotin synthetase (*bioB*)	0.48
HP1412	hypothetical protein	0.58
HP1458	thioredoxin	0.43
HP1464	conserved hypothetical secreted protein	0.55
HP1465	ABC transporter, ATP-binding protein (HI1087)	0.51
HP1466	conserved hypothetical integral membrane protein	0.58
HP1469	outer membrane protein (*omp31*)	0.59
HP1485	proline dipeptidase (*pepQ*)	0.51
HP1497	peptidyl-tRNA hydrolase (*pth*)	0.59
HP1530	purine nucleoside phosphorylase (*punB*)	0.58
HP1531	hypothetical protein	0.23
HP1542	hypothetical protein	0.38
HP1550	protein-export membrane protein (*secD*)	0.45
HP1587	conserved hypothetical protein	0.61
Genes upregulated in high salt		
HP0007	hypothetical protein	1.91
HP0017	virB4 homolog (*virB4*)	1.75
HP0131	hypothetical protein	1.87
HP0140	L-lactate permease (*lctP*)	2.18
HP0225	hypothetical protein	1.71
HP0243	*napA*	1.74
HP0261	hypothetical protein	1.96
HP0316	hypothetical protein	1.70
HP0350	hypothetical protein	1.65
HP0376	ferrochelatase (*hemH*)	1.61
HP0400	penicillin tolerance protein (*lytB*)	1.63
HP0440	DNA topoisomerase I (*topA*)	1.81
HP0441	VirB4 homolog	2.04
HP0444	hypothetical protein	1.68
HP0448	hypothetical protein	1.62
HP0460	hypothetical protein	2.72
HP0461	hypothetical protein	2.30
HP0488	hypothetical protein	1.62
HP0536	cag pathogenicity island protein (*cag15*)	2.11
HP0612	hypothetical protein	1.77
HP0670	hypothetical protein	1.68
HP0689	hypothetical protein	1.70
HP0694	hypothetical protein	1.76
HP0724	anaerobic C4-dicarboxylate transport protein (*dcuA*)	1.64
HP0784	hypothetical protein	1.95
HP0846	type I restriction enzyme R protein (*hsdR*)	1.76
HP0854	GMP reductase (*guaC*)	1.76
HP0855	alginate O-acetylation protein (*algI*)	1.64
HP0871	CDP-diglyceride hydrolase (*cdh*)	2.77
HP0887	vacuolating cytotoxin (*vacA*)	1.81
HP0895	hypothetical protein	1.64
HP0939	amino acid ABC transporter, permease protein (*yckJ*)	1.90
HP0943	D-amino acid dehydrogenase (*dadA*)	1.64

HP0991	hypothetical protein	1.80
HP1024	co-chaperone-curved DNA binding protein A (*cbpA*)	2.15
HP1025	heat shock regulator (*hspR*)	2.26
HP1026	hypothetical helicase-like protein	2.42
HP1186	carbonic anhydrase (*cah*)	1.85
HP1193	aldo-keto reductase	2.58
HP1239	hypothetical protein	1.89
HP1290	nicotinamide mononucleotide transporter (*pnuC*)	1.70
HP1322	hypothetical protein	1.69
HP1327	hypothetical protein	1.64
HP1351	hypothetical protein	1.92
HP1352	adenine specific DNA methyltransferase (*hpyAIVM*)	1.84
HP1563	alkyl hydroperoxide reductase (*tsaA*)	1.63

[a] *H. pylori* were grown in Brucella broth containing either 0.5% or 1.25% NaCl. RNA-seq was performed as described in the methods. The fold change in transcript levels in response to high salt conditions was then calculated as a ratio (number of RNA-seq reads from cultures containing 1.25% NaCl compared to number of reads from cultures containing 0.5% NaCl).

Operon structure	Function
	predicted (HP0444), DNA transfer (HP0441), DNA replication (HP0440)
	guanonsine monophosphate reductase (HP0854), lipopolysaccharide synthesis (HP0855)
	amino acid dehydrogenase (HP0943); amino acid transporter (HP0939)
	chaperone (HP1024), heat shock regulator (HP1025), predicted (HP1026)
	DNA methylase (HP1352), restriction endonuclease (HP1351)
	lipopolysaacharide synthesis (HP0003), riboflavin synthesis (HP0002)
	panthothenic acid synthesis (HP0034), redicted (HP0035)
	chemotaxis (tlpB, HP0103), glycosyl transferase (HP0102)
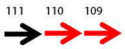	heat shock chaperone (HP0109, HP0110)
	cytochrome C oxidase (HP0144, HP0145)
	DNA recombinase (recA, HP0153), enolase (HP0154)
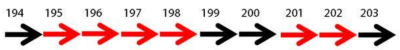	acyl carrier protein reductase (HP0195), lipid A synthesis (lpxD, HP0196), S-adenosine methione synthetase (metK, HP0197), nucleoside diphosphate kinase (HP0198), phospholipid synthesis protein (plsX, HP0201) acyl carrier protein synthase (fabH, HP0202)
	Fe-S cluster assembly (HP0220, HP0221)
	predicted (HP0284, HP0285)
	cysteine rich protein (HP0335, HP0336)
	ribosome protein (rpl9, HP0514), heat shock protease (hslV, HP0515)
	acyl carrier protein reductase (FabH, HP0561), acyl carrier protein (acpP, HP0559)
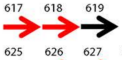	tRNA synthetase (aspS, HP0617), adenylate kinase (adk, HP0618)
	diaminopimelate/lysine synthesis (HP0626), cysteine rich protein (HP0627, HP0628)
	predicted (HP0681, HP0682)
	succinyl coA synthetase (HP0691, HP0692)
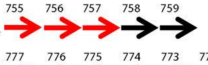	predicted (HP0755, HP0756, HP0755)
	uridine monophosphate kinase (HP0777), predicted (HP0773)
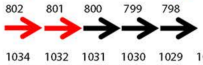	riboflavin synthesis (ribA, HP0802), molybdopterin biosynthetic pathway (HP0801)
	ATP binding protein (HP1034), flagellar motor switch (FliM, HP1031)
	phosphogluconate aldolase (HP1099), cysteine rich protein (HP1098), predicted (HP1097),
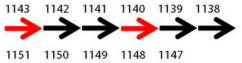	predicted (HP1143), acetyl coA carboxylase synthetase (HP1140)
	ribosomal protein (rps16, HP1151), predicted (HP1150)
	ribosomal proteins (HP1319 to HP1298)
	ABC transport system (HP1466, HP1465, HP1464)
	nucleoside phosphorylase (punB, HP1530), predicted (HP1531)
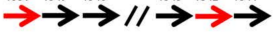	protein export (secD, HP1550), predicted (HP1542)

Figure 4. Operons regulated in response to salt. Multiple salt-responsive genes identified using RNA-seq were mapped to the same operons. Fifteen genes upregulated in response to high salt conditions were mapped to 5 operons (green arrows), and 68 downregulated genes were mapped to 27 operons (red arrows). Black arrows indicate genes for which transcription was unchanged. Gene numbers and protein functions are listed.

Table 5. Selectively released proteins encoded by genes that were salt responsive in RNA-seq experiments

Gene/Protein	Description	Fold change[a] (1.25% vs 0.5%)
HP0003	3-deoxy-d-manno-octulosonic acid 8-phosphate synthetase (KdsA)	0.61
HP0089	Pfs; Mtn; MqnB	0.50
HP0204	hypothetical protein	0.54
HP0618	adenylate kinase (Adk)	0.46
HP0630	modulator of drug activity (Mda66)	0.57
HP0865	deoxyuridine 5'-triphosphate nucleotidohydrolase (Dut)	0.60
HP0871	CDP-diglyceride hydrolase (Cdh)	2.77
HP0887	vacuolating cytotoxin (VacA)	1.81
HP1098	hypothetical secreted protein (HcpC)	0.35
HP1099	2-keto-3-deoxy-6-phosphogluconate aldolase (Eda)	0.58
HP1117	hypothetical secreted protein (HcpX)	0.54
HP1118	gamma-glutamyltranspeptidase (Ggt)	0.49
HP1186	carbonic anhydrase	1.85
HP1299	methionine amino peptidase (Map)	0.54
HP1458	thioredoxin-2 (Trx2)	0.43
HP1469	outer membrane protein (Omp31, HorJ)	0.59

[a]*H. pylori* was grown in Brucella broth containing either 0.5% or 1.25% NaCl. RNA-seq was performed as described in the methods. The fold change in transcript levels in response to high salt conditions was then calculated as a ratio (number of RNA-seq reads from cultures containing 1.25% NaCl compared to reads from cultures containing 0.5% NaCl).

Discussion

Consumption of a high salt diet is an important risk factor for development of gastric adenocarcinoma (12-14, 140, 142). In response to high salt conditions in vitro, *H. pylori* undergoes alterations in gene transcription and altered production of multiple proteins (15, 16, 25, 144). These changes potentially influence gastric cancer risk. In this manuscript, we tested the hypothesis that growth of *H. pylori* in a high salt environment alters the composition of the exoproteome. We also used RNA-seq methods to analyze the effects of high salt concentrations on the *H. pylori* transcriptome and compared the transcriptomic results with proteomic results.

Previous studies identified *H. pylori* proteins that are selectively released into the culture supernatant under routine culture conditions (33, 35, 147, 148), and the current experiments showed that the most of these proteins are also selectively released under high salt conditions. Many of these proteins are predicted to have signal sequences that facilitate translocation of the proteins across the inner membrane (33), but the mechanism underlying selective release across the outer membrane is unknown.

One of the key findings in the current study was the detection of higher levels of the VacA toxin in culture supernatants of cultures containing high salt concentrations, compared to supernatants from cultures grown in conventional culture medium. RNA-seq and RT-qPCR experiments showed that *vacA* transcription was increased in response to high salt concentrations. Therefore, we presume that the increased levels of VacA in culture supernatant in response to high salt conditions are attributable, at least in part, to increased *vacA* transcription. Notably, the magnitude of change in *vacA* transcription detected by RNA-seq or quantitative RT-qPCR experiments was

substantially less than the magnitude of change in VacA levels detected in proteomic analyses or Western blotting experiments. A previous proteomic analysis showed that levels of VacA protein detected in the membrane fraction of *H. pylori* grown in high salt conditions were reduced, in comparison to VacA levels in corresponding fractions from bacteria grown in low-salt conditions (18). Therefore, it seems likely that high salt conditions not only upregulate *vacA* transcription, but also may have other effects such as promoting VacA release from the outer membrane into the extracellular space.

Several previous studies analyzed effects of high salt concentrations on VacA transcription or production. One study detected increased *vacA* transcription after exposure of *H. pylori* to high salt conditions for 15 to 60 minutes, using an RNAse protection assay (175), and another study detected increased *vacA* transcription in response to high salt conditions for 1 h, using RT-qPCR methods (34). In contrast, other studies did not detect alterations in *vacA* transcription in bacteria exposed to high salt conditions for longer time periods (25, 144). The current study confirms that *vacA* transcription increases in response to high salt conditions for 1 h.

Consistent with results of previous studies (33), we detected multiple OMPs in the culture supernatant. We detected increased abundance of outer membrane proteins in the culture supernatants of cultures containing high salt concentrations, compared to supernatants of cultures grown in conventional culture medium. Hop outer membrane proteins have multiple features in common with autotransporter proteins (176), and therefore, we hypothesized that portions of Hop outer membrane proteins corresponding to passenger domains might be translocated across the outer membrane and released into the extracellular space. Instead, we detected all portions of the outer

membrane proteins selected for analysis (including the predicted C-terminal beta-barrel domains) in the culture supernatant. Although the methodology for the current study included the use of ultracentrifugation to remove outer membrane vesicles from culture supernatant, we speculate that the outer membrane proteins detected in the culture supernatant might be components of small vesicles or membrane fragments that were not completely removed by ultracentrifugation. A recent study reported that *H. pylori* outer membrane vesicles exhibit varying properties at different stages of the growth cycle (177), which provides a possible explanation for the detection of outer membrane proteins in the culture supernatant mainly at the 24 hour time point compared to later time points.

RNA-seq studies showed that growth of *H. pylori* in high salt conditions leads to altered transcription of numerous *H. pylori* genes, including genes encoding proteins that are selectively released into the culture supernatant. In agreement with the results of a previous RNA-seq analysis (25), the magnitude of salt-induced changes in transcription observed in the current study were relatively small. Differences in the set of salt-responsive genes identified in the current study compared to a previous study (25) are presumably attributable to differences in the time points selected for analysis, as well as the use of a different *H. pylori* strain in the previous study. The mechanisms by which high salt conditions alter *H. pylori* gene transcription are not yet understood.

We hypothesized that differences in the relative abundance of proteins in culture supernatants of cultures grown in high salt conditions compared to routine conditions might result from effects of high salt conditions on *H. pylori* gene transcription. However, there was relatively little overlap in the list of salt-responsive genes identified

by RNA-seq compared to the list of salt-responsive proteins identified in proteomic studies. The limited concordance may be partly attributable to differences in the time points at which the proteomic and transcriptomic analyses were performed. In addition, it seems likely that the effect of high salt conditions on composition of the exoproteome is not dependent solely on transcriptional changes, but also may reflect the capacity of high salt conditions to stimulate release of proteins from the outer membrane into the extracellular space.

In summary, these data indicate that *H. pylori* exposure to high environmental salt concentrations results in alterations of the exoproteome. When taken together with several previous papers showing effects of salt concentrations on *H. pylori* cellular proteins and *H. pylori* gene transcription (15, 18, 25, 144), the data indicate that many properties of the bacteria are altered in response to changes in environmental salt concentration. We propose that these salt-induced changes contribute to the increased risk of gastric cancer observed in *H. pylori*-infected individuals who consume a high salt diet.

Chapter 3

FUNCTIONAL PROPERTIES OF *Helicobacter pylori* VACA TOXIN m1 AND m2 VARIANTS

Introduction

Helicobacter pylori is highly adapted for colonization of the human stomach, and persistent colonization with these bacteria is a risk factor for development of gastric cancer and peptic ulcer disease (7, 178). *H. pylori* secretes several proteins that contribute to the pathogenesis of these diseases. One such protein, VacA toxin, is secreted through a type V (autotransporter) secretion pathway and released into the extracellular space as a soluble protein (132, 133, 145, 179-185). CagA, an oncogenic effector protein, is secreted and translocated into gastric cells by a type IV secretion system (19-22, 186). Numerous other proteins are released into the extracellular space, either by bacterial autolysis or through more selective processes that remain poorly understood (33, 35, 147, 148, 156).

The *vacA* gene encodes a 140 kDa protein, which undergoes proteolytic cleavage of an amino terminal signal sequence and a C-terminal β-barrel domain to yield a secreted 88 kDa protein (27, 30, 31). The secreted 88 kDa VacA protein is comprised of an N-terminal p33 domain and a C-terminal p55 domain (31, 187). Although *vacA* is present in all *H. pylori* strains, there is a high level of sequence diversity among *vacA* alleles. The three main regions of sequence diversity have been designated: a 5' region encoding the signal sequence and the amino-terminus of the 88

kDa protein (s-region), intermediate region (i-region), and mid-region (m-region) (9, 103, 134) (Figure 1). Multiple combinations of these regions (for example, s1i1m1, s1i1m2, s2i2m2) can arise through natural transformation and homologous recombination. Sequence variation in the s-region is the main determinant of VacA activity (105, 106, 134), but sequence variation in other regions also influences toxin activity (103, 113, 188). Epidemiological studies have shown that *H. pylori* strains containing specific *vacA* allelic types (for example, s1i1m1) are associated with an increased risk of gastric cancer and peptic ulcer disease, compared to strains that contain other *vacA* allelic types (e.g., s2i2m2) (9, 103, 115, 134, 189-191).

Two main families of *vacA* alleles, m1 and m2, are recognized based on diversity in the region encoding the p55 domain (100, 134). Both m1 and m2 *vacA* allelic types are common throughout the world, and subfamilies of m1 or m2 *vacA* alleles are present in specific geographic regions (107). A prototypical m1 VacA protein and a prototypical m2 VacA protein exhibit 55% amino acid sequence diversity within a ~281 amino acid segment of the p55 domain (100). The exact boundaries of the VacA m-region have not been defined. Phylogenetic analysis indicates that there is a relatively strong selective pressure for preservation of m1 and m2 *vacA* alleles, such that chimeric alleles arising through recombination (containing both m1 and m2 elements) are uncommon (100). Based on this observation, it has been proposed that m1 and m2 forms of VacA have distinct activities that each confer a selective advantage compared to m1-m2 chimeric forms of the protein (100).

Crystallographic and electron microscopic analyses indicate that VacA has a predominantly β-helical structure throughout both the p55 and p33 domains (48, 49, 55,

56). Thus far, structural analyses have only been undertaken for s1i1m1 forms of VacA, but other forms presumably have a similar overall β-helical structure. When comparing m1 and m2 forms of VacA, the sites of amino acid polymorphisms are predicted to be clustered and surface-exposed (55, 100).

Most studies of VacA activity have analyzed s1i1m1 forms of the toxin. Type s1i1m1 VacA can cause a wide range of cellular alterations in cultured epithelial cells, including stimulating intracellular vacuole formation, membrane depolarization, mitochondrial alterations, altering cell signaling, autophagy, disruption of cell-cell junctions, and potentially cell death (178, 179, 181, 183, 191, 192). VacA also can cause alterations in immune cells, including inhibition of the activation and proliferation of human T-cells and B-cells and altered signal transduction in macrophages (179, 180, 184, 193, 194). Most of the reported VacA-induced cellular alterations are attributed to its capacity to form membrane channels in host cells, and therefore, VacA is classified as a pore-forming toxin (195-197).

Previous studies of m2 VacA protein have used mostly non-gastric cell lines (such as HeLa or RK-13 cells), which are of uncertain relevance to *H. pylori* biology in the human stomach. Early studies reported that m2 VacA proteins have a reduced capacity to cause vacuolation of HeLa cells, compared to m1 VacA proteins (112, 113). Conversely, several studies reported that m1 and m2 VacA have similar capacity to vacuolate RK-13 cells (rabbit kidney origin), leading to the hypothesis that m1 and m2 proteins differ in cell type specificity (112, 113). Two studies suggested that m1 VacA exhibits increased binding to HeLa cells compared to m2 VacA proteins (113, 198). Notably, there have been several limitations in previous comparative studies of m1 and

m2 VacA proteins. Some studies compared m1 and m2 VacA proteins produced by wild-type *H. pylori* strains, which have variations outside of the m-region of VacA (112, 113). Due to the difficulty of purifying the m2 forms of VacA, most studies have used concentrated broth culture supernatants or water extracts of intact bacteria as sources of m2 VacA (112, 113, 199). The presence of numerous bacterial proteins in these preparations can potentially influence cellular responses and complicate the interpretations. Further, the standardization of VacA in broth culture supernatants or water extracts to ensure equivalent VacA concentrations has been challenging. Some studies used polyclonal antibodies against m1 and m2 VacA that potentially differ in affinities (113). Therefore, most comparative studies of m1 and m2 VacA proteins have provided few insights into the mechanisms or structural features underlying observed differences in activity.

In this current study, we sought to investigate the activity of m2 forms of VacA on gastric epithelial cells and elucidate the mechanistic basis for any observed differences in activity between m1 and m2 forms. We describe the generation of *H. pylori* strains producing chimeric VacA proteins in which segments of the p55 domain (m1 in the parental strain) were replaced by corresponding m2 sequences. We report the results of comparative experiments in which these proteins were added to cultured human gastric epithelial cells or human gastric organoids grown as monolayers. The experiments demonstrate sequence variation in the N-terminal portion of the VacA p55 domain influences toxin activity and VacA binding to transformed cell lines, thereby influencing toxin potency. Importantly, both m1 and m2 forms of the toxin are capable of causing alterations in all of the cell lines tested, as well as human gastric organoids.

The capacity of m2 VacA proteins to cause alterations in gastric epithelial cells is consistent with the widespread presence of m2 *vacA* alleles in *H. pylori* strains throughout the world.

Materials and Methods

H. pylori culture methods

H. pylori strains were cultured on Trypticase soy agar plates containing 5% sheep blood at 37°C in room air supplemented with 5% CO_2. Liquid cultures were grown in Brucella broth containing 1x cholesterol (Gibco).

Generation of *H. pylori* mutant strains

Plasmids containing chimeric *vacA* sequences, derived in part from *H. pylori* strain 60190 (type m1 *vacA;* Genbank accession number Q48245.1) and in part from *H. pylori* strain Tx30a (type m2 *vacA;* Genbank accession number Q48253.1), and encoding a strep tag (strep-tag II) at a position corresponding to amino acid 808 in *vacA* from strain 60190 (Str_{808}), were designed as shown in Figure 5 and were synthesized by Genscript. A previously described counter-selection approach (56) was used to construct the mutant strains. *H. pylori* strain 60190 Δ*rdxA* containing a *cat::rdxA* cassette replacing amino acids 420 to amino acid 820 in *vacA* (AflII and NheI restriction sites) (VM218) was transformed with the plasmids described above. Metronidazole-resistant transformants were isolated and expanded and genomic DNA was isolated.

Introduction of the desired mutations was confirmed by PCR and sequencing the PCR-amplified regions of interest. Mutant strains are described in Table 6.

VacA purification

H. pylori strains were grown in broth culture for two days, and bacteria were removed by centrifugation at 7,500 x *g* for 15 min. Ammonium sulfate was added to the supernatant, resulting in a 50% saturated solution of ammonium sulfate. Precipitated proteins were pelleted by centrifugation at 7,500 x *g* for 15 min and resuspended in phosphate-buffered saline (PBS) containing 1 mM EDTA and 0.02% sodium azide. Strep-tagged VacA proteins were incubated with Strep-Tactin resin (IBA) in a gravity column. The resin and associated proteins were washed with wash buffer (50 mM Tris, 150 mM NaCl [pH 8.0]), and subsequently VacA was eluted with elution buffer (50 mM Tris, 150 mM NaCl, and 5 mM D-desthiobiotin [pH 8.0]) (56).

Negative stain electron microscopy

Samples were prepared for electron microscopy (EM) analysis by diluting the samples to 40 µg/mL in 20 mM of HEPES buffer and applying about 5 µL to a glow-discharged copper grid covered with carbon-coated collodion film. After washing grids in 4 drops of water and staining in uranyl formate (0.75%), samples were imaged by electron microscopy (Morgagni) at a magnification of 28,000x (200).

Cell culture methodology

HeLa cells (human cervix origin) and AZ-521 cells (human duodenal origin) were grown in minimal essential medium (modified Eagle medium containing Earle's salts and L-glutamine) supplemented with 10% FBS and nonessential amino acid solution 100x (Sigma), and AGS cells (human gastric origin) were grown in RPMI 1640 medium (containing L-glutamine and 25 mM Hepes) supplemented with 10% FBS in a 5% CO_2 atmosphere at 37°C.

Cell vacuolation and neutral red assay

Wild-type (WT) and mutant VacA proteins were tested for vacuolating activity using a neutral red uptake assay (201). Cells were seeded in tissue culture-treated flat bottom 96-well plates at a density of 1-2.5 x 10^4 cells per well and incubated overnight at 37°C in room air supplemented with 5% CO_2. Oligomeric purified VacA was acid-activated with 200 mM HCl until a pH of 3.0 was reached, and the acid-activated VacA then was added to adherent cells in media supplemented with 5 mM ammonium chloride. After incubation for 4 h or 24 h at 37°C in room air supplemented with 5% CO_2, vacuolation was quantified by removing media and adding neutral red dye (201). Once the dye was taken up by vacuolated cells, the cells were washed three times with 0.9% saline. Acid alcohol (97% ethanol and 3% HCl) was added to release the dye and OD_{540} was determined using a plate reader.

VacA-induced cell death

Cell death was assessed using the ATPlite Luminescence Assay (Perkin Elmer) (88). AZ-521 cells were grown in minimal essential medium (modified Eagle medium

containing Earle's salts and L-glutamine) supplemented with 10% FBS and MEM non-essential amino acid solution in a 5% CO_2 atmosphere at 37°C. Cells were plated on black-walled tissue culture-treated plates with a clear bottom (Corning). Acid-activated VacA was added to 1-2.5 x10^4 cells per well as described above for neutral red assays. After incubation for 24 h, the assay was completed following the instructions provided by the manufacturer.

Assessing VacA binding to cells and internalization using fluorescent microscopy

HeLa or AGS cells were plated onto glass coverslips in wells of a 24-well plate at a density of 7 x 10^4 cells/ml and incubated overnight. VacA proteins were labeled with Alexa 488 (Molecular Probes) (56, 202). To assess VacA binding to cells, 5 µg/mL (~60 nM) of each fluorescently labeled acid-activated VacA variant was added to cells for 1 h and incubated at 4°C. When assessing VacA internalization, 5 µg/mL of each labeled VacA variant was acid-activated, added to cells and cells were incubated for 5 minutes at 37°C. The degree of labeling [DOL = (moles dye)/(mole protein] of VacA typically ranged from 4.5 to 10 moles dye/mole protein and was calculated as described in Alexa Fluor 488 Microscale Protein Labeling Kit product information sheet. The VacA-containing media was removed and fresh media with 5 mM of ammonium chloride was added, and cells then were incubated at 37°C for 4 h. The cells were washed once with PBS and fixed with 4% paraformaldehyde (PFA). Cell membranes were stained with Wheat Germ Agglutinin Alexa Fluor 594 Conjugate (WGA) (Molecular Probes) and nuclei were stained with DAPI (Invitrogen) according to the manufacturer's instructions.

All cells were imaged using confocal microscopy (LSM710) and analyzing using ImageJ. VacA co-trafficking studies were performed by fluorescently labeling two different VacA preparations with Alexa 488 or Alexa 594.

Cell depolarization

AZ521 cells were detached with trypsin/EDTA then incubated with 1,5-Bis (5-oxo-3-propylisoxazol-4-yl) pentamethine oxonol (oxonol VI) (Millipore Sigma) (final concentration 2.5 μM) for 15 min at 37 °C (41). A cell suspension (2 ml) was placed in a stirred quartz cuvette at 37 °C in a PerkinElmer Life Sciences LS50B fluorimeter. After stabilization of the fluorescence signal (excitation 585 nm, slit 10 nm; emission, 645 nm, slit 5 nm), acid-activated VacA (final concentration 20 μg/ml) or an acidified buffer control was added to the cells. The fluorescent signal was monitored for about 3.5 minutes after addition of VacA.

VacA interactions with cultured human organoids

De-identified donor gastric tissue specimens of corpus origin were obtained from sleeve gastrectomy surgeries and gastric glands were isolated as described previously, using IRB-approved protocols (203, 204). Gastric spheroid cultures were established following a 1 h incubation with 0.5 U/mL of collagenase in a 37 °C water bath at 200 rpm, samples were vortexed to release the glands, and centrifuged at 4 °C for 5 min. After resuspending the pellet in cold DPBS (Hyclone GE Healthcare Life Sciences) and vortexing for 30 s, glands were removed from the supernatant fraction, transferred to a 50 mL tube, pelleted and transferred to Matrigel (Corning, Bedford, MA, USA). The

Matrigel-suspended glands were added to prewarmed 24-well plates and overlaid with conditioned L-WRN media composed of Advance DMEM/F12 (Gibco) and supplemented with 10 mM HEPES, 10 μM Y-27632 and 10 μM SB431542 (Tocris). Cells were maintained as described in (205).

To generate two-dimensional monolayer cultures, gastric spheroids from three different human donors were dissociated using trypsin and mechanical dissociation. Cells were then added to transwells (Thermo Fisher) previously coated with type I collagen, overlaid with L-WRNA conditioned medium containing penicillin and streptomycin, and cultured until confluent. Fluorescently labeled acid-activated VacA was added to either the apical or basolateral side as described above. Cells were washed with PBS and fixed as indicated above, and transwells were cut out using a scalpel and mounted using Prolong gold antifade (Invitrogen). VacA binding was assessed using confocal microscopy as described above. To quantify VacA intensity, z-stacks were merged and maximum intensity was analyzed in ImageJ. Integrated density values were divided by the number of nuclei in the field.

VacA-induced vacuolation was quantified using a neutral red uptake assay similar to that used for transformed cell lines (described above) but modified for compatibility with transwells. Acid-activated VacA proteins were added to either the apical or basolateral compartments in medium containing 5 mM ammonium chloride and cells were incubated for 24 h at 37°C in room air supplemented with 5% CO_2. Vacuolation was then quantified by removing media and adding neutral red dye to both the apical and basolateral compartments for 20 minutes. Cell surfaces on both sides of the transwell then were washed three times with 0.9% saline. Acid alcohol was added to

the apical compartment to release the dye, 75 µL of dye-cell mixture was transferred to a 96 well plate, and OD_{540} was determined.

Statistical analysis

Statistical significance of vacuolation and cell death data were determined by two-way ANOVA. Microscopy data were analyzed using ANOVA and Dunnett's or Dunn's multiple test corrections for parametric and non-parametric analyses, respectively. Neutral red data to assess vacuolation of epithelial monolayers derived from human gastric organoids were analyzed by two-way ANOVA with Bonferroni multiple corrections. Mann Whitney used to evaluate the significance of differences in VacA binding to cells derived from gastric organoids.

Results

Replacement of m1 VacA sequences with m2 sequences

To undertake comparative analyses of type m1 and type m2 forms of VacA, we generated *H. pylori* strains in which segments of the *vacA* m-region in strain 60190 (which harbors a type s1/i1/m1 *vacA* allele) were replaced with corresponding segments of *vacA* from strain Tx30a (type s2/i2/m2 *vacA*) (Table 6, Figure 5A). Each of the chimeric *vacA* genes was also engineered to encode a Strep-tag II, which allows purification of the secreted proteins.

One of the strains (RRC4) was designed so that the *vacA* region encoding nearly the entire p55 domain was altered (corresponding to a change from m1 to m2;

designated m2 in Figure 5). We also engineered *H. pylori* strains in which smaller regions of the m-region were altered. In one strain (RRC3) the 5' portion of the m-region was changed from m1 to m2 (designated m2m1 in Figure 5), and in the other strain (RRC2) the 3' portion of the m-region was changed from m1 to m2 (designated m1m2 in Figure 5). Figure 5B shows the cryo-EM structure of a hexamer formed by wild-type VacA from strain 60190 and depicts regions that were replaced with VacA sequences from strain Tx30a (48, 49). Each of these chimeric VacA proteins was secreted into the extracellular space, and the secreted proteins were successfully purified by use of the Strep-tag II. SDS-PAGE and Coomassie blue staining showed that all the secreted proteins were similar in size (about 88 kDa) (Figure 6A). To determine if the VacA variants retained the ability to oligomerize, we utilized negative stain electron microscopy (EM). All of the m2 VacA chimeras assembled into flower-shaped oligomeric structures (Figure 6B), similar to m1 VacA. Collectively, these experiments suggested that the replacement of various segments of the parental m1 sequence with corresponding m2 sequences did not have detrimental effects on protein folding.

Table 6. *H. pylori* mutant strains

***H. pylori* strain name**	**Description of strain or VacA protein**	**VacA type**
VM218	Strain 60190 with *cat::rdxA* cassette replacing VacA amino acids 420-820	*vacA* null mutant
60190-Str_{808}	Wild-type VacA secreted from *H. pylori* strain 60190 engineered to produce VacA containing a Strep-tag II introduced at amino acid 808 (56)	m1
RRC2	60190-Str_{808} containing VacA amino acid sequences from *H. pylori* strain Tx30a replacing amino acids 625-804	m1/m2
RRC3	60190-Str_{808} containing VacA amino acid sequences from *H. pylori* strain Tx30a replacing amino acids 315-623	m2/m1
RRC4	60190-Str_{808} containing VacA amino acid sequences from *H. pylori* strain Tx30a replacing amino acids 315-804	m2
RRC5	60190-Str_{808} containing VacA amino acid sequences from *H. pylori* strain Tx30a replacing amino acids 299-347, which includes a 23 amino acid deletion	299-347 m2
RRC6	60190-Str_{808} containing VacA amino acid sequences from *H. pylori* strain Tx30a replacing amino acids 462-485, which includes a 25 amino acid insertion	462-485 m2
RRC7	60190-Str_{808} containing the changes described for RRC5 plus the changes described for RRC6	double mutant

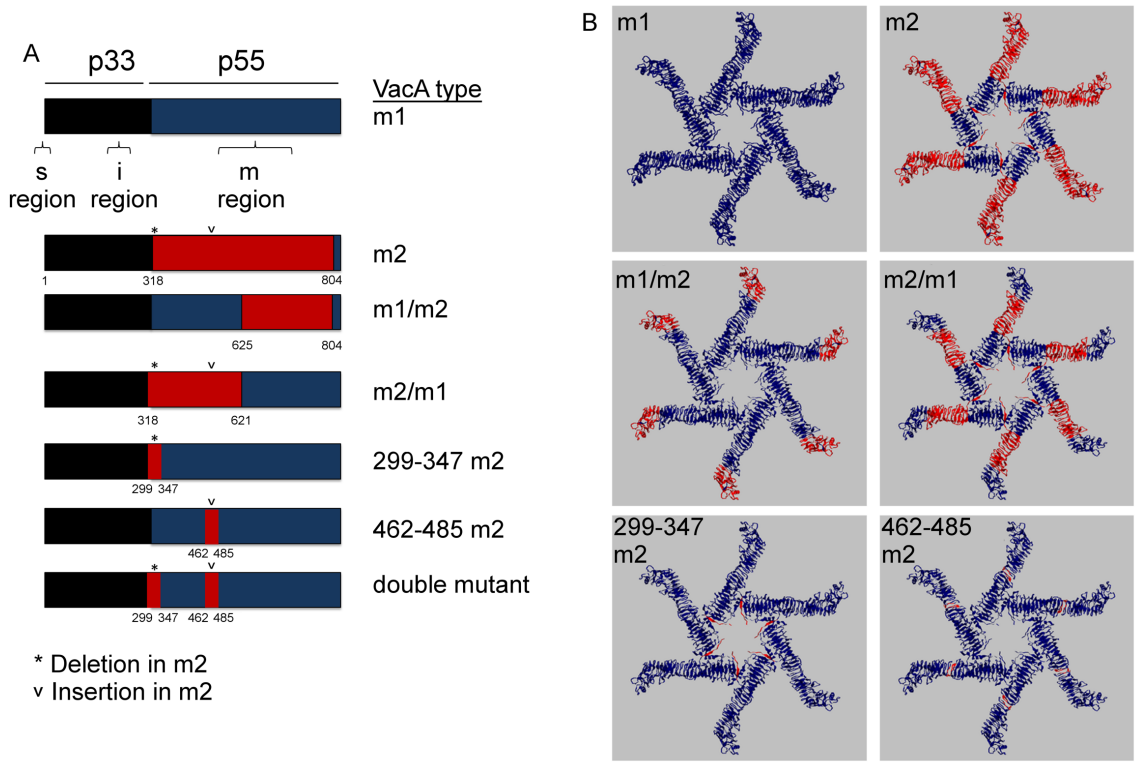

Figure 5. Schematic depiction of VacA proteins analyzed in this study. *vacA* segments from *H. pylori* strain Tx30a (which contains type m2 VacA) were introduced in place of corresponding *vacA* segments in strain 60190. Strain designations are explained in Table 1. (A) In the schematic, the p33 domain of VacA is depicted in black, the p55 domain containing native m1 VacA sequences is blue, and regions containing m2 VacA sequences from strain Tx30a are red. Amino acid numbers of swapped regions are listed below each schematic (based on numbering of VacA from strain 60190). Asterisks indicate position of a 23-amino acid region present in VacA from strain 60190 but absent in VacA from strain Tx30a. Caret symbols indicate position of a 25-amino acid region present in VacA from strain Tx30a but absent in VacA from strain 60190. (B) The cryo-EM structure of a hexamer formed by VacA from wild-type 60190 (type m1 VacA) is shown (PDB 6NYF). Regions in which m1 sequences were replaced with m2 sequences are shown in red. Blue indicates regions in which VacA sequences of the parental strain are unchanged.

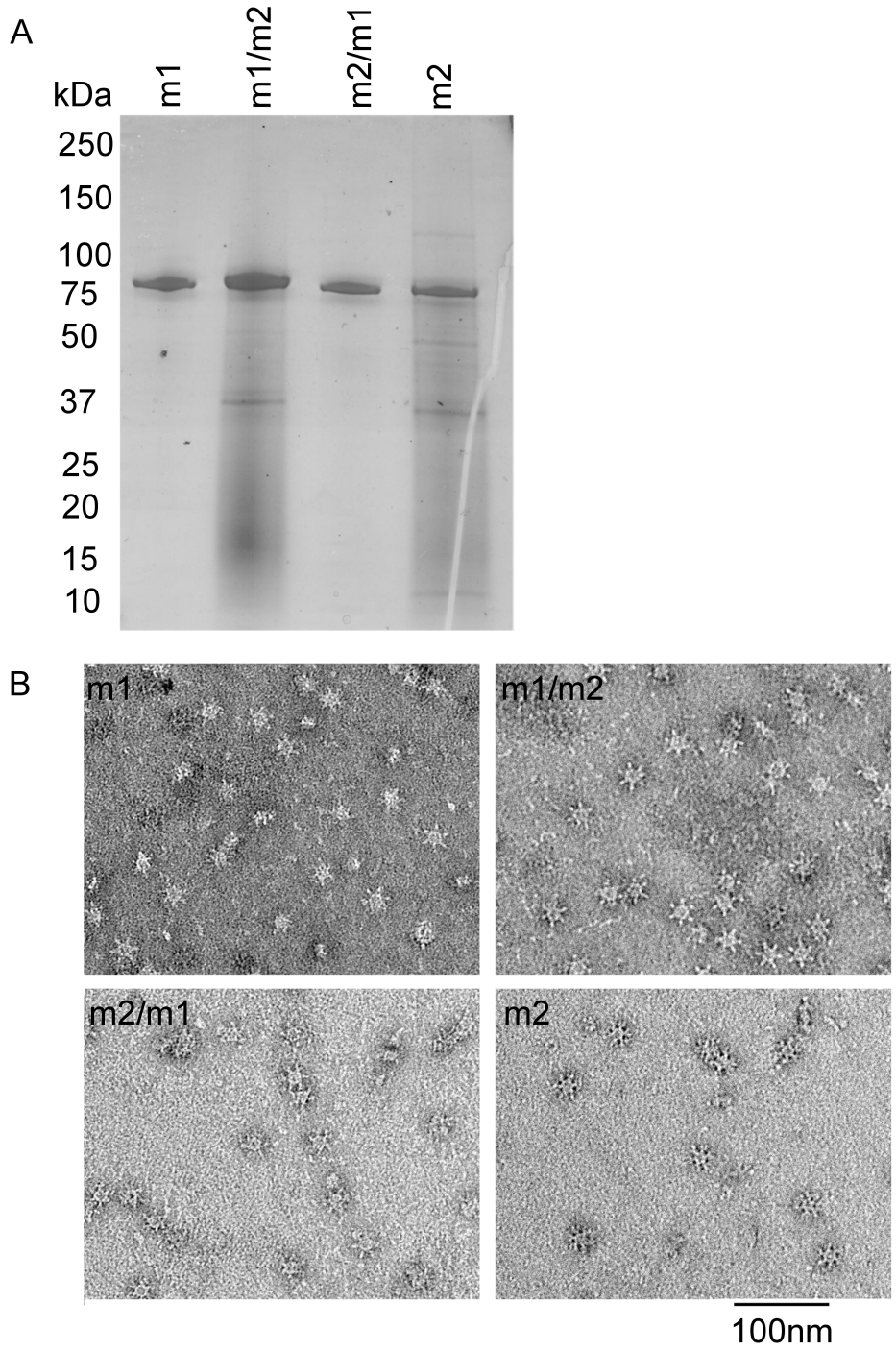

Figure 6. Properties of VacA chimeras in which regions in VacA from strain 60190 (type m1) were replaced with corresponding regions of VacA from strain Tx30a (type m2 VacA). (A) VacA proteins were purified from *H. pylori* culture supernatants and analyzed by SDS-PAGE and Coomassie blue staining. (B) Negative stain electron microscopy revealed that all of the VacA proteins assemble into water-soluble oligomers.

Cell-vacuolating effects of VacA

When added to cultured epithelial cells, s1m1 VacA causes multiple cellular alterations, including cell vacuolation (132, 179-181, 191). To compare the vacuolating activity of the m1/m2, m2/m1 and m2 forms of VacA with that of the m1 form, we tested the effects of the proteins on HeLa cells (which are commonly used for assessing VacA activity) and AGS gastric epithelial cells. Vacuolation was quantified using a neutral red uptake assay, as described in Methods. The m1 VacA form and the m1/m2 form had similar activities, and these activities were significantly greater than those of the m2/m1 or m2 forms in both HeLa cell and AGS cell assays (Figure 7). These results provided evidence that sequence variation in the N-terminal portion of the p55 domain influences toxin potency. Because we consistently obtained relatively low yields of purified m2 protein compared to other forms of VacA, we used the m2/m1 VacA protein for subsequent experiments.

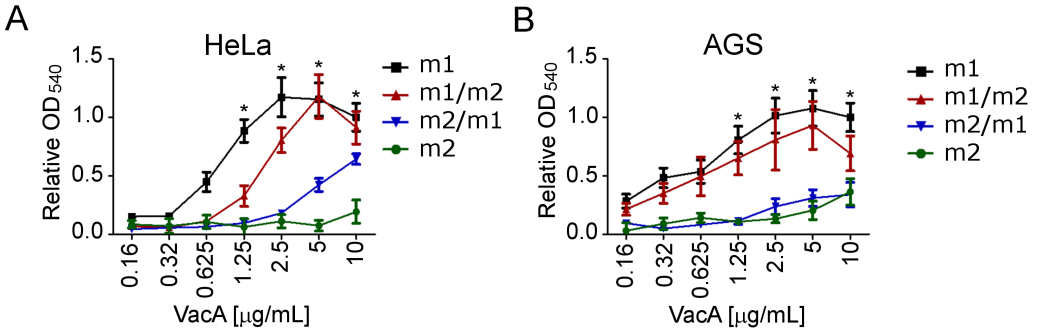

Figure 7. Cell-vacuolating activity of VacA proteins. Purified VacA proteins were acid-activated, serially diluted and added to (A) HeLa or (B) AGS cells in the presence of 5 mM ammonium chloride for 24 h. Neutral red uptake assays were performed to assess cell vacuolation (quantified by measuring optical density at 540 nm). Data from two or three independent experiments were normalized to results for the m1 VacA control. *, $p < 0.05$ for m2/m1 or m2 VacA proteins compared to the m1 VacA type.

Effects of VacA proteins on AZ-521 cells

AZ-521 cells, a duodenal cell line, are highly susceptible to cell death in response to s1m1 forms of VacA (88), but the effects of m2 forms of VacA on these cells have not been studied in detail. Therefore, we tested the effects of the chimeric VacA proteins on this cell line. Type m1 and m1/m2 types of VacA caused similar levels of vacuolation in AZ-521 cells, and these VacA forms induced significantly greater vacuolation compared to the m2/m1 form (Figure 8A). Similar to the results of the vacuolation studies, the m1 and m1/m2 VacA types induced significantly greater cell death compared to the m2/m1 form (Figure 8B).

When added to AZ521 cells, type s1m1 VacA causes depolarization of the plasma membrane potential (41). To compare the depolarizing activities of the different forms of VacA, we conducted cell depolarization assays, as described in the Methods. A reduced fluorescent signal was detected for cells incubated with m2/m1 VacA compared to the m1 and m1/m2 types (Figure 8C), indicating that the N-terminal of the p55 domain contributes to the ability of VacA to depolarize the membrane of AZ-521 cells.

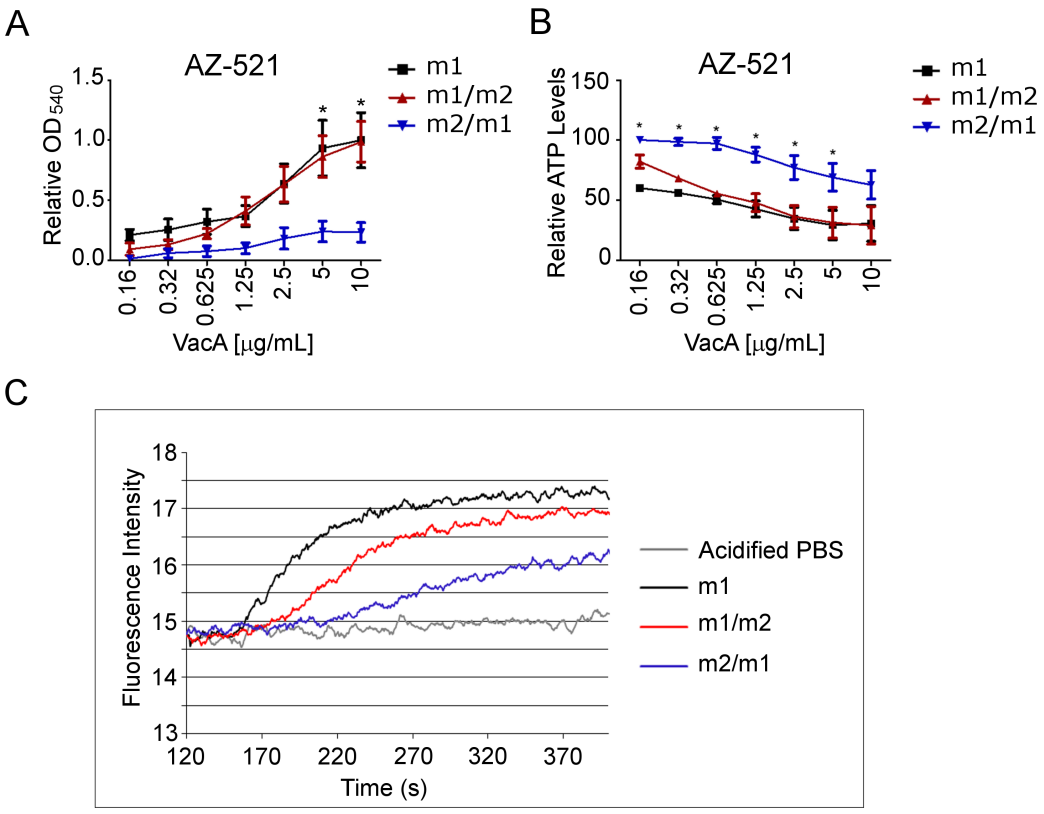

Figure 8. Effects of VacA proteins on AZ-521 cells. (A) AZ-521 cells were incubated with the indicated purified acid-activated VacA proteins for 4 h in the presence of 5 mM ammonium chloride. Data were normalized to results for the m1 VacA control. *, $p < 0.05$ for m2/m1 VacA compared to m1 VacA. (B) AZ-521 cells were incubated with VacA proteins for 24 h and ATP levels were analyzed using the ATPlite reagent. Data from three independent experiments were normalized to results for control cells incubated with medium only. *, $p < 0.05$ for m2/m1 compared to m1 VacA. (C) AZ-521 cells were loaded with oxonol VI (a probe used to monitor membrane potential). Following stabilization of the fluorescent signal for 2.5 minutes, acid-activated VacA proteins (20 μg/ml) or acidified PBS was added to cells. The fluorescent signal was monitored for about 3.5 minutes after addition of VacA. m2/m1 VacA has reduced ability to alter membrane potential compared to m1 VacA. The graph shows representative data from three independent experiments.

Analysis of a strain-specific insertions or deletions in the m-region

The results shown in Figure 7 suggest that differences in the activity of m1 and m2 forms of VacA are mainly due to sequence differences in the N-terminal portion of the p55 domain. Two of the most striking differences in this region are a ~23-amino acid segment at the junction of the p33 and p55 domains (denoted as the d-region in some publications) (109, 206), typically present in m1 but not m2 VacA proteins, and a ~25-amino acid segment within the p55 domain of m2 but not m1 VacA proteins. To determine if these regions are important determinants of VacA activity, we generated strains (RRC5 and RRC6) engineered to produce VacA proteins in which these segments were individually altered (Figure 5). We also generated a strain (RRC7) producing a VacA protein in which both regions were altered. All of these mutants secreted VacA, similar to the parental strain (data not shown). When tested for activity in vacuolation and cell death assays, each of these mutants exhibited activity that was not significantly different compared to that of the parental m1 VacA protein suggesting that cumulative differences between m1 and m2 VacA forms account for differences in activity (Figure 9).

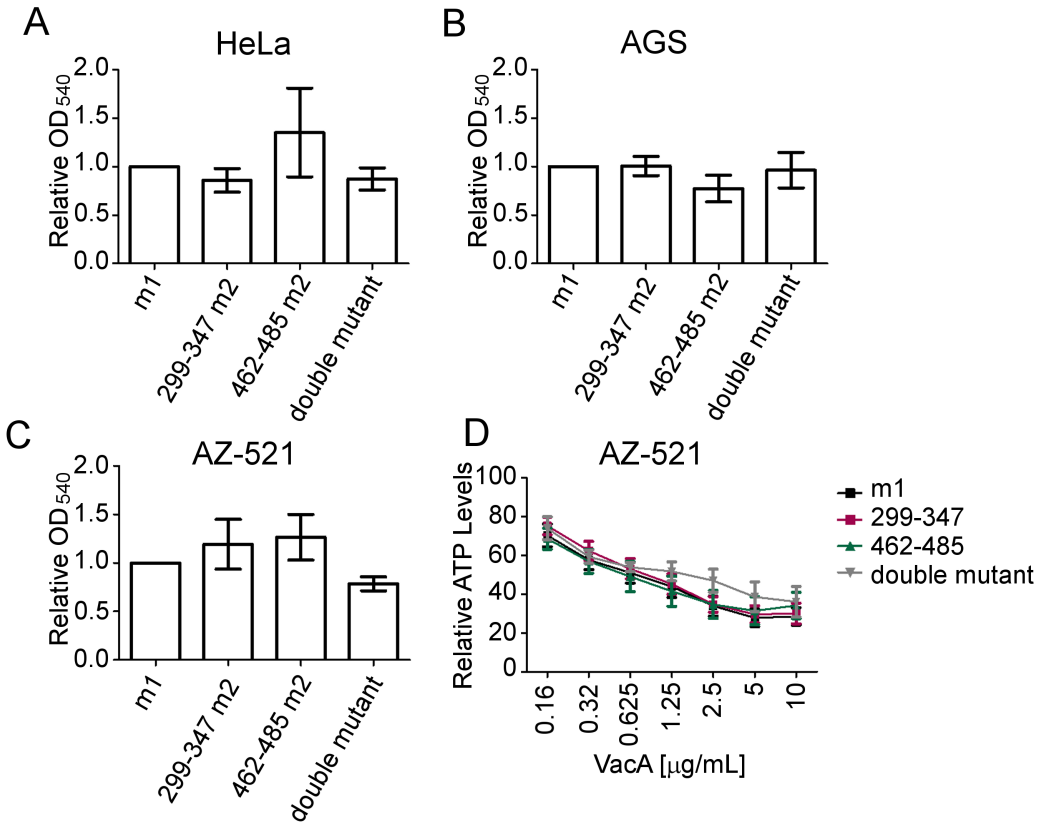

Figure 9. Strain-specific VacA insertions or deletions are not determinants of toxin activity. VacA proteins in which the segment at the p33-p55 junction is deleted (299-347 m2), a ~ 25 segment is inserted into the p55 domain (462-485 m2), or both alterations (double mutant) are depicted in Figure 1. VacA preparations were acid-activated and added (final concentration 5 μg/ml) to (A) HeLa or (B) AGS cells for 24 h or (C) AZ-521 cells for 4 h in the presence of 5 mM ammonium chloride. Neutral red uptake was measured as described in Methods. Data from three to seven independent experiments were normalized to results for the m1 VacA control. (D) To analyze cell death, AZ-521 cells were incubated with the indicated concentrations of VacA for 24 h and luminescence was measured after the addition of the ATPlite reagent. Data from three independent experiments were normalized to results for control cells incubated with medium only. There were no significant differences between m1 VacA and VacA mutants in analyses of cell vacuolation or cell death (two-way ANOVA).

VacA cellular binding, internalization, and localization

We next compared the ability of the different forms of VacA to interact with host cells. AGS or HeLa cells were incubated with fluorescently labeled VacA proteins at 4°C (to assess VacA binding to cells) or 37°C (to assess VacA internalization into cells), and the cells were then visualized by fluorescence microscopy. These studies revealed that the m1 form of VacA binds to both HeLa and AGS cells at higher levels compared to the m2/m1 form (Figure 10). The m1 form was also internalized at higher levels by HeLa and AGS cells compared to the m2/m1 form (Figure 11).

To determine if the different activities of m1 and m2/m1 VacA proteins might be attributable to differences in intracellular localization, we labeled m1 and m2/m1 forms of VacA with different fluorophores (Alexa 488 or 594) and added the proteins to cells, either consecutively or simultaneously. The VacA-treated cells were then incubated at 37°C for 4 h. Confocal microscopy revealed substantial co-localization of the two VacA types (Figure 12). Collectively, these results suggest that reduced binding of the m2/m1 VacA form to cells compared to the m1 type correlates with reduced internalization of the m2/m1 toxin. However, once m2/m1 VacA is internalized, it localizes in the same intracellular compartments as the m1 VacA type.

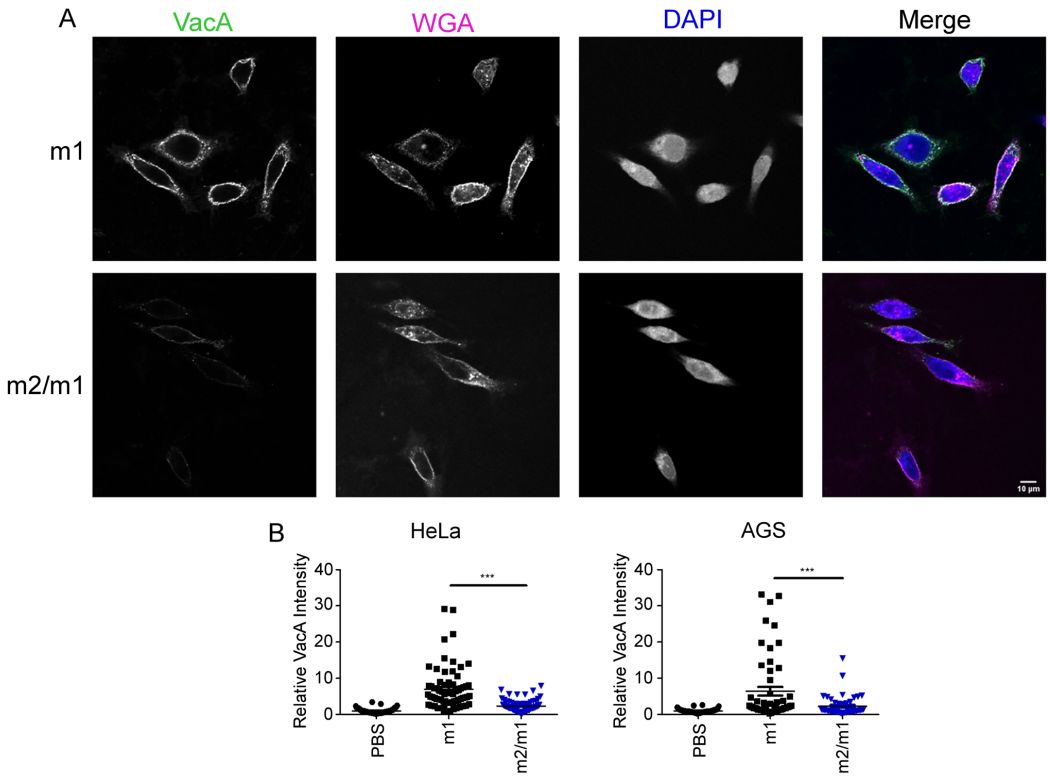

Figure 10. m2/m1 VacA exhibits reduced binding to AGS cells compared to the m1 form. (A) AGS cells were treated with 5 µg/mL of acid-activated fluorescently labeled VacA (green) for 1 h at 4°C to evaluate toxin binding to cells. Cell membranes were stained with fluorescently labeled WGA (magenta), a cell membrane marker, and DAPI (blue) for nuclear staining. Cells were outlined in ImageJ and the VacA fluorescence intensity was quantified. Experiments with HeLa cells yielded similar results (images not shown). The m1 form of toxin binds to HeLa (B) and AGS cells (C) at higher levels compared to m2/m1 VacA. Data points represent results from three (HeLa) or four (AGS) independent experiments (analysis of ≥10 cells per condition per experiment). ***, $p < 0.001$

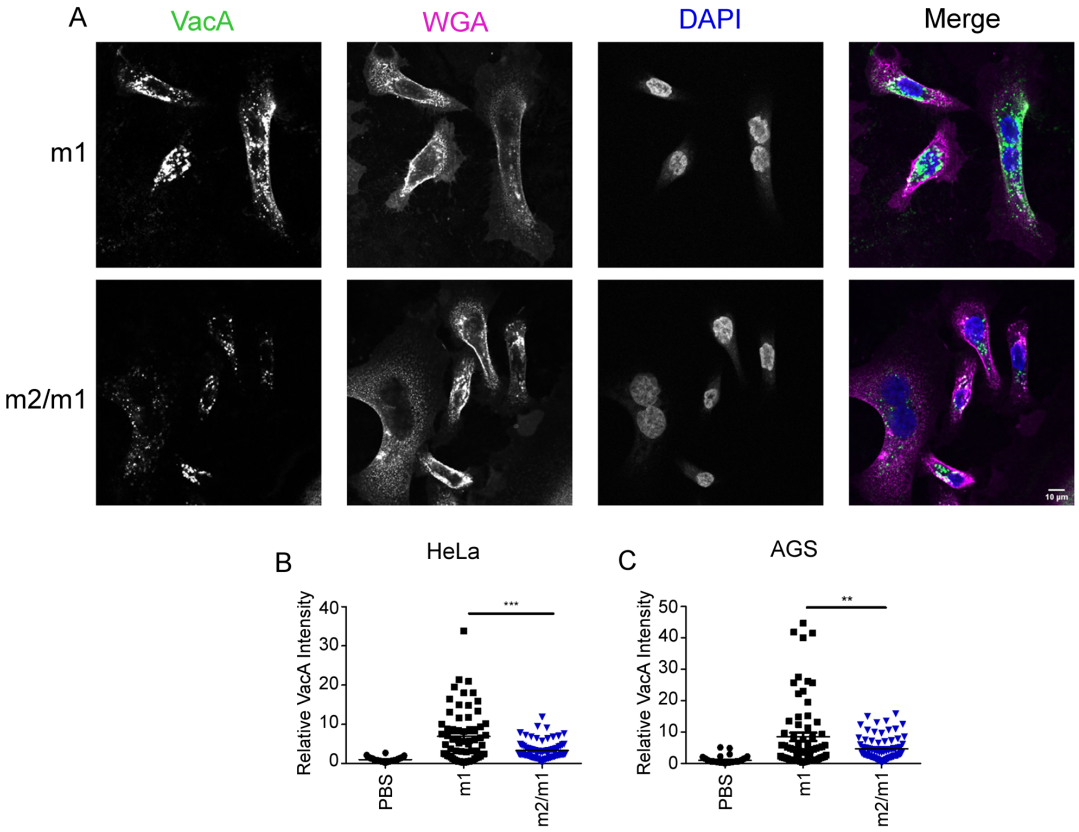

Figure 11. m2/m1 VacA exhibits reduced internalization into AGS cells compared to the m1 form. HeLa and AGS cells were treated with 5 μg/mL of fluorescently labeled acid-activated VacA (green) for 5 minutes. The medium overlying cells was replaced with fresh medium containing 5 mM ammonium chloride, and cells then were incubated for 4 h at 37°C. Cell membranes were stained with fluorescently labeled WGA (magenta), a cell membrane marker, and DAPI (blue) for nuclear staining. Cells were outlined in ImageJ and the VacA fluorescence intensity was quantified. (A) Images for experiments with AGS cells are shown. Experiments with HeLa cells yielded similar results (images not shown). The m1 form of toxin is internalized by HeLa (B) and AGS cells (C) at higher levels compared to m2/m1 VacA. Data points represent results from three (HeLa) or four (AGS) independent experiments (analysis of ≥15 cells per condition per experiment). **, $p<0.01$ and ***, $p< 0.001$

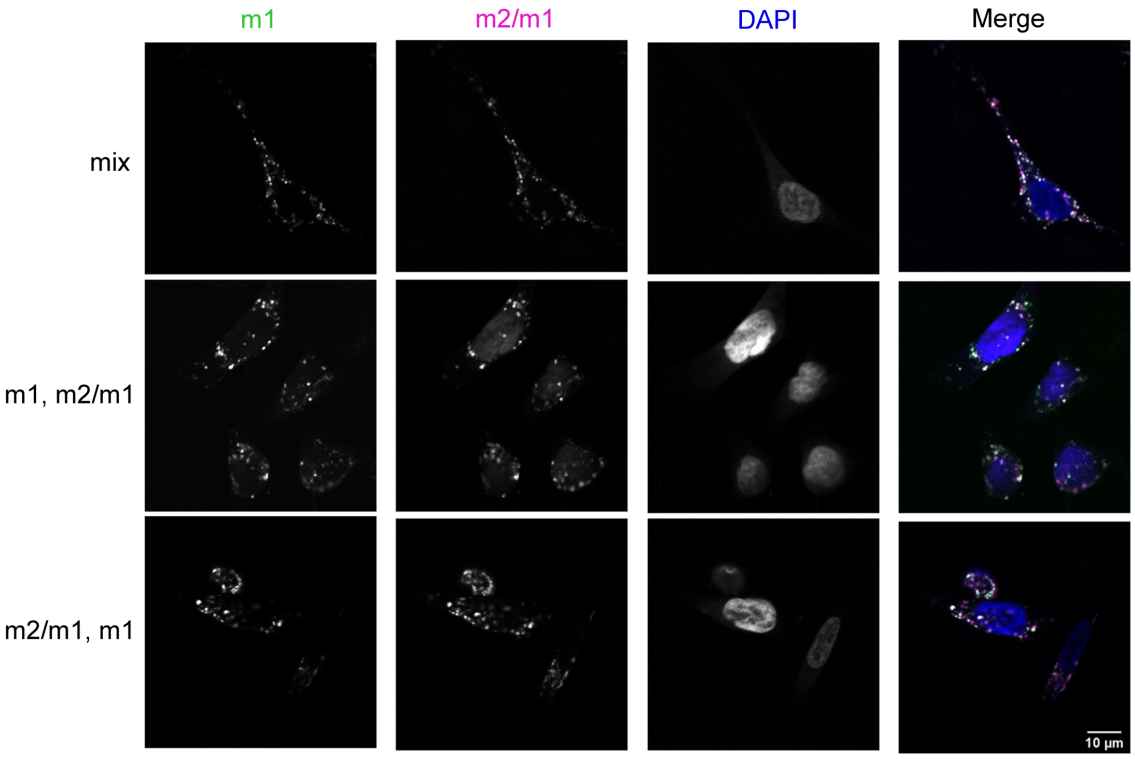

Figure 12. m1 and m2/m1 VacA co-localize within intracellular compartments. m1 and m2/m1 VacA types were labeled with different fluorophores (m1, green; m2/m1, magenta) and added either simultaneously ("mix") or consecutively ("m1, m2/m1" or "m2/m1, m1") to AGS cells. In the latter case, cells were treated with 5 µg/mL of the first fluorescently labeled acid-activated VacA protein for 5 minutes, washed, and then treated with the second labeled protein for 5 minutes. The medium overlying cells was replaced with fresh medium containing 5 mM ammonium chloride, and cells then were incubated for 4 h at 37°C. Co-localization of m1 and m2/m1 toxin is indicated by a white color in the merged images (right panels).

VacA interactions with human gastric organoids

We also assessed VacA interactions with polarized monolayers derived from human gastric organoids, grown on transwell filters. In initial experiments, we tested organoid cell lines derived from gastric tissue of three different human donors and added VacA proteins to either the apical (top) or basolateral (bottom) compartment of the chambers. Both m1 and m2/m1 VacA proteins caused cell vacuolation (assessed by neutral red uptake assay) when added to the basolateral compartment but not the apical compartment (Figure 13). There were no significant differences in vacuolating activity when comparing m1 and m2/m1 VacA (Figure 13). We then selected one of the organoid cell lines for further studies and analyzed VacA binding to the cells. Fluorescently labeled VacA proteins were added to either the apical (top) or basolateral (bottom) compartment, the cells were incubated at 4°C, and then were visualized using fluorescence microscopy. Significantly higher levels of VacA binding were detected when the proteins were added to the basolateral chamber than when added to the apical chamber (Figure 14). Similar to the results observed in experiments with cultured transformed cells, the levels of m1 binding to the gastric organoids were higher than levels of m2/m1 binding (Figure 14).

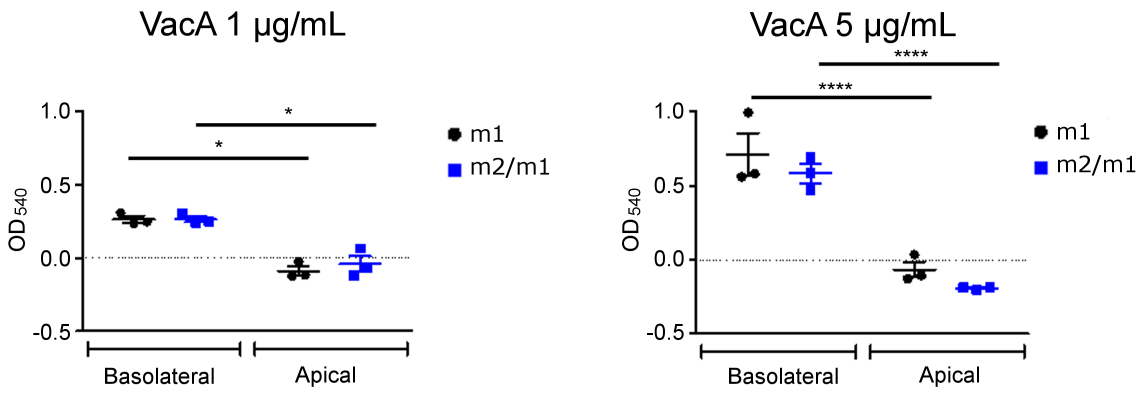

Figure 13. Vacuolation of epithelial monolayers derived from human gastric organoids. Acid-activated VacA proteins were added at the indicated concentrations to either the apical or basolateral compartments of transwells containing epithelial monolayers derived from human gastric organoids. Epithelial monolayers derived from three different human donors were tested. Cells were incubated for 24 h at 37°C, and VacA-induced vacuolation was quantified by a neutral red dye uptake assay as described in Methods. *, $p<0.05$ and ****, $p<0.0001$

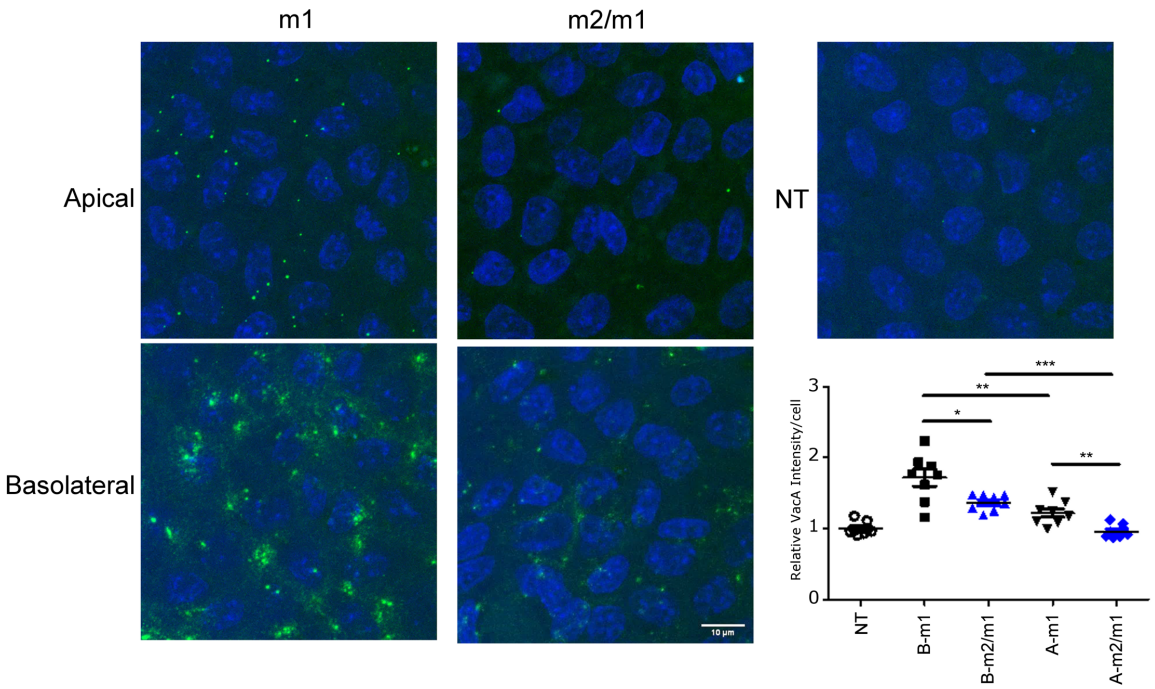

Figure 14. Binding of m1 and m2/m1 VacA to epithelial monolayers derived from human gastric organoids. Fluorescently labeled acid-activated VacA proteins (5 µg/mL) were added to the apical or basolateral compartments of transwells containing human gastric epithelial cells for 1 h at 4°C to assess toxin binding (green). Nuclei were stained with DAPI (blue). Cell-associated VacA was quantified as described in Methods. A, apical; B, basolateral. Each data point represents results from 4 fields per condition per experiment (two independent experiments). B-m1 vs. B-m2/m1 p = 0.0379; A-m1 vs A-m2/m1 p = 0.003; B-m1 vs A-m1 p = 0.007; B-m2/m1 vs A-m2/m1 p = 0.0002

Discussion

In the current study, we analyzed the functional correlates of sequence diversity (corresponding to m1 and m2 variations) in the VacA p55 domain. We found that a chimeric m2/m1 VacA protein was less potent in inducing vacuolation in multiple transformed cell lines than the parental m1 VacA protein. The m1 form of the toxin also induced greater cellular depolarization and cell death in AZ521 cells, a duodenal cell line, compared to the m2/m1 toxin. The region responsible for the observed difference in potency was mapped to the N-terminal portion of the p55 domain.

Previous studies compared the activity of different forms of VacA in the context of non-gastric cells (HeLa cells and RK-13 cells) and reported that m1 and m2 forms of VacA had similar vacuolating activity when tested on RK-13 cells, whereas the m1 form was more active than the m2 form when tested on HeLa cells (112, 113, 198). Therefore, it was proposed that m2 forms of VacA have a cell type-specific activity. The current study focuses on gastric or duodenal epithelial cells, which are presumably more biologically relevant than non-gastric cell types.

Nearly all previously published studies of m2 VacA proteins analyzed *H. pylori* broth culture supernatants or *H. pylori* extracts containing VacA, instead of purified m2 VacA protein (112, 113, 199). One likely reason for the rare use of purified m2 VacA proteins in previous studies relates to difficulty in purifying sufficient quantities of the m2 protein. Most strains producing s2m2 forms of VacA secrete relatively low levels of VacA compared to strains producing s1m1 forms of VacA; this difference has been attributed to different levels of *vacA* transcription (207). In the current study, we manipulated a parental strain (containing an s1m1 *vacA* allele and secreting high levels

of VacA) to yield strains containing modified forms of *vacA* (harboring segments of m2 *vacA*), which allowed the *vacA* promoter region to remain unchanged in all of the strains tested. The construction of these strains and use of a strep tag for purification allowed us to purify sufficient quantities of m2 VacA proteins to allow analyses of VacA activity. Nevertheless, we consistently purified lower amounts of VacA from the strain in which the entire m1 region was replaced with an m2 sequence than from the parental strain. The reasons for this phenomenon remain unclear.

Our current studies revealed that the m2/m1 VacA chimera exhibits decreased binding to the plasma membrane of AGS gastric epithelial cells, compared to the parental m1 protein. The reduced level of binding presumably accounts for the reduced level of m2/m1 VacA protein internalized into host cells, as well as the observed reduction in activity. Several putative cell-surface receptors for m1 VacA on epithelial cells have been reported, including receptor protein tyrosine phosphatase alpha and beta (RPTPα and RPTPβ) (51, 59, 64, 65), lipoprotein receptor-related protein-1 (LPR1) (63), epidermal growth factor receptor (EGFR) (208), sphingomyelin (60, 61), heparan sulfate, glycosphingolipids and phospholipids (179, 181, 190, 191). The relative importance of these individual receptors in mediating VacA binding to cells or VacA internalization into host cells remains unclear (199, 209). In future studies it will be important to investigate further the binding of m1 and m2 VacA proteins to specific receptors and evaluate if differential binding to specific receptors accounts for the observed differences in toxin potency.

In addition to analyzing VacA interactions with transformed cultured cell lines, we analyzed VacA interactions with human gastric organoids grown as monolayers, which

potentially replicate in vivo conditions more closely than cultured transformed cell lines. Unexpectedly, we found that VacA bound at higher levels to the basolateral surface of the monolayers compared to the apical surface. Similarly, VacA caused increased cell vacuolation following interaction with the basolateral surface compared to the apical surface. Preferential binding of VacA to the basolateral surface could potentially reflect a higher concentration of VacA receptors on this surface compared to the apical surface. Alternatively, mucus overlying the apical surface might impede VacA binding. We detected a small, statistically non-significant difference in binding of m1 and m2/m1 forms of VacA to the organoids, and the two types caused similar levels of cell vacuolation. The capacity of m2 VacA proteins to cause alterations in human gastric epithelial cells is consistent with the widespread presence of m2 *vacA* alleles in *H. pylori* strains throughout the world.

CHAPTER 4

SUMMARY AND FUTURE DIRECTIONS

Summary

Helicobacter pylori colonizes about half the world's population or about 4 billion individuals (1, 2). Although most remain asymptomatic, a small fraction of infected individuals develop severe disease attributed to *H. pylori*, such as gastric cancer or peptic ulceration (2, 7). Differences in disease outcomes have been attributed to a number of factors, including variations in host genetic characteristics, environmental exposures, and *H. pylori* strain characteristics (8, 9). These factors also may account for geographic variations in incidences of gastric disease, with regions such as East Asia and South America reporting higher incidences of gastric cancer than several other parts of the world.

In this dissertation, I focused on proteins secreted by *H. pylori*, particularly the secreted VacA toxin. Animal studies have shown that gastric cancer rates are increased in animals fed a high salt diet. Additionally, epidemiologic studies have shown that humans colonized with *H. pylori* strains producing specific forms of VacA are more likely to experience severe disease outcomes. I conducted experiments designed to increase our understanding of these two topics. The goals of these studies were two-fold: to identify secreted *H. pylori* proteins that are upregulated in a high salt environment and to determine the contribution of the VacA m-region to toxin activities.

Effect of environmental salt concentration on the *H. pylori* exoproteome

Epidemiologic studies have linked consuming a high salt diet in conjunction with *H. pylori* infection to an increased risk of gastric cancer (11, 12). Similarly, studies using the Mongolian gerbil model have shown that *H. pylori*-infected animals consuming a high salt diet develop more severe gastric inflammation, higher gastric pH, and higher incidences of gastric cancer than animals consuming a regular diet (13, 126). However, the mechanisms underlying these observations are poorly understood.

Studies focused on changes occurring in *H. pylori* under stressful conditions, such as high salt concentration, have revealed that the virulence factor CagA is upregulated in high salt environments (13, 16, 17). Analyses of the *H. pylori* membrane proteome and *H. pylori* gene expression have revealed multiple other changes in response to high salt conditions (18, 25). Among the proteins or genes that were regulated in response to changes in environmental salt concentration, several have been implicated as important for *H. pylori* pathogenesis. Proteins shown to be increased in abundance in response to high salt conditions included the outer membrane proteins HopQ and SabA and fibronectin domain-containing protein. Membrane proteins with decreased abundance in response to high salt conditions included VacA and two VacA-like proteins (ImaA and FaaA) (18).

In this study, I analyzed changes in expression and abundance of secreted *H. pylori* proteins in response to varying salt concentrations. My data show that twenty-five proteins are selectively released into the culture supernatants in all 6 of the culture conditions tested (medium containing 0.5%, 1.0%, or 1.25% NaCl, and time points of 24 h or 36 h). I found that thirty-one selectively released proteins were more abundant in

the culture supernatant in one or both high salt conditions (1.0% and 1.25%) compared to the baseline salt condition (0.5%). Surprisingly, this list included many outer membrane proteins (OMPs), including HopQ. Although the methodology included the use of ultracentrifugation to remove outer membrane vesicles from culture supernatant, we speculate that the outer membrane proteins detected in the culture supernatant might be components of small vesicles or membrane fragments that were not completely removed by ultracentrifugation. When investigating transcriptional changes in the *H. pylori* genome in response to high salt, we found that 46 genes were upregulated.

The salt-responsive proteins identified by proteomic analysis and salt-responsive genes identified by RNA-seq analysis were mostly non-concordant, but the secreted toxin VacA was salt-responsive in both analyses. These data were confirmed using (RT)-PCR analysis and western blotting. Nearly all the VacA peptides detected in the supernatant from cultures containing increased salt concentration mapped to the secreted 88 kDa toxin. Therefore, exposure to high salt conditions did not strip the VacA β-barrel domain from the membrane.

These results indicate that environmental salt concentration influences the composition of the *H. pylori* exoproteome, which could contribute to the increased risk of gastric cancer associated with a high salt diet. These data also indicate that increased VacA protein abundance is associated with increased *vacA* transcript levels in high salt conditions. At present, it is unknown if the underlying mechanism involves transcriptional activators that become active in response to high salt conditions or if there are post-transcriptional changes. One study reported that *vacA* mRNA is

stabilized in high salt environments (34). In addition, a previous study reported that *H. pylori* grown in high salt conditions has decreased levels of membrane-associated VacA, which suggests that high salt conditions may increase VacA secretion (18). In our study we also found that several secreted proteases were also upregulated in response to high salt. I hypothesize that one of these proteases could be responsible for increased proteolysis of the VacA protoxin, resulting in increased VacA secretion and release into the extracellular space.

Functional properties of *H. pylori* VacA m1 and m2 variants

Since vacuolating cytotoxin A and its ability to induce vacuole formation in eukaryotic cells were discovered, this protein has been implicated in a number of cellular activities, including inducing cell death, autophagy, causing mitochondrial alterations, disrupting epithelial barriers, and altering cell signaling (74, 78, 79, 82, 84-88, 90-92). Studies of VacA activity have primarily been done using the s1i1m1 form of VacA. Epidemiologic studies have shown that the risk for peptic ulcer disease or gastric cancer is higher in patients colonized with *H. pylori* secreting this form of toxin compared to the s2i2m2 form. Many previous studies comparing activities of different VacA types used non-gastric cell lines, such as HeLa (cervical) and RK13 (rabbit kidney) (112, 113, 129). I sought to understand the contribution of the m-region to VacA activities in relevant gastric cell lines. I also aimed to determine the mechanistic basis for the noted differences in activity.

To accomplish these goals, I generated *H. pylori* strains producing chimeric proteins in which VacA m1 segments of a parental strain were replaced by

corresponding m2 sequences. In comparison to the parental m1 VacA protein, a chimeric protein containing m2 sequences in the N-terminal portion of the m-region (m2/m1) caused less vacuolation in HeLa cells and AGS cells. The m2/m1 VacA type also induced less plasma membrane depolarization and cell death of AZ-521 duodenal cells. The presence of two strain-specific insertions or deletions, which could potentially correspond to the addition or removal of a β-helix rung within or adjacent to the m-region, did not influence toxin activity.

To determine why m1 and m2 VacA types exhibited differences in activity, we tested their ability to associate and to be internalized by HeLa cells and AGS cells. In comparison to the m2/m1 form of VacA, the m1 form of VacA exhibited higher levels of binding and internalization. In these cell lines, it appears that the difference in activity (vacuolation) is due in part to a difference in toxin binding.

Human gastric epithelial monolayers, which more closely resemble the epithelial populations in the stomach, were also utilized to assess vacuolation, binding and internalization of VacA. I found that similar amounts of both VacA types bound and were internalized by the gastric epithelial cells. The ability of the m2 VacA type to bind, be internalized, and cause cell vacuolation helps us to understand why this form has not been selected against in nature and is present in *H. pylori* strains around the world. Differences in m1 and m2 VacA types have been mapped to the surface of the protein, which suggests that these forms of toxin might interact with different host cell receptors and that the receptor favored by the m2/m1 VacA type is not present or expressed at low levels on HeLa, AGS, and AZ-521 cell lines.

Surprisingly, more VacA bound to the basolateral surface compared to the apical surface of human gastric epithelial monolayers. It is currently unknown if this phenomenon is due to the presence of mucus on the apical surface inhibiting VacA binding or if this is due to differential expression of receptors. This is an important topic for investigation in future studies.

Future Directions

Thus far, most studies of VacA have utilized *in vitro* assays and model systems (HeLa, AZ-521 and AGS cells) to study VacA activities. These methods allow for quick and easy testing of VacA activity, but these systems may not be optimal for replicating the human gastric environment. Use of *ex vivo* and *in vivo* models potentially allows a better understanding of VacA activity and the toxin's contribution to disease state. Below I propose using the gerbil model and gastric organoids to gain new insights into the role of VacA in gastric cancer.

***In vivo* effects of high salt diet and VacA on disease**

In vivo studies of the role of VacA in disease have been limited and analysis of the effects of VacA in animals on a high salt diet are non-existent. We have shown that VacA production is upregulated when *H. pylori* is grown under high salt conditions compared to normal laboratory conditions. I hypothesize that VacA would also be upregulated in *H. pylori*-infected animals consuming a high salt diet. Future studies could utilize the Mongolian gerbil model, an established *H. pylori* infection model,

consuming a normal diet (0.25% sodium chloride) or a high salt diet (8.25% sodium chloride). Changes in expression of VacA can be monitored using RT-PCR analysis of gastric tissue extracts, a method previously used to monitor changes in *cagA* expression in response to a high salt environment (13).

Most gerbil studies thus far have utilized *H. pylori* strain 7.13, which does not produce VacA (125, 127). Using alternate strains (for example, strains PZ5056G and J166) will allow us to study VacA, diet, disease and VacA-CagA interplay. *H. pylori* gerbil adapted strain PZ5056G can result in gastric cancer in the gerbil model (210). Alternatively, mouse strain J166 also secretes an active s1i1m1 VacA and can colonize gerbils (unpublished). Evaluating the effects of wild-type and *vacA* null mutant PZ5056G or J166 in animals receiving a normal and high salt could provide new insights into VacA-CagA interplay, since the strains produce both CagA and s1i1m1 VacA. CagA and VacA have been shown to have an antagonistic relationship by dampening the effects of one another in host cells. A working theory is that this relationship extends the life of host cells, while allowing VacA to intoxicate neighboring cells to release nutrients (185). VacA has been shown to limit CagA-induced nuclear translocation of NFAT, while CagA inhibits VacA induced-apoptosis (87, 185, 211, 212).

A study by Winter et al. analyzed the role of the VacA i-region in colonization of *H. pylori* and the development of metaplasia (124). The group found that mice infected with a strain producing s1i1 VacA acquired extensive metaplasia and gastric inflammation compared to mice infected with strains producing s1i2 or s2i2 VacA (124). This study indicates that differences in disease state can be attributed to differing forms of VacA. The role of the VacA m-region has yet to be explored in any animal model.

Using the gerbil model instead of mice to investigate the role of the m-region in the development of disease will allow for a greater range of disease states to be investigated. In human gastric organoids both m1 and m2 forms are active, implying that both VacA types would be active *in vivo*. I hypothesize that VacA-producing *H. pylori* strains have a colonization advantage, and that gerbils infected with m1 VacA-producing strains may only develop slightly more disease compared to the m2 VacA-producing strain.

Preferential binding of VacA to the basolateral surface of human gastric epithelial monolayers

My studies suggest that VacA preferentially binds the basolateral surface of human gastric organoid monolayers. I propose that this is due to mucus production interfering with the ability of purified VacA to interact with the apical surface or due to differential receptor expression by the apical and basolateral surfaces. Mucus production has been observed on the apical side of the polarized cells. To elucidate if the observed difference in VacA binding to the basolateral and apical surfaces is because of mucus production, the apical compartment of epithelial monolayers could be treated with the mucolytic agent, N-acetylcysteine (NAC). After treating cells with NAC, VacA internalization, binding and vacuolation can be assessed using methods described in Chapter 3. If we do not see an increase in VacA activity once added to the NAC-treated apical compartment, one can assume that the difference in VacA binding is attributable to differential receptor expression by the apical and basolateral compartments. A study has shown that the *cag* type IV secretion system pilus formation

primarily occurs at the basolateral side of polarized cells due to integrin-β_1 being primarily expressed on the basolateral surface (186). It was proposed that HtrA, a secreted serine protease, cleaves epithelial junctional proteins, allowing *H. pylori to* migrate from the apical to basolateral compartments (186). Thus, it is plausible that VacA can also preferentially localize to the basolateral surface of human gastric epithelial monolayers.

Cellular targets of VacA in human gastric organoids

Human gastric organoids have been shown to express genes specific for all five major gastric epithelial cell subsets (parietal cells, chief cells, surface mucus cells, mucus neck cells, and enteroendocrine cells) (204). VacA has been shown to inhibit gastric acid secretion from parietal cells, but whether or not VacA interacts with the other epithelial cell types present in the gastric environment is unknown (213, 214). Due to the relatively large number of putative VacA receptors, I suspect that VacA will interact with a number of these cell types. Assessing binding, internalization, and localization of VacA to certain cell types can be accomplished using fluorescent VacA in conjunction with fluorescent cell markers. Understanding the targeting of VacA to specific cell types can potentially help us develop a better understanding of VacA actions *in vivo*.

REFERENCES

1. Atherton JC, Blaser MJ. 2009. Coadaptation of *Helicobacter pylori* and humans: ancient history, modern implications. J Clin Invest 119:2475-2487.
2. Cover TL, Blaser MJ. 2009. *Helicobacter pylori* in health and disease. Gastroenterology 136:1863-1873.
3. Marshall BJ, Warren JR. 1984. Unidentified curved bacilli in the stomach of patients with gastritis and peptic ulceration. Lancet 1:1311-5.
4. Moodley Y, Linz B, Bond RP, Nieuwoudt M, Soodyall H, Schlebusch CM, Bernhoft S, Hale J, Suerbaum S, Mugisha L, van der Merwe SW, Achtman M. 2012. Age of the association between Helicobacter pylori and man. PLoS Pathog 8:e1002693.
5. Fuchs CS, Mayer RJ. 1995. Gastric carcinoma. N Engl J Med 333:32-41.
6. Forman D, Newell DG, Fullerton F, Yarnell JW, Stacey AR, Wald N, Sitas F. 1991. Association between infection with Helicobacter pylori and risk of gastric cancer: evidence from a prospective investigation. BMJ 302:1302-5.
7. Suerbaum S, Michetti P. 2002. *Helicobacter pylori* infection. N Engl J Med 347:1175-1186.
8. Rawla P, Barsouk A. 2019. Epidemiology of gastric cancer: global trends, risk factors and prevention. Prz Gastroenterol 14:26-38.
9. Cover TL. 2016. *Helicobacter pylori* Diversity and Gastric Cancer Risk. MBio 7:e01869-15.
10. Gore RM. 1997. Gastric cancer. Clinical and pathologic features. Radiol Clin North Am 35:295-310.
11. Cover TL, Peek RM, Jr. 2013. Diet, microbial virulence, and *Helicobacter pylori*-induced gastric cancer. Gut Microbes 4:482-493.
12. Tsugane S. 2005. Salt, salted food intake, and risk of gastric cancer: epidemiologic evidence. Cancer Sci 96:1-6.
13. Gaddy JA, Radin JN, Loh JT, Zhang F, Washington MK, Peek RM, Jr., Algood HM, Cover TL. 2013. High dietary salt intake exacerbates *Helicobacter pylori*-induced gastric carcinogenesis. Infect Immun 81:2258-2267.
14. Fox JG, Rogers AB, Ihrig M, Taylor NS, Whary MT, Dockray G, Varro A, Wang TC. 2003. *Helicobacter pylori*-associated gastric cancer in INS-GAS mice is gender specific. Cancer Res 63:942-950.
15. Gancz H, Jones KR, Merrell DS. 2008. Sodium chloride affects *Helicobacter pylori* growth and gene expression. J Bacteriol 190:4100-4105.
16. Loh JT, Friedman DB, Piazuelo MB, Bravo LE, Wilson KT, Peek RM, Jr., Correa P, Cover TL. 2012. Analysis of *Helicobacter pylori cagA* promoter elements required for salt-induced upregulation of CagA expression. Infect Immun 80:3094-3106.
17. Loh JT, Torres VJ, Cover TL. 2007. Regulation of *Helicobacter pylori cagA* expression in response to salt. Cancer Res 67:4709-4715.
18. Voss BJ, Loh JT, Hill S, Rose KL, McDonald WH, Cover TL. 2015. Alteration of the *Helicobacter pylori* membrane proteome in response to changes in environmental salt concentration. Proteomics Clin Appl 9:1021-1034.

19. Backert S, Tegtmeyer N, Fischer W. 2015. Composition, structure and function of the *Helicobacter pylori cag* pathogenicity island encoded type IV secretion system. Future Microbiol 10:955-965.
20. Frick-Cheng AE, Pyburn TM, Voss BJ, McDonald WH, Ohi MD, Cover TL. 2016. Molecular and Structural Analysis of the *Helicobacter pylori cag* Type IV Secretion System Core Complex. MBio 7:e02001-2015.
21. Hatakeyama M. 2014. *Helicobacter pylori* CagA and gastric cancer: a paradigm for hit-and-run carcinogenesis. Cell Host Microbe 15:306-316.
22. Odenbreit S, Puls J, Sedlmaier B, Gerland E, Fischer W, Haas R. 2000. Translocation of *Helicobacter pylori* CagA into gastric epithelial cells by type IV secretion. Science 287:1497-1500.
23. Tegtmeyer N, Neddermann M, Asche CI, Backert S. 2017. Subversion of host kinases: a key network in cellular signaling hijacked by Helicobacter pylori CagA. Mol Microbiol 105:358-372.
24. Hatakeyama M. 2004. Oncogenic mechanisms of the Helicobacter pylori CagA protein. Nat Rev Cancer 4:688-94.
25. Loh JT, Beckett AC, Scholz MB, Cover TL. 2018. High-Salt Conditions Alter Transcription of Helicobacter pylori Genes Encoding Outer Membrane Proteins. Infect Immun 86.
26. Cover TL, Blaser MJ. 1992. Purification and characterization of the vacuolating toxin from *Helicobacter pylori*. J Biol Chem 267:10570-10575.
27. Cover TL, Tummuru MK, Cao P, Thompson SA, Blaser MJ. 1994. Divergence of genetic sequences for the vacuolating cytotoxin among *Helicobacter pylori* strains. J Biol Chem 269:10566-10573.
28. Leunk RD, Johnson PT, David BC, Kraft WG, Morgan DR. 1988. Cytotoxic activity in broth-culture filtrates of Campylobacter pylori. J Med Microbiol 26:93-9.
29. Phadnis SH, Ilver D, Janzon L, Normark S, Westblom TU. 1994. Pathological significance and molecular characterization of the vacuolating toxin gene of Helicobacter pylori. Infect Immun 62:1557-65.
30. Schmitt W, Haas R. 1994. Genetic analysis of the *Helicobacter pylori* vacuolating cytotoxin: structural similarities with the IgA protease type of exported protein. Mol Microbiol 12:307-319.
31. Telford JL, Ghiara P, Dell'Orco M, Comanducci M, Burroni D, Bugnoli M, Tecce MF, Censini S, Covacci A, Xiang Z, et al. 1994. Gene structure of the *Helicobacter pylori* cytotoxin and evidence of its key role in gastric disease. J Exp Med 179:1653-1658.
32. Forsyth MH, Cover TL. 1999. Mutational analysis of the vacA promoter provides insight into gene transcription in Helicobacter pylori. J Bacteriol 181:2261-6.
33. Snider CA, Voss BJ, McDonald WH, Cover TL. 2016. Growth phase-dependent composition of the Helicobacter pylori exoproteome. J Proteomics 130:94-107.
34. Amilon KR, Letley DP, Winter JA, Robinson K, Atherton JC. 2015. Expression of the Helicobacter pylori virulence factor vacuolating cytotoxin A (vacA) is influenced by a potential stem-loop structure in the 5' untranslated region of the transcript. Mol Microbiol 98:831-46.

35. Bumann D, Aksu S, Wendland M, Janek K, Zimny-Arndt U, Sabarth N, Meyer TF, Jungblut PR. 2002. Proteome analysis of secreted proteins of the gastric pathogen *Helicobacter pylori*. Infect Immun 70:3396-3403.
36. Nguyen VQ, Caprioli RM, Cover TL. 2001. Carboxy-terminal proteolytic processing of *Helicobacter pylori* vacuolating toxin. Infect Immun 69:543-546.
37. Torres VJ, McClain MS, Cover TL. 2004. Interactions between p-33 and p-55 domains of the *Helicobacter pylori* vacuolating cytotoxin (VacA). J Biol Chem 279:2324-2331.
38. Torres VJ, Ivie SE, McClain MS, Cover TL. 2005. Functional properties of the p33 and p55 domains of the Helicobacter pylori vacuolating cytotoxin. J Biol Chem 280:21107-14.
39. de Bernard M, Burroni D, Papini E, Rappuoli R, Telford J, Montecucco C. 1998. Identification of the Helicobacter pylori VacA toxin domain active in the cell cytosol. Infect Immun 66:6014-6.
40. Kim S, Chamberlain AK, Bowie JU. 2004. Membrane channel structure of Helicobacter pylori vacuolating toxin: role of multiple GXXXG motifs in cylindrical channels. Proc Natl Acad Sci U S A 101:5988-91.
41. McClain MS, Iwamoto H, Cao P, Vinion-Dubiel AD, Li Y, Szabo G, Shao Z, Cover TL. 2003. Essential role of a GXXXG motif for membrane channel formation by *Helicobacter pylori* vacuolating toxin. J Biol Chem 278:12101-12108.
42. Vinion-Dubiel AD, McClain MS, Czajkowsky DM, Iwamoto H, Ye D, Cao P, Schraw W, Szabo G, Blanke SR, Shao Z, Cover TL. 1999. A dominant negative mutant of Helicobacter pylori vacuolating toxin (VacA) inhibits VacA-induced cell vacuolation. J Biol Chem 274:37736-42.
43. McClain MS, Czajkowsky DM, Torres VJ, Szabo G, Shao Z, Cover TL. 2006. Random mutagenesis of Helicobacter pylori vacA to identify amino acids essential for vacuolating cytotoxic activity. Infect Immun 74:6188-95.
44. Ye D, Blanke SR. 2000. Mutational analysis of the Helicobacter pylori vacuolating toxin amino terminus: identification of amino acids essential for cellular vacuolation. Infect Immun 68:4354-7.
45. Chambers MG, Pyburn TM, Gonzalez-Rivera C, Collier SE, Eli I, Yip CK, Takizawa Y, Lacy DB, Cover TL, Ohi MD. 2013. Structural analysis of the oligomeric states of *Helicobacter pylori* VacA toxin. J Mol Biol 425:524-535.
46. El-Bez C, Adrian M, Dubochet J, Cover TL. 2005. High resolution structural analysis of Helicobacter pylori VacA toxin oligomers by cryo-negative staining electron microscopy. J Struct Biol 151:215-28.
47. Lupetti P, Heuser JE, Manetti R, Massari P, Lanzavecchia S, Bellon PL, Dallai R, Rappuoli R, Telford JL. 1996. Oligomeric and subunit structure of the Helicobacter pylori vacuolating cytotoxin. J Cell Biol 133:801-7.
48. Su M, Erwin AL, Campbell AM, Pyburn TM, Salay LE, Hanks JL, Lacy DB, Akey DL, Cover TL, Ohi MD. 2019. Cryo-EM Analysis Reveals Structural Basis of *Helicobacter pylori* VacA Toxin Oligomerization. J Mol Biol 431:1956-1965.
49. Zhang K, Zhang H, Li S, Pintilie GD, Mou TC, Gao Y, Zhang Q, van den Bedem H, Schmid MF, Au SWN, Chiu W. 2019. Cryo-EM structures of *Helicobacter pylori* vacuolating cytotoxin A oligomeric assemblies at near-atomic resolution. Proc Natl Acad Sci U S A 116:6800-6805.

50. Cover TL, Hanson PI, Heuser JE. 1997. Acid-induced dissociation of VacA, the Helicobacter pylori vacuolating cytotoxin, reveals its pattern of assembly. J Cell Biol 138:759-69.
51. Yahiro K, Niidome T, Kimura M, Hatakeyama T, Aoyagi H, Kurazono H, Imagawa K, Wada A, Moss J, Hirayama T. 1999. Activation of Helicobacter pylori VacA toxin by alkaline or acid conditions increases its binding to a 250-kDa receptor protein-tyrosine phosphatase beta. J Biol Chem 274:36693-9.
52. de Bernard M, Papini E, de Filippis V, Gottardi E, Telford J, Manetti R, Fontana A, Rappuoli R, Montecucco C. 1995. Low pH activates the vacuolating toxin of Helicobacter pylori, which becomes acid and pepsin resistant. J Biol Chem 270:23937-40.
53. McClain MS, Schraw W, Ricci V, Boquet P, Cover TL. 2000. Acid activation of Helicobacter pylori vacuolating cytotoxin (VacA) results in toxin internalization by eukaryotic cells. Mol Microbiol 37:433-42.
54. Pyburn TM, Foegeding NJ, Gonzalez-Rivera C, McDonald NA, Gould KL, Cover TL, Ohi MD. 2016. Structural organization of membrane-inserted hexamers formed by Helicobacter pylori VacA toxin. Mol Microbiol 102:22-36.
55. Gangwer KA, Mushrush DJ, Stauff DL, Spiller B, McClain MS, Cover TL, Lacy DB. 2007. Crystal structure of the Helicobacter pylori vacuolating toxin p55 domain. Proc Natl Acad Sci U S A 104:16293-8.
56. Gonzalez-Rivera C, Campbell AM, Rutherford SA, Pyburn TM, Foegeding NJ, Barke TL, Spiller BW, McClain MS, Ohi MD, Lacy DB, Cover TL. 2016. A Nonoligomerizing Mutant Form of Helicobacter pylori VacA Allows Structural Analysis of the p33 Domain. Infect Immun 84:2662-70.
57. Genisset C, Galeotti CL, Lupetti P, Mercati D, Skibinski DA, Barone S, Battistutta R, de Bernard M, Telford JL. 2006. A Helicobacter pylori vacuolating toxin mutant that fails to oligomerize has a dominant negative phenotype. Infect Immun 74:1786-94.
58. Ivie SE, McClain MS, Torres VJ, Algood HM, Lacy DB, Yang R, Blanke SR, Cover TL. 2008. Helicobacter pylori VacA subdomain required for intracellular toxin activity and assembly of functional oligomeric complexes. Infect Immun 76:2843-51.
59. Fujikawa A, Shirasaka D, Yamamoto S, Ota H, Yahiro K, Fukada M, Shintani T, Wada A, Aoyama N, Hirayama T, Fukamachi H, Noda M. 2003. Mice deficient in protein tyrosine phosphatase receptor type Z are resistant to gastric ulcer induction by VacA of Helicobacter pylori. Nat Genet 33:375-81.
60. Gupta VR, Patel HK, Kostolansky SS, Ballivian RA, Eichberg J, Blanke SR. 2008. Sphingomyelin functions as a novel receptor for *Helicobacter pylori* VacA. PLoS Pathog 4:e1000073.
61. Gupta VR, Wilson BA, Blanke SR. 2010. Sphingomyelin is important for the cellular entry and intracellular localization of Helicobacter pylori VacA. Cell Microbiol 12:1517-33.
62. Sewald X, Gebert-Vogl B, Prassl S, Barwig I, Weiss E, Fabbri M, Osicka R, Schiemann M, Busch DH, Semmrich M, Holzmann B, Sebo P, Haas R. 2008. Integrin subunit CD18 Is the T-lymphocyte receptor for the Helicobacter pylori vacuolating cytotoxin. Cell Host Microbe 3:20-9.

63. Yahiro K, Satoh M, Nakano M, Hisatsune J, Isomoto H, Sap J, Suzuki H, Nomura F, Noda M, Moss J, Hirayama T. 2012. Low-density lipoprotein receptor-related protein-1 (LRP1) mediates autophagy and apoptosis caused by *Helicobacter pylori* VacA. J Biol Chem 287:31104-31115.
64. Yahiro K, Wada A, Nakayama M, Kimura T, Ogushi K, Niidome T, Aoyagi H, Yoshino K, Yonezawa K, Moss J, Hirayama T. 2003. Protein-tyrosine phosphatase alpha, RPTP alpha, is a Helicobacter pylori VacA receptor. J Biol Chem 278:19183-9.
65. Yahiro K, Wada A, Yamasaki E, Nakayama M, Nishi Y, Hisatsune J, Morinaga N, Sap J, Noda M, Moss J, Hirayama T. 2004. Essential domain of receptor tyrosine phosphatase beta (RPTPbeta) for interaction with Helicobacter pylori vacuolating cytotoxin. J Biol Chem 279:51013-21.
66. Geisse NA, Cover TL, Henderson RM, Edwardson JM. 2004. Targeting of Helicobacter pylori vacuolating toxin to lipid raft membrane domains analysed by atomic force microscopy. Biochem J 381:911-7.
67. Patel HK, Willhite DC, Patel RM, Ye D, Williams CL, Torres EM, Marty KB, MacDonald RA, Blanke SR. 2002. Plasma membrane cholesterol modulates cellular vacuolation induced by the Helicobacter pylori vacuolating cytotoxin. Infect Immun 70:4112-23.
68. Raghunathan K, Foegeding NJ, Campbell AM, Cover TL, Ohi MD, Kenworthy AK. 2018. Determinants of Raft Partitioning of the Helicobacter pylori Pore-Forming Toxin VacA. Infect Immun 86.
69. Schraw W, Li Y, McClain MS, van der Goot FG, Cover TL. 2002. Association of Helicobacter pylori vacuolating toxin (VacA) with lipid rafts. J Biol Chem 277:34642-50.
70. Gauthier NC, Monzo P, Gonzalez T, Doye A, Oldani A, Gounon P, Ricci V, Cormont M, Boquet P. 2007. Early endosomes associated with dynamic F-actin structures are required for late trafficking of H. pylori VacA toxin. J Cell Biol 177:343-54.
71. Gauthier NC, Monzo P, Kaddai V, Doye A, Ricci V, Boquet P. 2005. Helicobacter pylori VacA cytotoxin: a probe for a clathrin-independent and Cdc42-dependent pinocytic pathway routed to late endosomes. Mol Biol Cell 16:4852-66.
72. Gauthier NC, Ricci V, Gounon P, Doye A, Tauc M, Poujeol P, Boquet P. 2004. Glycosylphosphatidylinositol-anchored proteins and actin cytoskeleton modulate chloride transport by channels formed by the Helicobacter pylori vacuolating cytotoxin VacA in HeLa cells. J Biol Chem 279:9481-9.
73. Sewald X, Jimenez-Soto L, Haas R. 2011. PKC-dependent endocytosis of the Helicobacter pylori vacuolating cytotoxin in primary T lymphocytes. Cell Microbiol 13:482-96.
74. Calore F, Genisset C, Casellato A, Rossato M, Codolo G, Esposti MD, Scorrano L, de Bernard M. 2010. Endosome-mitochondria juxtaposition during apoptosis induced by H. pylori VacA. Cell Death Differ 17:1707-16.
75. Willhite DC, Blanke SR. 2004. Helicobacter pylori vacuolating cytotoxin enters cells, localizes to the mitochondria, and induces mitochondrial membrane permeability changes correlated to toxin channel activity. Cell Microbiol 6:143-54.

76. Kern B, Jain U, Utsch C, Otto A, Busch B, Jimenez-Soto L, Becher D, Haas R. 2015. Characterization of Helicobacter pylori VacA-containing vacuoles (VCVs), VacA intracellular trafficking and interference with calcium signalling in T lymphocytes. Cell Microbiol 17:1811-32.
77. Boncristiano M, Paccani SR, Barone S, Ulivieri C, Patrussi L, Ilver D, Amedei A, D'Elios MM, Telford JL, Baldari CT. 2003. The Helicobacter pylori vacuolating toxin inhibits T cell activation by two independent mechanisms. J Exp Med 198:1887-97.
78. Hisatsune J, Yamasaki E, Nakayama M, Shirasaka D, Kurazono H, Katagata Y, Inoue H, Han J, Sap J, Yahiro K, Moss J, Hirayama T. 2007. Helicobacter pylori VacA enhances prostaglandin E2 production through induction of cyclooxygenase 2 expression via a p38 mitogen-activated protein kinase/activating transcription factor 2 cascade in AZ-521 cells. Infect Immun 75:4472-81.
79. Nakayama M, Kimura M, Wada A, Yahiro K, Ogushi K, Niidome T, Fujikawa A, Shirasaka D, Aoyama N, Kurazono H, Noda M, Moss J, Hirayama T. 2004. *Helicobacter pylori* VacA activates the p38/activating transcription factor 2-mediated signal pathway in AZ-521 cells. J Biol Chem 279:7024-7028.
80. Caputo R, Tuccillo C, Manzo BA, Zarrilli R, Tortora G, Blanco Cdel V, Ricci V, Ciardiello F, Romano M. 2003. Helicobacter pylori VacA toxin up-regulates vascular endothelial growth factor expression in MKN 28 gastric cells through an epidermal growth factor receptor-, cyclooxygenase-2-dependent mechanism. Clin Cancer Res 9:2015-21.
81. Nakayama M, Hisatsune J, Yamasaki E, Isomoto H, Kurazono H, Hatakeyama M, Azuma T, Yamaoka Y, Yahiro K, Moss J, Hirayama T. 2009. Helicobacter pylori VacA-induced inhibition of GSK3 through the PI3K/Akt signaling pathway. J Biol Chem 284:1612-9.
82. Genisset C, Puhar A, Calore F, de Bernard M, Dell'Antone P, Montecucco C. 2007. The concerted action of the Helicobacter pylori cytotoxin VacA and of the v-ATPase proton pump induces swelling of isolated endosomes. Cell Microbiol 9:1481-90.
83. Morbiato L, Tombola F, Campello S, Del Giudice G, Rappuoli R, Zoratti M, Papini E. 2001. Vacuolation induced by VacA toxin of Helicobacter pylori requires the intracellular accumulation of membrane permeant bases, Cl(-) and water. FEBS Lett 508:479-83.
84. Ricci V, Sommi P, Fiocca R, Romano M, Solcia E, Ventura U. 1997. Helicobacter pylori vacuolating toxin accumulates within the endosomal-vacuolar compartment of cultured gastric cells and potentiates the vacuolating activity of ammonia. J Pathol 183:453-9.
85. Cover TL, Krishna US, Israel DA, Peek RM, Jr. 2003. Induction of gastric epithelial cell apoptosis by Helicobacter pylori vacuolating cytotoxin. Cancer Res 63:951-7.
86. Kuck D, Kolmerer B, Iking-Konert C, Krammer PH, Stremmel W, Rudi J. 2001. Vacuolating cytotoxin of Helicobacter pylori induces apoptosis in the human gastric epithelial cell line AGS. Infect Immun 69:5080-7.

87. Oldani A, Cormont M, Hofman V, Chiozzi V, Oregioni O, Canonici A, Sciullo A, Sommi P, Fabbri A, Ricci V, Boquet P. 2009. Helicobacter pylori counteracts the apoptotic action of its VacA toxin by injecting the CagA protein into gastric epithelial cells. PLoS Pathog 5:e1000603.
88. Radin JN, Gonzalez-Rivera C, Ivie SE, McClain MS, Cover TL. 2011. Helicobacter pylori VacA induces programmed necrosis in gastric epithelial cells. Infect Immun 79:2535-43.
89. Ricci V. 2016. Relationship between VacA Toxin and Host Cell Autophagy in Helicobacter pylori Infection of the Human Stomach: A Few Answers, Many Questions. Toxins (Basel) 8.
90. Amieva MR, Vogelmann R, Covacci A, Tompkins LS, Nelson WJ, Falkow S. 2003. Disruption of the epithelial apical-junctional complex by Helicobacter pylori CagA. Science 300:1430-4.
91. Papini E, Satin B, Norais N, de Bernard M, Telford JL, Rappuoli R, Montecucco C. 1998. Selective increase of the permeability of polarized epithelial cell monolayers by Helicobacter pylori vacuolating toxin. J Clin Invest 102:813-20.
92. Pelicic V, Reyrat JM, Sartori L, Pagliaccia C, Rappuoli R, Telford JL, Montecucco C, Papini E. 1999. Helicobacter pylori VacA cytotoxin associated with the bacteria increases epithelial permeability independently of its vacuolating activity. Microbiology 145 (Pt 8):2043-2050.
93. Yamasaki E, Wada A, Kumatori A, Nakagawa I, Funao J, Nakayama M, Hisatsune J, Kimura M, Moss J, Hirayama T. 2006. Helicobacter pylori vacuolating cytotoxin induces activation of the proapoptotic proteins Bax and Bak, leading to cytochrome c release and cell death, independent of vacuolation. J Biol Chem 281:11250-9.
94. Gebert B, Fischer W, Weiss E, Hoffmann R, Haas R. 2003. Helicobacter pylori vacuolating cytotoxin inhibits T lymphocyte activation. Science 301:1099-102.
95. Sundrud MS, Torres VJ, Unutmaz D, Cover TL. 2004. Inhibition of primary human T cell proliferation by Helicobacter pylori vacuolating toxin (VacA) is independent of VacA effects on IL-2 secretion. Proc Natl Acad Sci U S A 101:7727-32.
96. Torres VJ, VanCompernolle SE, Sundrud MS, Unutmaz D, Cover TL. 2007. Helicobacter pylori vacuolating cytotoxin inhibits activation-induced proliferation of human T and B lymphocyte subsets. J Immunol 179:5433-40.
97. Allen LA. 2000. Modulating phagocyte activation: the pros and cons of Helicobacter pylori virulence factors. J Exp Med 191:1451-4.
98. Zheng PY, Jones NL. 2003. Helicobacter pylori strains expressing the vacuolating cytotoxin interrupt phagosome maturation in macrophages by recruiting and retaining TACO (coronin 1) protein. Cell Microbiol 5:25-40.
99. Ito Y, Azuma T, Ito S, Suto H, Miyaji H, Yamazaki Y, Kohli Y, Kuriyama M. 1998. Full-length sequence analysis of the vacA gene from cytotoxic and noncytotoxic Helicobacter pylori. J Infect Dis 178:1391-8.
100. Gangwer KA, Shaffer CL, Suerbaum S, Lacy DB, Cover TL, Bordenstein SR. 2010. Molecular evolution of the Helicobacter pylori vacuolating toxin gene vacA. J Bacteriol 192:6126-35.

101. Duncan SS, Valk PL, McClain MS, Shaffer CL, Metcalf JA, Bordenstein SR, Cover TL. 2013. Comparative genomic analysis of East Asian and non-Asian *Helicobacter pylori* strains identifies rapidly evolving genes. PLoS One 8:e55120.
102. Atherton JC, Cao P, Peek RM, Jr., Tummuru MK, Blaser MJ, Cover TL. 1995. Mosaicism in vacuolating cytotoxin alleles of *Helicobacter pylori*. Association of specific *vacA* types with cytotoxin production and peptic ulceration. J Biol Chem 270:17771-17777.
103. Rhead JL, Letley DP, Mohammadi M, Hussein N, Mohagheghi MA, Eshagh Hosseini M, Atherton JC. 2007. A new *Helicobacter pylori* vacuolating cytotoxin determinant, the intermediate region, is associated with gastric cancer. Gastroenterology 133:926-936.
104. Letley DP, Atherton JC. 2000. Natural diversity in the N terminus of the mature vacuolating cytotoxin of *Helicobacter pylori* determines cytotoxin activity. J Bacteriol 182:3278-3280.
105. Letley DP, Rhead JL, Twells RJ, Dove B, Atherton JC. 2003. Determinants of non-toxicity in the gastric pathogen Helicobacter pylori. J Biol Chem 278:26734-41.
106. McClain MS, Cao P, Iwamoto H, Vinion-Dubiel AD, Szabo G, Shao Z, Cover TL. 2001. A 12-Amino-Acid Segment, Present in Type s2 but Not Type s1 Helicobacter pylori VacA Proteins, Abolishes Cytotoxin Activity and Alters Membrane Channel Formation. J Bacteriol 183:6499-508.
107. Van Doorn LJ, Figueiredo C, Megraud F, Pena S, Midolo P, Queiroz DM, Carneiro F, Vanderborght B, Pegado MD, Sanna R, De Boer W, Schneeberger PM, Correa P, Ng EK, Atherton J, Blaser MJ, Quint WG. 1999. Geographic distribution of *vacA* allelic types of *Helicobacter pylori*. Gastroenterology 116:823-830.
108. Ogiwara H, Sugimoto M, Ohno T, Vilaichone RK, Mahachai V, Graham DY, Yamaoka Y. 2009. Role of deletion located between the intermediate and middle regions of the *Helicobacter pylori* vacA gene in cases of gastroduodenal diseases. J Clin Microbiol 47:3493-3500.
109. Tombola F, Pagliaccia C, Campello S, Telford JL, Montecucco C, Papini E, Zoratti M. 2001. How the loop and middle regions influence the properties of *Helicobacter pylori* VacA channels. Biophys J 81:3204-3215.
110. Burroni D, Lupetti P, Pagliaccia C, Reyrat JM, Dallai R, Rappuoli R, Telford JL. 1998. Deletion of the major proteolytic site of the Helicobacter pylori cytotoxin does not influence toxin activity but favors assembly of the toxin into hexameric structures. Infect Immun 66:5547-50.
111. Gonzalez-Rivera C, Algood HM, Radin JN, McClain MS, Cover TL. 2012. The intermediate region of *Helicobacter pylori* VacA is a determinant of toxin potency in a Jurkat T cell assay. Infect Immun 80:2578-2588.
112. Ji X, Fernandez T, Burroni D, Pagliaccia C, Atherton JC, Reyrat JM, Rappuoli R, Telford JL. 2000. Cell specificity of helicobacter pylori cytotoxin is determined by a short region in the polymorphic midregion. Infect Immun 68:3754-7.
113. Pagliaccia C, de Bernard M, Lupetti P, Ji X, Burroni D, Cover TL, Papini E, Rappuoli R, Telford JL, Reyrat JM. 1998. The m2 form of the Helicobacter pylori

cytotoxin has cell type-specific vacuolating activity. Proc Natl Acad Sci U S A 95:10212-7.
114. Figueiredo C, Machado JC, Pharoah P, Seruca R, Sousa S, Carvalho R, Capelinha AF, Quint W, Caldas C, van Doorn LJ, Carneiro F, Sobrinho-Simoes M. 2002. *Helicobacter pylori* and interleukin 1 genotyping: an opportunity to identify high-risk individuals for gastric carcinoma. J Natl Cancer Inst 94:1680-1687.
115. Matos JI, de Sousa HA, Marcos-Pinto R, Dinis-Ribeiro M. 2013. *Helicobacter pylori* CagA and VacA genotypes and gastric phenotype: a meta-analysis. Eur J Gastroenterol Hepatol 25:1431-1441.
116. Machado JC, Figueiredo C, Canedo P, Pharoah P, Carvalho R, Nabais S, Castro Alves C, Campos ML, Van Doorn LJ, Caldas C, Seruca R, Carneiro F, Sobrinho-Simoes M. 2003. A proinflammatory genetic profile increases the risk for chronic atrophic gastritis and gastric carcinoma. Gastroenterology 125:364-71.
117. Atherton JC, Peek RM, Jr., Tham KT, Cover TL, Blaser MJ. 1997. Clinical and pathological importance of heterogeneity in vacA, the vacuolating cytotoxin gene of Helicobacter pylori. Gastroenterology 112:92-9.
118. van Doorn LJ, Figueiredo C, Sanna R, Plaisier A, Schneeberger P, de Boer W, Quint W. 1998. Clinical relevance of the cagA, vacA, and iceA status of Helicobacter pylori. Gastroenterology 115:58-66.
119. Ghiara P, Marchetti M, Blaser MJ, Tummuru MK, Cover TL, Segal ED, Tompkins LS, Rappuoli R. 1995. Role of the Helicobacter pylori virulence factors vacuolating cytotoxin, CagA, and urease in a mouse model of disease. Infect Immun 63:4154-60.
120. Supajatura V, Ushio H, Wada A, Yahiro K, Okumura K, Ogawa H, Hirayama T, Ra C. 2002. Cutting edge: VacA, a vacuolating cytotoxin of Helicobacter pylori, directly activates mast cells for migration and production of proinflammatory cytokines. J Immunol 168:2603-7.
121. Eaton KA, Cover TL, Tummuru MK, Blaser MJ, Krakowka S. 1997. Role of vacuolating cytotoxin in gastritis due to Helicobacter pylori in gnotobiotic piglets. Infect Immun 65:3462-4.
122. Salama NR, Otto G, Tompkins L, Falkow S. 2001. Vacuolating cytotoxin of Helicobacter pylori plays a role during colonization in a mouse model of infection. Infect Immun 69:730-6.
123. Oertli M, Noben M, Engler DB, Semper RP, Reuter S, Maxeiner J, Gerhard M, Taube C, Muller A. 2013. *Helicobacter pylori* gamma-glutamyl transpeptidase and vacuolating cytotoxin promote gastric persistence and immune tolerance. Proc Natl Acad Sci U S A 110:3047-3052.
124. Winter JA, Letley DP, Cook KW, Rhead JL, Zaitoun AA, Ingram RJ, Amilon KR, Croxall NJ, Kaye PV, Robinson K, Atherton JC. 2014. A role for the vacuolating cytotoxin, VacA, in colonization and Helicobacter pylori-induced metaplasia in the stomach. J Infect Dis 210:954-63.
125. Loh JT, Gaddy JA, Algood HM, Gaudieri S, Mallal S, Cover TL. 2015. Helicobacter pylori adaptation in vivo in response to a high-salt diet. Infect Immun 83:4871-83.

126. Beckett AC, Piazuelo MB, Noto JM, Peek RM, Jr., Washington MK, Algood HM, Cover TL. 2016. Dietary composition influences incidence of Helicobacter pylori-induced iron deficiency anemia and gastric ulceration. Infect Immun doi:10.1128/IAI.00479-16.
127. McClain MS, Shaffer CL, Israel DA, Peek RM, Cover TL. 2009. Genome sequence analysis of Helicobacter pylori strains associated with gastric ulceration and gastric cancer. Bmc Genomics 10.
128. Ogura K, Maeda S, Nakao M, Watanabe T, Tada M, Kyutoku T, Yoshida H, Shiratori Y, Omata M. 2000. Virulence factors of Helicobacter pylori responsible for gastric diseases in Mongolian gerbil. J Exp Med 192:1601-10.
129. Wang WC, Wang HJ, Kuo CH. 2001. Two distinctive cell binding patterns by vacuolating toxin fused with glutathione S-transferase: one high-affinity m1-specific binding and the other lower-affinity binding for variant m forms. Biochemistry 40:11887-96.
130. Blaser MJ, Berg DE. 2001. *Helicobacter pylori* genetic diversity and risk of human disease. J Clin Invest 107:767-773.
131. Suerbaum S, Josenhans C. 2007. *Helicobacter pylori* evolution and phenotypic diversification in a changing host. Nat Rev Microbiol 5:441-452.
132. Cover TL, Blaser MJ. 1992. Purification and characterization of the vacuolating toxin from Helicobacter pylori. J Biol Chem 267:10570-5.
133. Cover TL, Blanke SR. 2005. Helicobacter pylori VacA, a paradigm for toxin multifunctionality. Nat Rev Microbiol 3:320-32.
134. Atherton JC, Cao P, Peek RM, Jr., Tummuru MK, Blaser MJ, Cover TL. 1995. Mosaicism in vacuolating cytotoxin alleles of Helicobacter pylori. Association of specific vacA types with cytotoxin production and peptic ulceration. J Biol Chem 270:17771-7.
135. Olbermann P, Josenhans C, Moodley Y, Uhr M, Stamer C, Vauterin M, Suerbaum S, Achtman M, Linz B. 2010. A global overview of the genetic and functional diversity in the Helicobacter pylori cag pathogenicity island. PLoS Genet 6:e1001069.
136. Cao P, Cover TL. 2002. Two different families of *hopQ* alleles in *Helicobacter pylori*. J Clin Microbiol 40:4504-4511.
137. Mahdavi J, Sonden B, Hurtig M, Olfat FO, Forsberg L, Roche N, Angstrom J, Larsson T, Teneberg S, Karlsson KA, Altraja S, Wadstrom T, Kersulyte D, Berg DE, Dubois A, Petersson C, Magnusson KE, Norberg T, Lindh F, Lundskog BB, Arnqvist A, Hammarstrom L, Boren T. 2002. *Helicobacter pylori* SabA adhesin in persistent infection and chronic inflammation. Science 297:573-578.
138. Ilver D, Arnqvist A, Ogren J, Frick IM, Kersulyte D, Incecik ET, Berg DE, Covacci A, Engstrand L, Boren T. 1998. *Helicobacter pylori* adhesin binding fucosylated histo-blood group antigens revealed by retagging. Science 279:373-377.
139. Berthenet E, Yahara K, Thorell K, Pascoe B, Meric G, Mikhail JM, Engstrand L, Enroth H, Burette A, Megraud F, Varon C, Atherton JC, Smith S, Wilkinson TS, Hitchings MD, Falush D, Sheppard SK. 2018. A GWAS on *Helicobacter pylori* strains points to genetic variants associated with gastric cancer risk. BMC Biol 16:84.

140. Cover TL, Peek RM, Jr. 2013. Diet, microbial virulence, and Helicobacter pylori-induced gastric cancer. Gut Microbes 4:482-93.
141. Gaddy JA, Radin JN, Loh JT, Zhang F, Washington MK, Peek RM, Jr., Algood HM, Cover TL. 2013. High Dietary Salt Intake Exacerbates Helicobacter pylori-Induced Gastric Carcinogenesis. Infect Immun 81:2258-67.
142. Fox JG, Dangler CA, Taylor NS, King A, Koh TJ, Wang TC. 1999. High-salt diet induces gastric epithelial hyperplasia and parietal cell loss, and enhances *Helicobacter pylori* colonization in C57BL/6 mice. Cancer Res 59:4823-4828.
143. Loh JT, Lin AS, Beckett AC, McClain MS, Cover TL. 2018. Role of a stem-loop structure in *Helicobacter pylori cagA* transcript stability. Infect Immun doi:10.1128/IAI.00692-18.
144. Loh JT, Torres VJ, Cover TL. 2007. Regulation of Helicobacter pylori cagA expression in response to salt. Cancer Res 67:4709-15.
145. Fischer W, Buhrdorf R, Gerland E, Haas R. 2001. Outer membrane targeting of passenger proteins by the vacuolating cytotoxin autotransporter of *Helicobacter pylori*. Infect Immun 69:6769-6775.
146. Cover TL, Blanke SR. 2005. *Helicobacter pylori* VacA, a paradigm for toxin multifunctionality. Nat Rev Microbiol 3:320-332.
147. Kim N, Weeks DL, Shin JM, Scott DR, Young MK, Sachs G. 2002. Proteins released by Helicobacter pylori in vitro. J Bacteriol 184:6155-62.
148. Smith TG, Lim JM, Weinberg MV, Wells L, Hoover TR. 2007. Direct analysis of the extracellular proteome from two strains of *Helicobacter pylori*. Proteomics 7:2240-2245.
149. Hawrylik SJ, Wasilko DJ, Haskell SL, Gootz TD, Lee SE. 1994. Bisulfite or sulfite inhibits growth of *Helicobacter pylori*. J Clin Microbiol 32:790-792.
150. Voss BJ, Gaddy JA, McDonald WH, Cover TL. 2014. Analysis of Surface-Exposed Outer Membrane Proteins in Helicobacter pylori. J Bacteriol 196:2455-2471.
151. Schraw W, Li Y, McClain MS, van der Goot FG, Cover TL. 2002. Association of *Helicobacter pylori* vacuolating toxin (VacA) with lipid rafts. J Biol Chem 277:34642-34650.
152. Lo CC, Chain PS. 2014. Rapid evaluation and quality control of next generation sequencing data with FaQCs. BMC Bioinformatics 15:366.
153. Bray NL, Pimentel H, Melsted P, Pachter L. 2016. Near-optimal probabilistic RNA-seq quantification. Nat Biotechnol 34:525-527.
154. Tomb JF, White O, Kerlavage AR, Clayton RA, Sutton GG, Fleischmann RD, Ketchum KA, Klenk HP, Gill S, Dougherty BA, Nelson K, Quackenbush J, Zhou LX, Kirkness EF, Peterson S, Loftus B, Richardson D, Dodson R, Khalak HG, Glodek A, McKenney K, Fitzegerald LM, Lee N, Adams MD, Hickey EK, Berg DE, Gocayne JD, Utterback TR, Peterson JD, Kelley JM, Cotton MD, Weldman JM, Fujii C, Bowman C, Watthey L, Wallin E, Hayes WS, Weidman JM, Fujii C, Borodovsky M, Karp PD, Smith HO, Fraser CM, Venter JC. 1997. The complete genome sequence of the gastric pathogen *Helicobacter pylori*. Nature 388:539-547.

155. Robinson MD, McCarthy DJ, Smyth GK. 2010. edgeR: a Bioconductor package for differential expression analysis of digital gene expression data. Bioinformatics 26:139-140.
156. Phadnis SH, Parlow MH, Levy M, Ilver D, Caulkins CM, Connors JB, Dunn BE. 1996. Surface localization of *Helicobacter pylori* urease and a heat shock protein homolog requires bacterial autolysis. Infect Immun 64:905-912.
157. Cao P, McClain MS, Forsyth MH, Cover TL. 1998. Extracellular release of antigenic proteins by Helicobacter pylori. Infect Immun 66:2984-6.
158. Ogura M, Perez JC, Mittl PR, Lee HK, Dailide G, Tan S, Ito Y, Secka O, Dailidiene D, Putty K, Berg DE, Kalia A. 2007. *Helicobacter pylori* evolution: lineage- specific adaptations in homologs of eukaryotic Sel1-like genes. PLoS Comput Biol 3:1455-1467.
159. Basak C, Pathak SK, Bhattacharyya A, Pathak S, Basu J, Kundu M. 2005. The secreted peptidyl prolyl cis,trans-isomerase HP0175 of *Helicobacter pylori* induces apoptosis of gastric epithelial cells in a TLR4- and apoptosis signal-regulating kinase 1-dependent manner. J Immunol 174:5672-5680.
160. Halder P, Datta C, Kumar R, Sharma AK, Basu J, Kundu M. 2015. The secreted antigen, HP0175, of *Helicobacter pylori* links the unfolded protein response (UPR) to autophagy in gastric epithelial cells. Cell Microbiol 17:714-729.
161. Amedei A, Munari F, Bella CD, Niccolai E, Benagiano M, Bencini L, Cianchi F, Farsi M, Emmi G, Zanotti G, de Bernard M, Kundu M, D'Elios MM. 2014. *Helicobacter pylori* secreted peptidyl prolyl cis, trans-isomerase drives Th17 inflammation in gastric adenocarcinoma. Intern Emerg Med 9:303-309.
162. Deml L, Aigner M, Decker J, Eckhardt A, Schutz C, Mittl PR, Barabas S, Denk S, Knoll G, Lehn N, Schneider-Brachert W. 2005. Characterization of the *Helicobacter pylori* cysteine-rich protein A as a T-helper cell type 1 polarizing agent. Infect Immun 73:4732-4742.
163. Dumrese C, Slomianka L, Ziegler U, Choi SS, Kalia A, Fulurija A, Lu W, Berg DE, Benghezal M, Marshall B, Mittl PR. 2009. The secreted *Helicobacter* cysteine-rich protein A causes adherence of human monocytes and differentiation into a macrophage-like phenotype. FEBS Lett 583:1637-1643.
164. Hoy B, Lower M, Weydig C, Carra G, Tegtmeyer N, Geppert T, Schroder P, Sewald N, Backert S, Schneider G, Wessler S. 2010. *Helicobacter pylori* HtrA is a new secreted virulence factor that cleaves E-cadherin to disrupt intercellular adhesion. EMBO Rep 11:798-804.
165. Tegtmeyer N, Wessler S, Necchi V, Rohde M, Harrer A, Rau TT, Asche CI, Boehm M, Loessner H, Figueiredo C, Naumann M, Palmisano R, Solcia E, Ricci V, Backert S. 2017. *Helicobacter pylori* Employs a Unique Basolateral Type IV Secretion Mechanism for CagA Delivery. Cell Host Microbe 22:552-560
166. Shibayama K, Kamachi K, Nagata N, Yagi T, Nada T, Doi Y, Shibata N, Yokoyama K, Yamane K, Kato H, Iinuma Y, Arakawa Y. 2003. A novel apoptosis-inducing protein from Helicobacter pylori. Mol Microbiol 47:443-51.
167. Schmees C, Prinz C, Treptau T, Rad R, Hengst L, Voland P, Bauer S, Brenner L, Schmid RM, Gerhard M. 2007. Inhibition of T-cell proliferation by *Helicobacter pylori* gamma-glutamyl transpeptidase. Gastroenterology 132:1820-1833.

168. Tavares R, Pathak SK. 2018. Induction of TNF, CXCL8 and IL-1beta in macrophages by *Helicobacter pylori* secreted protein HP1173 occurs via MAP-kinases, NF-kappaB and AP-1 signaling pathways. Microb Pathog 125:295-305.
169. Li J, Meng FL, He LH, Zhang JZ. 2012. Secreted protein HP1286 of *Helicobacter pylori* strain 26695 induces apoptosis of AGS cells. Biomed Environ Sci 25:614-619.
170. Tavares R, Pathak SK. 2017. *Helicobacter pylori* Secreted Protein HP1286 Triggers Apoptosis in Macrophages via TNF-Independent and ERK MAPK-Dependent Pathways. Front Cell Infect Microbiol 7:58.
171. Capitani N, Codolo G, Vallese F, Minervini G, Grassi A, Cianchi F, Troilo A, Fischer W, Zanotti G, Baldari CT, de Bernard M, D'Elios MM. 2019. The lipoprotein HP1454 of *Helicobacter pylori* regulates T-cell response by shaping T-cell receptor signalling. Cell Microbiol 21:e13006.
172. Almagro Armenteros JJ, Tsirigos KD, Sonderby CK, Petersen TN, Winther O, Brunak S, von Heijne G, Nielsen H. 2019. SignalP 5.0 improves signal peptide predictions using deep neural networks. Nat Biotechnol 37:420-423.
173. Hayat S, Elofsson A. 2012. BOCTOPUS: improved topology prediction of transmembrane beta barrel proteins. Bioinformatics 28:516-522.
174. Sharma CM, Hoffmann S, Darfeuille F, Reignier J, Findeiss S, Sittka A, Chabas S, Reiche K, Hackermuller J, Reinhardt R, Stadler PF, Vogel J. 2010. The primary transcriptome of the major human pathogen Helicobacter pylori. Nature 464:250-5.
175. Gancz H, Jones KR, Merrell DS. 2008. Sodium chloride affects Helicobacter pylori growth and gene expression. J Bacteriol 190:4100-5.
176. Coppens F, Castaldo G, Debraekeleer A, Subedi S, Moonens K, Lo A, Remaut H. 2018. Hop-family *Helicobacter* outer membrane adhesins form a novel class of Type 5-like secretion proteins with an interrupted beta-barrel domain. Mol Microbiol 110:33-46.
177. Zavan L, Bitto NJ, Johnston EL, Greening DW, Kaparakis-Liaskos M. 2018. *Helicobacter pylori* Growth Stage Determines the Size, Protein Composition, and Preferential Cargo Packaging of Outer Membrane Vesicles. Proteomics doi:10.1002/pmic.201800209:e1800209.
178. Cover TL, Blaser MJ. 2009. Helicobacter pylori in health and disease. Gastroenterology 136:1863-73.
179. Foegeding NJ, Caston RR, McClain MS, Ohi MD, Cover TL. 2016. An Overview of *Helicobacter pylori* VacA Toxin Biology. Toxins (Basel) 8.
180. Junaid M, Linn AK, Javadi MB, Al-Gubare S, Ali N, Katzenmeier G. 2016. Vacuolating cytotoxin A (VacA) - A multi-talented pore-forming toxin from *Helicobacter pylori*. Toxicon 118:27-35.
181. Kim IJ, Blanke SR. 2012. Remodeling the host environment: modulation of the gastric epithelium by the *Helicobacter pylori* vacuolating toxin (VacA). Front Cell Infect Microbiol 2:37.
182. Palframan SL, Kwok T, Gabriel K. 2012. Vacuolating cytotoxin A (VacA), a key toxin for *Helicobacter pylori* pathogenesis. Front Cell Infect Microbiol 2:92.

183. Backert S, Tegtmeyer N. 2010. The versatility of the *Helicobacter pylori* vacuolating cytotoxin vacA in signal transduction and molecular crosstalk. Toxins (Basel) 2:69-92.
184. Boquet P, Ricci V. 2012. Intoxication strategy of *Helicobacter pylori* VacA toxin. Trends Microbiol 20:165-174.
185. Jones KR, Whitmire JM, Merrell DS. 2010. A Tale of Two Toxins: *Helicobacter pylori* CagA and VacA Modulate Host Pathways that Impact Disease. Front Microbiol 1:115.
186. Tegtmeyer N, Wessler S, Necchi V, Rohde M, Harrer A, Rau TT, Asche CI, Boehm M, Loessner H, Figueiredo C, Naumann M, Palmisano R, Solcia E, Ricci V, Backert S. 2017. Helicobacter pylori Employs a Unique Basolateral Type IV Secretion Mechanism for CagA Delivery. Cell Host Microbe 22:552-560 e5.
187. Torres VJ, McClain MS, Cover TL. 2004. Interactions between p-33 and p-55 domains of the Helicobacter pylori vacuolating cytotoxin (VacA). J Biol Chem 279:2324-31.
188. Gonzalez-Rivera C, Algood HM, Radin JN, McClain MS, Cover TL. 2012. The intermediate region of Helicobacter pylori VacA is a determinant of toxin potency in a Jurkat T cell assay. Infect Immun 80:2578-88.
189. Figueiredo C, Machado JC, Pharoah P, Seruca R, Sousa S, Carvalho R, Capelinha AF, Quint W, Caldas C, van Doorn LJ, Carneiro F, Sobrinho-Simoes M. 2002. Helicobacter pylori and interleukin 1 genotyping: an opportunity to identify high-risk individuals for gastric carcinoma. J Natl Cancer Inst 94:1680-7.
190. Ferreira RM, Machado JC, Figueiredo C. 2014. Clinical relevance of *Helicobacter pylori vacA* and *cagA* genotypes in gastric carcinoma. Best Pract Res Clin Gastroenterol 28:1003-1015.
191. McClain MS, Beckett AC, Cover TL. 2017. *Helicobacter pylori* Vacuolating Toxin and Gastric Cancer. Toxins (Basel) 9.
192. Capurro MI, Greenfield LK, Prashar A, Xia S, Abdullah M, Wong H, Zhong XZ, Bertaux-Skeirik N, Chakrabarti J, Siddiqui I, O'Brien C, Dong X, Robinson L, Peek RM, Jr., Philpott DJ, Zavros Y, Helmrath M, Jones NL. 2019. VacA generates a protective intracellular reservoir for *Helicobacter pylori* that is eliminated by activation of the lysosomal calcium channel TRPML1. Nat Microbiol 4:1411-1423.
193. Djekic A, Muller A. 2016. The Immunomodulator VacA Promotes Immune Tolerance and Persistent *Helicobacter pylori* Infection through Its Activities on T-Cells and Antigen-Presenting Cells. Toxins (Basel) 8.
194. Utsch C, Haas R. 2016. VacA's Induction of VacA-Containing Vacuoles (VCVs) and Their Immunomodulatory Activities on Human T Cells. Toxins (Basel) 8.
195. Czajkowsky DM, Iwamoto H, Cover TL, Shao Z. 1999. The vacuolating toxin from Helicobacter pylori forms hexameric pores in lipid bilayers at low pH. Proc Natl Acad Sci U S A 96:2001-6.
196. Iwamoto H, Czajkowsky DM, Cover TL, Szabo G, Shao Z. 1999. VacA from Helicobacter pylori: a hexameric chloride channel. FEBS Lett 450:101-4.
197. Tombola F, Carlesso C, Szabo I, de Bernard M, Reyrat JM, Telford JL, Rappuoli R, Montecucco C, Papini E, Zoratti M. 1999. Helicobacter pylori vacuolating toxin

forms anion-selective channels in planar lipid bilayers: possible implications for the mechanism of cellular vacuolation. Biophys J 76:1401-9.
198. Wang WC, Wang HJ, Kuo CH. 2001. Two distinctive cell binding patterns by vacuolating toxin fused with glutathione S-transferase: one high-affinity m1-specific binding and the other lower-affinity binding for variant m forms. Biochemistry 40:11887-11896.
199. Skibinski DA, Genisset C, Barone S, Telford JL. 2006. The cell-specific phenotype of the polymorphic vacA midregion is independent of the appearance of the cell surface receptor protein tyrosine phosphatase beta. Infect Immun 74:49-55.
200. Chambers MG, Pyburn TM, Gonzalez-Rivera C, Collier SE, Eli I, Yip CK, Takizawa Y, Lacy DB, Cover TL, Ohi MD. 2013. Structural analysis of the oligomeric states of Helicobacter pylori VacA toxin. J Mol Biol 425:524-35.
201. Cover TL, Puryear W, Perez-Perez GI, Blaser MJ. 1991. Effect of urease on HeLa cell vacuolation induced by *Helicobacter pylori* cytotoxin. Infect Immun 59:1264-1270.
202. Foegeding NJ, Raghunathan K, Campbell AM, Kim SW, Lau KS, Kenworthy AK, Cover TL, Ohi MD. 2019. Intracellular Degradation of *Helicobacter pylori* VacA Toxin as a Determinant of Gastric Epithelial Cell Viability. Infect Immun 87.
203. Sebrell TA, Hashimi M, Sidar B, Wilkinson RA, Kirpotina L, Quinn MT, Malkoc Z, Taylor PJ, Wilking JN, Bimczok D. 2019. A Novel Gastric Spheroid Co-culture Model Reveals Chemokine-Dependent Recruitment of Human Dendritic Cells to the Gastric Epithelium. Cell Mol Gastroenterol Hepatol 8:157-171 e3.
204. Sebrell TA, Sidar B, Bruns R, Wilkinson RA, Wiedenheft B, Taylor PJ, Perrino BA, Samuelson LC, Wilking JN, Bimczok D. 2018. Live imaging analysis of human gastric epithelial spheroids reveals spontaneous rupture, rotation and fusion events. Cell Tissue Res 371:293-307.
205. Miyoshi H, Stappenbeck TS. 2013. In vitro expansion and genetic modification of gastrointestinal stem cells in spheroid culture. Nat Protoc 8:2471-2482.
206. Ogiwara H, Sugimoto M, Ohno T, Vilaichone RK, Mahachai V, Graham DY, Yamaoka Y. 2009. Role of deletion located between the intermediate and middle regions of the Helicobacter pylori vacA gene in cases of gastroduodenal diseases. J Clin Microbiol 47:3493-500.
207. Forsyth MH, Atherton JC, Blaser MJ, Cover TL. 1998. Heterogeneity in levels of vacuolating cytotoxin gene (vacA) transcription among Helicobacter pylori strains. Infect Immun 66:3088-94.
208. Seto K, Hayashi-Kuwabara Y, Yoneta T, Suda H, Tamaki H. 1998. Vacuolation induced by cytotoxin from *Helicobacter pylori* is mediated by the EGF receptor in HeLa cells. FEBS Lett 431:347-350.
209. De Guzman BB, Hisatsune J, Nakayama M, Yahiro K, Wada A, Yamasaki E, Nishi Y, Yamazaki S, Azuma T, Ito Y, Ohtani M, van der Wijk T, den Hertog J, Moss J, Hirayama T. 2005. Cytotoxicity and recognition of receptor-like protein tyrosine phosphatases, RPTPalpha and RPTPbeta, by *Helicobacter pylori* m2VacA. Cell Microbiol 7:1285-1293.
210. Chaturvedi R, de Sablet T, Asim M, Piazuelo MB, Barry DP, Verriere TG, Sierra JC, Hardbower DM, Delgado AG, Schneider BG, Israel DA, Romero-Gallo J,

Nagy TA, Morgan DR, Murray-Stewart T, Bravo LE, Peek RM, Jr., Fox JG, Woster PM, Casero RA, Jr., Correa P, Wilson KT. 2015. Increased Helicobacter pylori-associated gastric cancer risk in the Andean region of Colombia is mediated by spermine oxidase. Oncogene 34:3429-40.
211. Akada JK, Aoki H, Torigoe Y, Kitagawa T, Kurazono H, Hoshida H, Nishikawa J, Terai S, Matsuzaki M, Hirayama T, Nakazawa T, Akada R, Nakamura K. 2010. Helicobacter pylori CagA inhibits endocytosis of cytotoxin VacA in host cells. Dis Model Mech 3:605-17.
212. Yokoyama K, Higashi H, Ishikawa S, Fujii Y, Kondo S, Kato H, Azuma T, Wada A, Hirayama T, Aburatani H, Hatakeyama M. 2005. Functional antagonism between Helicobacter pylori CagA and vacuolating toxin VacA in control of the NFAT signaling pathway in gastric epithelial cells. Proc Natl Acad Sci U S A 102:9661-6.
213. Kobayashi H, Kamiya S, Suzuki T, Kohda K, Muramatsu S, Kurumada T, Ohta U, Miyazawa M, Kimura N, Mutoh N, Shirai T, Takagi A, Harasawa S, Tani N, Miwa T. 1996. The effect of Helicobacter pylori on gastric acid secretion by isolated parietal cells from a guinea pig. Association with production of vacuolating toxin by H. pylori. Scand J Gastroenterol 31:428-33.
214. Wang F, Xia P, Wu F, Wang D, Wang W, Ward T, Liu Y, Aikhionbare F, Guo Z, Powell M, Liu B, Bi F, Shaw A, Zhu Z, Elmoselhi A, Fan D, Cover TL, Ding X, Yao X. 2008. Helicobacter pylori VacA disrupts apical membrane-cytoskeletal interactions in gastric parietal cells. J Biol Chem 283:26714-25.